# MODIFICATION OF ZEOLITES FOR BIOSENSOR APPLICATIONS

A THESIS SUBMITTED TO
THE GRADUATE SCHOOL OF NATURAL AND APPLIED SCIENCES
OF
MIDDLE EAST TECHNICAL UNIVERSITY

BY

BERNA OZANSOY KASAP

IN PARTIAL FULFILLMENT OF THE REQUIREMENTS
FOR
THE DEGREE OF DOCTOR OF PHILOSOPHY
IN
MICRO AND NANOTECHNOLOGY

JANUARY 2018

Approval of the thesis:

**MODIFICATION OF ZEOLITES FOR BIOSENSOR APPLICATIONS**

submitted by **BERNA OZANSOY KASAP** in partial fulfillment of the requirements for the degree of **Doctor of Philosophy in Micro and Nanotechnology Department, Middle East Technical University** by,

Prof. Dr. Gülbin Dural Ünver _____
Dean, Graduate School of **Natural and Applied Sciences**

Assoc. Prof. Dr. Burcu AKATA KURÇ _____
Head of Department, **Micro and Nanotechnology**

Assoc. Prof. Dr. Burcu AKATA KURÇ _____
Supervisor, **Micro and Nanotechnology Dept., METU**

Prof. Dr. Raşit TURAN _____
Co-Advisor, **Physics Dept., METU**

**Examining Committee Members:**

Prof. Dr. Zafer EVİS _____
Engineering Sciences Dept., METU

Assoc. Prof. Dr. Burcu AKATA KURÇ _____
Micro and Nanotechnology Dept., METU

Assoc. Prof. Dr. Can ÖZEN _____
Biotechnology Dept., METU

Assoc. Prof. Dr. Eda Ayşe AKSOY _____
Pharmaceutical Basic Sciences Dept., Hacettepe University

Asst. Prof. Dr. Ceren HAKTANIR _____
Chemical Engineering Dept., Gazi University

**Date**: _____

**I hereby declare that all information in this document has been obtained and presented in accordance with academic rules and ethical conduct. I also declare that, as required by these rules and conduct, I have fully cited and referenced all material and results that are not original to this work.**

Name, Last name: Berna OZANSOY KASAP

Signature:

# ABSTRACT

## MODIFICATION OF ZEOLITES FOR BIOSENSOR APPLICATIONS

OZANSOY KASAP, BERNA
Ph.D., Department of Micro and Nanotechnology
Supervisor: Assoc. Prof. Dr. Burcu AKATA KURÇ
Co-Advisor: Prof. Dr. Raşit TURAN

JANUARY 2018, 134 pages

In the field of biosensor, zeolites are promising materials due to their large surface areas, mechanical and chemical stabilities, ion exchange capacities and controllable hydrophilicity/hydrophobicity. The powder form of zeolites was the only obstacle of their utilization for biosensor fabrication. In this study, drop-coating and polyethylenimine (PEI) coating methods were developed for improving and optimizing the zeolite usage in immobilization of enzymes. These methods were applied for fabrication of conductometric, amperometric and ion sensitive field effect transistor (ISFET) based biosensors.

The conductometric biosensors developed by drop coating method with silicalite were compared with biosensors produced by the frequently used glutaraldehyde (GA) cross-linking method which uses toxic reagent and partially denatures the enzyme. The usage of zeolite increased sensitivity by one-thirds and decreased relative standard deviation (RSD) values for inter-reproducibility by approximately half. The produced biosensors were applied for urea detection in real serum samples and a satisfactory correlation was found when compared with diacetyl monoxime

reaction. It is therefore asserted that this method is useful for application in real samples.

Application of drop-coating method in amperometric biosensors for glucose determination resulted in a prolonged response time due to thick zeolite layers, which were thinned by the PEI method and the response time decreased by a factor of ten. The sensitivity of GA based biosensor increased by 88% using nano beta (nano BEA) and by 34% using silicalite. Furthermore, RSD of reproducibility decreased by half and RSD of inter-reproducibility decreased significantly by a factor of three using zeolite. Consequently, the method developed in this thesis was found to be promising in the development of amperometric biosensors without using toxic compounds. PEI coating method was also applied to ion-sensitive field-effect transistors for urea determination. The obtained results showed that enzyme adsorption on PEI coating of zeolites can promote a wider linear range of biosensors and cause a decrease in the error of signal reproducibility and inter-reproducibility with enhanced sensitivity without using any toxic compounds.

This thesis is the first to study the incorporation of zeolite and gold nanoparticles for adsorption of creatinine deiminase on ISFET based biosensors. The effect of different types of zeolite frameworks, particle size variation and the presence of gold on zeolites (BEA-Gold) were investigated to improve the analytical characteristics of drop-coated zeolite modified ISFET based biosensors. The sensitivity of BEA-Gold based biosensor increased three fold compared to GA based biosensors which showed that gold nanoparticles can be used with zeolite to improve the characteristics of ISFET based biosensors.

**Keywords:** Zeolite, biosensor, urease, glucose oxide, creatinine deiminase, gold nanoparticle

# ÖZ

## BİYOSENSÖR UYGULAMALARI İÇİN ZEOLİTLERİN MODİFİKASYONU

OZANSOY KASAP, BERNA
Doktora, Mikto ve Nanoteknoloji Bölümü
Tez Yöneticisi: Doç. Dr. Burcu AKATA KURÇ
Ortak Tez Yöneticisi: Prof. Dr. Raşit TURAN

OCAK 2018, 134 pages

Biyosensör alanında zeolitler, geniş yüzey alanları, mekanik ve kimyasal stabiliteleri, iyon değiştirme kapasiteleri ve kontrol edilebilir hidrofiliklik/hidrofobiklikleriyle gelecek vadeden malzemelerdir. Zeolitlerin toz formları, biyosensör üretiminde kullanılmalarına tek engeldir. Bu çalışmada, enzimlerin immobilizasyonunda zeolit kullanımının iyileştirilmesi ve optimize edilmesi için damlatarak kaplama ve polietilenimin (PEI) kaplama yöntemleri geliştirilmiştir. Bu yöntemler, kondaktometrik, amperometrik ve iyon duyarlı alan etkili transistor (ISFET) bazlı biyosensörleri üretmek için uygulanmıştır.

Silikalit ile damlatarak kaplama yöntemiyle geliştirilen kondaktometrik biyosensörler, sıklıkla kullanılan toksik kimyasal içeren ve enzimi kısmen denatüre eden glutaraldehit (GA) çapraz bağlama yöntemiyle üretilen biyosensörlerle karşılaştırılmıştır. Zeolit kullanımı hassasiyeti üçte bir oranında arttırmış ve tekrar elde edilebilirlik için relatif standart sapma (RSD) değerlerini yaklaşık olarak yarıya düşürmüştür. Üretilen biyosensörler, gerçek serum örneklerinde üre tayini için uygulanmış ve diasetil monoksim reaksiyonu ile karşılaştırıldığında tatmin

edici bir korelasyon bulunmuştur. Bu nedenle, bu yöntemin gerçek örneklerde uygulanmasının kullanışlı olduğu öne sürülmektedir.

Damlatarak kaplama yönteminin amperometrik biosensörlerde glikoz tayini için uygulanması, kalın zeolit tabakaları sebebiyle tepki sürelerinin uzamasına yol açmıştır; PEI yöntemi ile zeolit tabakaları inceltilmiş ve tepki süresi on kat azalmıştır. GA bazlı biyosensör hassasiyeti, nano beta (nano BEA) kullanılarak % 88 ve silikalit kullanarak % 34 oranında artmıştır. Dahası, zeolit kullanarak tekrarlanabilirlik RSD'si yarı yarıya azalmış ve tekrar elde edilebilirlik RSD'si üç kat azalmıştır. Sonuç olarak, bu tezde geliştirilen yöntemin amperometrik biyosensörlerin toksik bileşik kullanmadan üretiminde gelecek vadettiği bulunmuştur. PEI kaplama yöntemi ayrıca üre tayini için iyon seçici alan etkili transistörlerde uygulanmıştır. Elde edilen sonuçlar, zeolitlerin PEI kaplama ile enzim adsorpsiyonunun, biyosensörlerin doğrusal aralığını arttırabileceğini ve herhangi bir toksik madde kullanmadan gelişmiş hasassiyet ile sinyal tekrarlanabilirlik ve tekrar elde edilebilirlik hatasının azalmasına sebep olacağını göstermiştir.

Bu tez, ISFET bazlı biyosensörler üzerindeki kreatinin deiminazın (CD) adsorpsiyonu için zeolit ve altın nanoparçacıklarının katılımını inceleyen ilk çalışmadır. Damlatarak kaplanmış zeolit modifiye ISFET bazlı biyosensörlerin, analitik özelliklerinin iyileştirilmesi amacıyla değişik zeolit yapılarının, parçacık boyutunun değişiminin ve zeolit üzerinde altının mevcudiyetinin (BEA-Gold) etkisi araştırılmıştır. BEA-Gold bazlı biyosensörlerin hassasiyeti GA bazlı biyosensöre göre üç kat artmıştır; bu sonuç ISFET bazlı biyosensörlerin özelliklerinin iyileştirilmesi için zeolit ile birlikte altın nanoparçacıklarının kullanılabileceğini göstermiştir.

**Anahtar Kelimeler:** Zeolit, biyosensör, üreaz, glikoz oksidaz, kreatinin deiminaz, altın nanopartikül

*Dedicated to my family for their endless love, support and encouragement*

## ACKNOWLEDGMENTS

I would like to express my deepest gratitude to my supervisor Assoc. Prof. Dr. Burcu Akata Kurç, for her excellent guidance, high level of patience and support during my Ph.D. study.

I would like to thank the thesis monitoring committee members Prof. Dr. Zafer Evis and Assoc. Prof. Dr. Can Özen for their precious comments and valuable time.

I would like to thanks my group members; Sezin Galioğlu Özaltuğ, Melda İşler Binay, Esin Soy Yapıcı, Duygu Kuzyaka, S. Kaan Kirdeciler, Ramona Davoudnezhad and Tayfun Taş for their friendship and help during my study. They lifted my spirit when I was having difficult times during the process of writing the thesis.

I would like to thank Seçkin Öztürk, Sedat Canlı, Dr. Tuğba Endoğan, Ali Güzel, Dr. Kemal Behlülgil, Dr. İbrahim Çam, İlker Yıldız, and Dr. Aysel Kızıltay for their guidance and valuable help in the experiments conducted at Central Laboratory of METU. I would also like to thank Özgür Erişen, Gözde Eke, Dr. Selin Süer, Merve Kaplan, Merve Cengiz, Leyla Karabey Molu, Hikmet Eren, Levent Yıldız and Uğur Özgürgil for their friendship and support during my study.

I owe gratitude to Prof. Dr. Sergei V. Dzyadevych, Dr. Oleksandr Soldatkin, Dr. Ivan Kucherenko, Dr. Svitlana V. Marchenko, Dr. Viktoriya M. Pyeshkova and Margaryta K. Shelyakina for their assistance and advice during my study.

I am also appreciative of the financial support that I received for this study through Scientific and Technical Research Council of Turkey (TUBITAK) and European Union project with the project number FP7-PEOPLE-2012-IRSES, 318524, Integrated Nanodevices-NANODEV.

It is a great pleasure to thank Sibel Baybalı and Aysel Ergen İşçi for their friendship and suport during this period.

Special thanks to my mother in law Şirin Kasap and my father in law Hadi Kasap for their love, patience, caring and support. Furthermore, I would like to thank Hatice Ozansoy for her friendship and support.

I am grateful to my family members; my mother Gülgün Ozansoy and my father Harun Ozansoy and my brother Arda Ozansoy for their love, patience and support.

I would like to give my endless gratitude to my dearest husband Onur Kasap, who supported and motivated me with his love and patience during the whole period of my study. My little daughter İpek Kasap also deserves praise for her understanding and love during this period.

**TABLE OF CONTENTS**

ABSTRACT…….……..v
ÖZ……..……vii
ACKNOWLEDGEMENTS…….....…….……..x
TABLE OF CONTENTS…….…….xii
LIST OF TABLES…….…….……xvii
LIST OF FIGURES…….……..xviii
LIST OF ABBREVIATIONS……...……...……..…xxii
CHAPTERS
1. INTRODUCTION…….....……1
1.1 Biosensors ..... 1
1.1.1 Conductometric Biosensors ..... 3
1.1.2 Amperometric Biosensors..... 5
1.1.3 Potentiometric Biosensors-Ion Sensitive Field Effect Transistor Based ..... 8
1.2 Enzyme Immobilization ..... 11
1.2.1 Adsorption..... 11
1.2.2 Entrapment ..... 12
1.2.3 Covalent Bonding ..... 13
1.2.4 Cross-Linking..... 14
1.3 Zeolites ..... 15
2. LITERATURE REVIEW ……19
2.1 Inorganic Materials as Support Materials for Biosensors ..... 19
2.2 Zeolite Thin Films..... 22
2.3 Protein Immobilization on Zeolites..... 24
2.4 Zeolite Modified Electrodes..... 26
2.5 Gold Nanoparticles in Biosensors ..... 29

2.6 Goal and Objectives ..... 30
3. EXPERIMENTAL PROCEDURE……...33
3.1 Synthesis of Zeolites and Zeolite Modified Electrodes ..... 33
3.1.1 Zeolite Synthesis ..... 33
3.1.1.1 Silicalite ..... 33
3.1.1.2 Beta (BEA) ..... 33
3.1.1.2.1 Ion Exchange of BEA with $Au^{3+}$ ..... 34
3.1.1.2.2 Reduction of $Au^{3+}$-Ion Exchanged BEA..... 34
3.1.1.3 Nano BEA ..... 34
3.1.2 Preparation of Zeolite Modified Electrodes ..... 35
3.1.2.1 Drop-Coating ..... 35
3.1.2.2 Polyethylenimine (PEI) Coating..... 37
3.1.2.3 Enzyme Immobilization on Zeolite Modified Electrochemical Transducers..... 37
3.2 Biosensor Set up..... 39
3.2.1 Conductometric Biosensors ..... 39
3.2.1.1 Materials ..... 39
3.2.1.2 Enzymatic Reaction ..... 39
3.2.1.3 Sensor Structure and Data Measurement..... 40
3.2.1.4 Urease Immobilization in GA vapor ..... 41
3.2.1.5 Urease immobilization in GA drop ..... 42
3.2.1.6 Urease immobilization on Nitrocellulose ..... 43
3.2.1.7 Urease Photopolymerization in PVA/SbQ ..... 43
3.2.2 Amperometric Biosensors..... 44
3.2.2.1 Materials ..... 44
3.2.2.2 Enzymatic Reaction ..... 44
3.2.2.3 Sensor Structure and Data Measurement..... 45
3.2.2.4 Glucose oxidase immobilization in GA vapor ..... 46
3.2.3 ISFET based Biosensors ..... 47
3.2.3.1 Urea Determination ..... 47

3.2.3.1.1 Materials ..... 47
3.2.3.1.2 Enzymatic reaction ..... 47
3.2.3.1.3 Sensor Structure and Data Measurement ..... 47
3.2.3.1.4 Urease immobilization in GA vapor for ISFET based biosensor ..... 49
3.2.3.2 Creatinine Determination ..... 49
3.2.3.2.1 Materials ..... 49
3.2.3.2.2 Enzymatic reaction ..... 50
3.2.3.2.3 Sensor Structure and Data Measurement ..... 50
3.2.3.2.4 Creatinine deiminase immobilization in GA vapor ..... 51
3.3 Material Characterization ..... 51
3.3.1 X-Ray Diffraction (XRD) ..... 51
3.3.2 Scanning Electron Microscopy (SEM) ..... 52
3.3.3 Scanning Transmission Electron Microscopy (STEM) ..... 52
3.3.4 Particle Size Analysis ..... 52
3.3.5 Surface Area Analysis ..... 52
3.3.6 Zeta Potential ..... 53
3.3.7 Inductively Coupled Plasma Optical Emission Spectrometry (ICP-OES) ..... 53
3.3.8 X-ray Photoelectron Spectroscopy (XPS) ..... 53
3.3.9 Contact Angle Measurement ..... 53
3.3.10 Atomic Force Microscopy (AFM) ..... 53
4.RESULTS AND DISCUSSIONS ..... 55
4.1 Synthesis and Characterization of Zeolites ..... 55
4.1.1 Silicalite ..... 55
4.1.2 BEA ..... 58
4.1.2.1 Modification of BEA ..... 60
4.2 Surface Modification for Zeolite Modified Electrochemical Biosensors ..... 65
4.2.1 Drop-Coating ..... 65

4.2.2 PEI Coating ..... 66
4.3 Zeolite Modified Electrochemical Biosensors ..... 69
4.3.1 Conductometric Biosensors ..... 69
4.3.1.1 Preparation of Silicalite-Based Electrodes ..... 69
4.3.1.2 Effect of Silicalite Amount on Transducer ..... 71
4.3.1.3 Effect of Adsorption Time ..... 72
4.3.1.4 Effect of Solution Properties ..... 72
4.3.1.5 Sensitivity ..... 75
4.3.1.6 Comparison of Urease Adsorption on Silicalite with Other Methods of Immobilization ..... 75
4.3.1.7 Signal Reproducibility and Operational Stability ..... 76
4.3.1.8 Biosensor Inter-Reproducibility ..... 78
4.3.1.9 Application of Developed Biosensor in Serum ..... 79
4.3.2 Amperometric Biosensors ..... 82
4.3.2.1 Preparation of Zeolite Modified Electrode ..... 82
4.3.2.2 Sensitivity ..... 83
4.3.2.3 Signal Reproducibility and Inter-Reproducibility ..... 86
4.3.3 ISFET Based Biosensors ..... 89
4.3.3.1 ISFET Based Biosensors for Urea ..... 89
4.3.3.1.1 Preparation of Zeolite Modified Transducers ..... 89
4.3.3.1.2 Sensitivity ..... 91
4.3.3.1.3 Signal Reproducibility and Inter-Reproducibility ..... 93
4.3.3.2 ISFET Based Biosensor Applications for Creatinine ..... 96
4.3.3.2.1 Preparation of Drop-coated Silicalite Modified Transducers ..... 97
4.3.3.2.2 Sensitivity ..... 97
4.3.3.2.3 Signal Reproducibility and Operational Stability ..... 99
4.3.3.2.4 Effect of Solution Properties ..... 101
4.3.3.2.5 Comparison of Creatinine Adsorption on Silicalite Developed by DZMT and PZMT ..... 103

4.3.3.2.5.1 Sensitivity ..... 104
4.3.3.2.5.2 Signal Reproducibility and Inter-Reproducibility .... 106
4.3.3.2.6 Effect of Zeolite Morphology, Particle Size and Gold Nanoparticle on Drop-Coated Zeolite Modified ISFET Based Biosensors ..... 107
4.3.3.2.6.1 Preparation of Drop-coated Zeolite Modified Electrode ..... 108
4.3.3.2.6.2 Sensitivity ..... 111
4.3.3.2.6.3 Signal Reproducibility and Inter-Reproducibility .... 114
5. SUMMARY, CONCLUSION AND FURTHER SUGGESTIONS……...117
REFERENCES……119
CURRICULUM VITAE……..129

## LIST OF TABLES

TABLES

Table 4.1 Physical properties of silicalite crystals ..... 57
Table 4.2 Physical properties of BEA crystals ..... 60
Table 4.3 ICP-OES results of Cal-BEA and BEA-Gold ..... 62
Table 4.4 The summary of zeolite, the type of biosensors and enzymes used in bioselective elements ..... 64
Table 4.5 Comparison of conductometric urease biosensors based on different methods of immobilization. ..... 76
Table 4.6 Comparison of operational characteristics of biosensors created using all types of urease immobilization ..... 96
Table 4.7 Characteristics of creatinine biosensor based on different types of enzyme immobilization ..... 99
Table 4.8 Comparison of characteristics of creatinine based biosensors ..... 105
Table 4.9 Summary of physicochemical characteristics of used zeolites..... 108
Table 4.10 Cross sectional SEM and AFM images of Silicalite, Cal-BEA, BEA-Gold and Cal-Nano BEA on silicon wafer ..... 110
Table 4.11 Contact angles of biosensor surfaces..... 111
Table 4.12 Characteristics of creatinine based biosensors with different types of enzyme immobilization ..... 114

## LIST OF FIGURES

FIGURES

Figure 1.1 A typical biosensor [2] ..... 2
Figure 1.2 Ion migration in the solution and electrolyte conductivity [7]..... 3
Figure 1.3. Scheme of conductometric biosensor set up [9] ..... 5
Figure 1.4 Amperometric measurement setup a) two-electrode and b) three-electrode..... 7
Figure 1.5 Schematic view of (a) MOSFET and (b) ISFET [14] ..... 9
Figure 1.6 Electric double layer close to the $SiO_2$ surface [15] ..... 10
Figure 1.7 Schematic representation of the main enzyme immobilization methods; a) adsorption, b) entrapment, c) covalent bonding, d) cross-linking. E: Enzyme 13
Figure 1.8 Possible forms of GA in aqueous solution [21] ..... 14
Figure 1.9 The binding of primary units of zeolites ..... 15
Figure 1.10 Pore structure of a) Silicalite (MFI), b) BEA [24] ..... 16
Figure 2.1 Types of bonding effective for the monolayer assembly of zeolite microcrystals on substrate [46]..... 24
Figure 3.1 Creation of drop-coated zeolite modified transducer, DZMT ..... 36
Figure 3.2 Schematic representation of transducers; (a) Drop-coated Zeolite Modified Transducer (DZMT)), (B) PEI-coated Zeolite Modified Transducer (PZMT), (C) Standard Membrane Transducer (SMT) ..... 38
Figure 3.3 Overall view of a) conductometric transducer and b) portable conductometric analyzer..... 41
Figure 3.4 Schematic representation of enzyme immobilization in GA vapor .... 42
Figure 3.5 The photograph of (a) amperometric transducer and (b) measuring device..... 46
Figure 3.6 The photograph of (a) pH- sensitive field effect transistor and ..... 48
Figure 4.1 XRD patterns of synthesized silicalites: a) Silicalite and b) Cal- Sil.. 56

Figure 4.2 SEM images of silicalite crystals a) Silicalite, and b) Cal-Sil ..... 57
Figure 4.3 The X-ray diffraction patterns of (a) BEA, (b) Cal-BEA, (c) Nano BEA, (d) Cal-Nano BEA ..... 58
Figure 4.4 SEM images of BEA crystals a) Cal-BEA, and b) Cal-Nano BEA .... 59
Figure 4.5 X-ray diffraction patterns of (a) Cal-BEA and (b) BEA-Gold ..... 61
Figure 4.6 SEM image of BEA-Gold ..... 62
Figure 4.7 (a) STEM dark field image of gold nanoparticles and (b) STEM-EDX spectra of gold nanoparticle selected in (a) ..... 63
Figure 4.8 XPS Au 4f core-level spectrum of BEA-Gold ..... 64
Figure 4.9 SEM image of conductometric transducer a) Bare and b) Drop-coated zeolite modified electrode using silicalite ..... 65
Figure 4.10 SEM images of PEI modified silicon wafers with silicalite using varying concentrations of PEI; a) 10%, b) 6% and c) 1% ..... 67
Figure 4.11 SEM images of Mucasol-PEI modified silicon wafers with silicalite using a) Mucasol -3% PEI, b) Mucasol -1% PEI c) Mucasol -0.5 % PEI..... 68
Figure 4.12 SEM images of the active region of conductometric transducer showing (a) bare electrode, (b) with silicalite layer and (c) higher magnification of the electrode with silicalite ..... 70
Figure 4.13 Response dependence of conductometric based urea biosensor on silicalite amount..... 71
Figure 4.14 Response dependence of conductometric based urea biosensor on urease adsorption time ..... 72
Figure 4.15 Response dependence of conductometric based urea biosensor on pH based on urease, (1) adsorbed on silicalite and (2) immobilized in GA vapor..... 73
Figure 4.16 Dependence of biosensor's responses on ionic strength, (1) adsorbed on silicalite and (2) immobilized in GA vapor ..... 74
Figure 4.17 Calibration curves for urea detection by biosensors, based on urease, (a) adsorbed on silicalite (b) urease immobilized in GA vapor..... 75
Figure 4.18 Operational stability of biosensors based on urease, adsorbed on silicalite (1) and immobilized in GA vapor (2) ..... 77

Figure 4.19 Inter-reproducibility of biosensors based on urease, adsorbed on silicalite (A), and immobilized in GA saturated vapor (B). ..... 78
Figure 4.20 Real experiment on urea determination by the developed biosensor using the method of standard additions in 5mM, pH 6.5 ..... 80
Figure 4.21 Comparison of measurement by biosensors based on silicalite-adsorbed urease and by the method of diacetyl monoxime reaction ..... 81
Figure 4.22 Reproducibility of the results of measurement of two serum samples: (1) sample with 42 mM and (2) sample with 29 mM of urea..... 82
Figure 4.23 Response curve of amperometric biosensor developed by drop coating of silicalite ..... 84
Figure 4.24 Cross sectional SEM images of amperometric electrodes with (a) drop-coated silicalite, (b) PEI-coated silicalite, (c) PEI-coated silicalite ..... 85
Figure 4.25 Calibration curves for glucose detection based on GOx adsorbed on (1) Nano BEA and (2) Silicalite, and GOx immobilized in (3) GA vapor ..... 86
Figure 4.26 Reproducibility of responses of biosensors based on GOx adsorbed on nano BEA (1) and Silicalite (2), and GOx immobilized in GA vapor (3)..... 87
Figure 4.27 Inter-reproducibility of biosensors based on GOD adsorbed on nano BEA (1) and Silicalite (2), and GOx immobilized in GA vapor (3) ..... 88
Figure 4.28 SEM images of the PZMTs developed by using zeolites at different magnifications: (a,-c) without zeolite, (d-f) Silicalite, (g-i) Nano BEA ..... 90
Figure 4.29 The responses of biosensors created by urease immobilization in (a) GA vapor, adsorption on (b) Silicalite, (c) Nano BEA, (d) Cal-Nano BEA ..... 91
Figure 4.30 Calibration curves for urea created by urease immobilization in (a) GA vapor, adsorption on (b) Silicalite, (c) Nano BEA, (d) Cal-Nano BEA ..... 92
Figure 4.31 Reproducibility of the responses created by urease immobilization in (a) GA vapor, adsorption on (b) Silicalite, (c) Nano BEA, (d) Cal-Nano BEA... 94
Figure 4.32 Inter-reproducibility of signals created by urease immobilization in (a) GA vapor, adsorption on (b) Silicalite, (c) Nano BEA, (d) Cal-Nano BEA ..... 95
Figure 4.33 SEM images of potentiometric transducers (sensitive parts): (a) bare surfaces and (b) surface covered with silicalite..... 97

Figure 4.34 Calibration curves of creatinine biosensors: (a) covalent cross-linking in GA vapor and (b) adsorption on drop-coated silicalite ..... 98
Figure 4.35 The reproducibility of drop-coated silicalite modified biosensor... 100
Figure 4.36 Storage stability of drop-coated silicalite modified biosensor,..... 101
Figure 4.37 Dependence of response of drop-coated silicalite modified biosensor on NaCl concentration ..... 102
Figure 4.38 Calibration curves for creatinine detection in presence of protein at various concentrations: (a) 0 %, (b) 0.1 %, (c) 0.5 % and (d) 1%..... 103
Figure 4.39 The calibration curves for determination of the creatinine in 5 mM phosphate buffer solution, pH 7.4. ..... 104
Figure 4.40 Results of the biosensor signal reproducibility for determination of creatinine content in 5 mM phosphate buffer, pH 7.4 at room temperature..... 106
Figure 4.41 Results of the biosensor signal inter-reproducibility for determination of creatinine content in 5 mM phosphate buffer, pH 7.4 at room temperature .. 107
Figure 4.42 The calibration curves for creatinine created by CD immobilization; (a) in GA vapor, adsorption on: (b) Silicalite, (c) BEA, (d) BEA-Gold and (e) Nano BEA ..... 112
Figure 4.43 Reproducibility of signals created by CD immobilization; (a) in GA vapor, adsorption on: (b) Silicalite,(c) BEA,(d) BEA-Gold and (e) Nano BEA 115

## LIST OF ABBREVIATIONS

| | |
|---|---|
| AFM | Atomic force microscopy |
| BEA | Zeolite beta |
| CD | Creatinine deiminase |
| Cal-BEA | Calcined beta |
| Cal-Nano BEA | Calcine nano beta |
| Cal-Sil | Calcined silicalite |
| DZMT | Drop-coated zeolite modified transducer |
| GA | Glutaraldehyde |
| GOx | Glucose oxidase |
| ICP-OES | Inductively coupled plasma optical emission spectrometry |
| ISFET | Ion sensitive field effect transistor |
| PEI | Polyethylenimine |
| PZMT | PEI-coated zeolite modified transducer |
| SEM | Scanning electron microscopy |
| Sil | Silicalite |
| SMT | Standard membrane transducer |
| STEM | Scanning transmission electron microscopy |
| TEAOH | Tetraethylammonium hydroxide |
| TEOS | Tetraethylorthosilicate |
| TPAOH | Tetrapropylammonium hydroxide |
| XPS | X-ray photoelectron spectroscopy |
| XRD | X-ray diffraction |
| ZMT | Zeolite membrane transducer |

# CHAPTER 1

# INTRODUCTION

## 1.1 Biosensors

A biosensor converts the modification of the physical or chemical properties of a bioselective element, which occurs as a result of biochemical interactions, into an electric or an optic signal whose amplitude depends on the concentration of defined analytes in the solution. It can detect and quantify specific analytes. According to International Union of Pure and Applied Chemistry, biosensor is "A device that uses specific biochemical reactions mediated by isolated enzymes, immune systems, tissues, organelles or whole cells to detect chemical compounds usually by electrical, thermal or optical signals" [1].

Functionally, the device consists of two parts:

• a bioselective element, that is, a detecting layer of immobilized material (enzymes, antibodies, receptors, organelles, microorganisms);

• a transducer (electrochemical, optical, thermal, piezoelectrical).

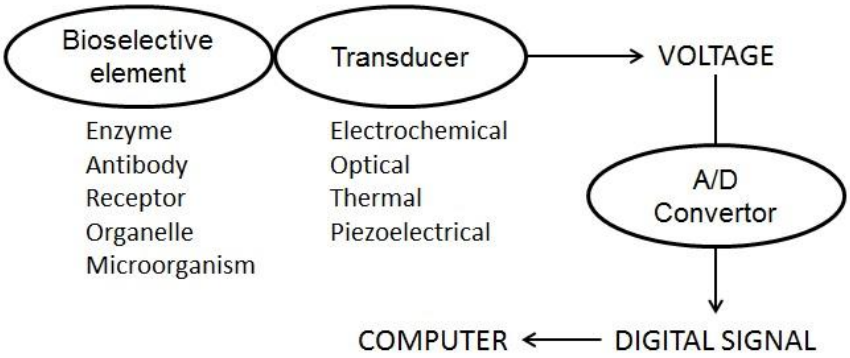


Figure 1.1 A typical biosensor [2]

Main analytical characteristics of biosensors are sensitivity, linear concentration range, limit of detection, response time, reproducibility, operational stability, storage stability and selectivity. The sensitivity is the slope of the calibration curve of the obtained biosensor. Linear concentration range is the range of analyte concentration where the biosensor response changes linearly with the concentration. Limit of detection is the lowest concentration of analyte that produces a statistically significant response. Response time is the time necessary to reach 90% of the steady-state response when analyte is added into the measurement cell. Reproducibility is a measure of the scatter or the drift in a series of observations or results performed over a period of time [3]. Inter-reproducibility is the deviation between the responses of different biosensors developed by the same procedure [4]. Operational stability can be defined as the retention of activity of bioselective material when in use. Storage stability depends on the conditions of storage; dry or wet storage, atmosphere, pH, existence of additives and buffer composition. There are two main methods for selectivity. In the first method, analyte calibration curve is compared to calibration curves of each interfering substances which are obtained at identical conditions. Selectivity is stated as the ratio of the response with analyte alone and with the interfering substance alone. In the other method, both analyte and interfering substances are injected to cell. The percentage of variation of response is expressed as selectivity [3,5].

The important working parameters of a biosensor, such as selectivity generally depends on bioselective element, whereas sensitivity and detection limit of a biosensor intensely relies on the physicochemical properties of the transducer which can be enhanced by use of proper materials and/or the design of new device architectures. Thus, the main endeavors in the biosensor development are focused on the exploration of various combinations of biological components (or their synthetic mimics) and/or nanomaterials with different transducers. Electrochemical transducers can be divided into three groups: conductometric, amperometric and potentiometric biosensors [6,7].

### 1.1.1 Conductometric Biosensors

Conductometric biosensors measure the conductivity of the solution. When a potential difference is applied to the electrode, an electric field occurs and this induces the migration of ions of the electrolyte; negative ions move towards anodes while positively charged ones move towards cathodes as presented in Figure 1.2.

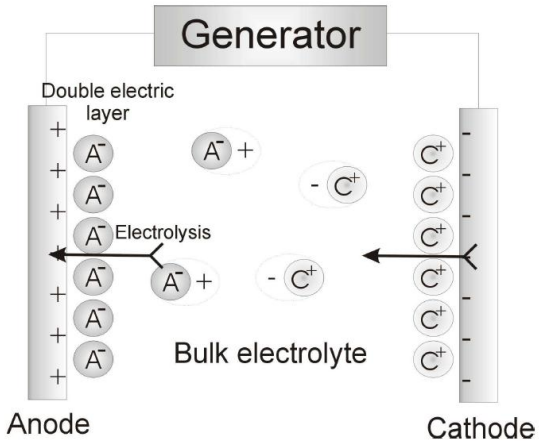


Figure 1.2 Ion migration in the solution and electrolyte conductivity [8]

This movement of ions causes a measurable current. According to Ohm's law conductivity of the solution can be calculated as follows:

$$S=I/V \tag{1.1}$$

where S is conductivity (value to reciprocal to resistance), I and V are induced current and applied voltage, respectively. Therefore, specific conductivity can be calculated as:

$$X=S(L/A) \tag{1.2}$$

where X is the specific conductivity, L is the distance between the immersed electrodes and A is the area of electrodes. There are several more parameters affecting the conductance. These parameters can be represented as a constant C and X can be given as:

$$X = C\,\Sigma(u_i\, c_i) \tag{1.3}$$

where $u_i$ is the mobility of an ion, $c_i$ is the concentration of an ion and C is the representation of the hidden parameters. Thus, the conductivity of the electrolyte solution depends on the ion concentration and mobility. When an enzymatic reaction occurs some ions can be produced or consumed as a result of the reaction and thereby alter the overall conductivity of the solution that can be measured by conductometric biosensors [8, 9].

The advantages of conductometric biosensors are suitability for miniaturization and low cost of production due to the simple structure of the electrodes. Additionally, they are not light sensitive and they can be used in various reactions since almost all enzymatic reactions involve consumption or production of charged species causing a change in the ionic composition of the tested sample. The most important disadvantage of this system is the low selectivity, due to the significant background conductivity of the solution but this can be overcome by using a differential measuring scheme which compensates for changes in background conductivity and influence of temperature variations [8].

The scheme of conductometric biosensor set up is presented in Figure 1.3. Conductivity measurements were performed by applying to each pair of

interdigitated electrodes a small-amplitude alternating voltage with the frequency 100 kHz and amplitude of 10 mV by a generator. The output differential signal between the pair of electrodes (the electrode with immobilized enzyme which is called working electrode and the electrode with only bovine serum albumin which is called reference electrode) was fed to a low-noise differential amplifier and then analyzed using lock-in amplifier, which was supplied with a reference signal from an internal oscillator. After the lock-in amplifier, the sensor output signal was recorded using registration device. Therefore, the dependence of the output signal on the substrate concentration in the solution was measured.

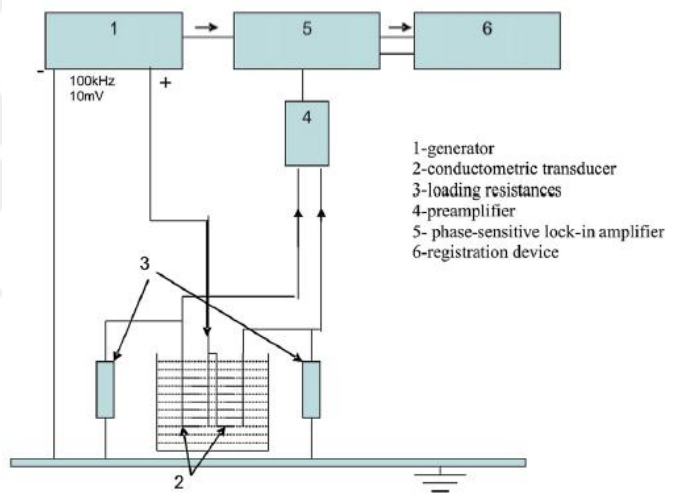


Figure 1.3. Scheme of conductometric biosensor set up [10]

### 1.1.2 Amperometric Biosensors

Amperometric biosensors are a class of the most widespread, numerous and successfully commercialized devices of biomolecular electronics. The development of the biosensors started from amperometric biosensors by adding enzyme (glucose oxidase) onto surface of oxygen electrode covered with half-permeable dialysis membrane leading to glucose-specific enzymatic electrode [11].

In amperometry, when a constant potential is applied, some redox species are oxidized or reduced so that an electrochemical reaction occurs on the transducer surface. Thus, this reaction results in a current change which is directly proportional to the amount of the oxidized or reduced electroactive species. The main factor that influences the results of the amperometric biosensor is the direct exchange of charged particles between the electrode and solution through the electron movement across the electron/solution interface (oxidation/reduction processes). The exchange reaction is presented below:

$$Ox + ze^- \leftrightarrow Red \tag{1.4}$$

Oxidized particles (Ox) accepts electrons while they are being reduced by reduced particles (Red) and reduced particles donates electrons while they are being oxidized where ze- is the number of electrons crossing the electron/solution interface.

The rate of electrochemical reaction on the electrode is the total current which is equal to the sum of cathode Ic (reduction) and anode Ia (oxidation) currents;

$$I = Ic + Ia \tag{1.5}$$

$$Ic = zFk_cC_{Ox} \tag{1.6}$$

$$I_a = -zFk_aC_{Red} \tag{1.7}$$

Where z is charge, F is Faraday constant, $C_{Ox}$ and $C_{Red}$ are concentrations of oxidized and reduced particles, respectively. $k_c$ and $k_a$ are rate coefficients which are the functions of electrode potential. These equations show that total current measured is a function of substrate concentration.

The current in an electrochemical cell at a constant voltage value applied is measured in amperometric transducers. These biosensors are composed of two or three electrodes.

In the two electrode amperometric measurement set up presented in Figure 1.4-a, same nodes are used for both supplying voltage and measuring potential drop. Because of this, only the total potential drop on the solution is measured instead of the net potential drop on the working electrode. To get rid of this problem (to eliminate the potential drop on the auxiliary electrode) a third electrode can be introduced (Figure 1.4-b). In this case, potential drop is measured through the reference electrode and net potential drop on working electrode can be measured.

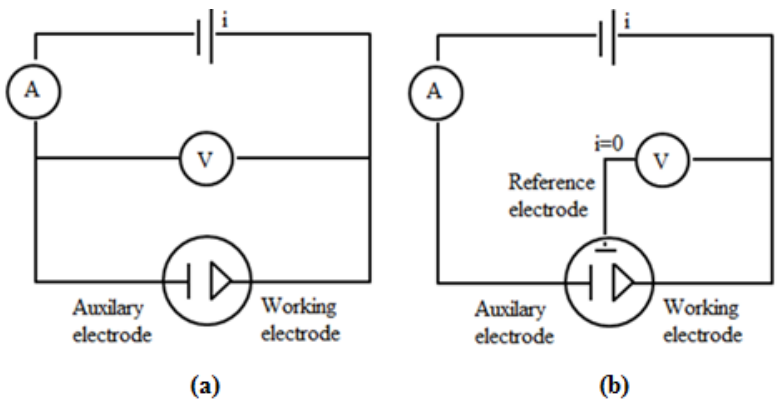


Figure 1.4 Amperometric measurement setup a) two-electrode and b) three-electrode

Moreover, there are three main classes of amperometric biosensors. The first group of biosensors (first generation biosensors) is based on the measurement of concentration of electroactive substrate or product. The widely used catalytic molecules are oxidases and dehydrogenases that generate easily oxidizable $H_2O_2$ and reduced NADH (nicotinamide adenine dinucleotide), respectively:

$$\text{Substrate} + O_2 \xrightarrow{\text{oxidase}} \text{Product} + H_2O_2 \quad (1.8)$$

$$\text{Substrate} + NAD^+ \xrightarrow{\text{dehydrogenease}} \text{Product} + NADH \quad (1.9)$$

The released $H_2O_2$ and NADH can be determined by applying modest potentials to the working electrode (+0.5-+0.8V against a Ag/AgCl reference electrode):

$$H_2O_2 \longrightarrow O_2 + 2H^+ + 2e^- \quad (1.10)$$

$$NADH \longrightarrow NAD^+ + H^+ + 2e^- \quad (1.11)$$

to produce a current signal which is proportional to substrate concentration [12].

Furthermore, alternative oxidizing agents which are called mediators can be used to get more efficient electron transfer during the enzymatic reactions (second generation biosensors). The most common mediators are ferrocene and ferrocyanide. Alternatively, direct electron transfer between active site of enzyme and transducer can be achieved in the construction of the biosensors (third generation biosensors). For this purpose, the redox enzyme is directly immobilized on the electrode surface. Cytochrome c peroxidase, horse-radish peroxidase at carbon electrodes produce catalytic currents in the presence of the substrates based on direct electron transfer [13]. This direct electron transfer was attributed to location of redox center at the protein periphery [14].

### 1.1.3 Potentiometric Biosensors-Ion Sensitive Field Effect Transistor Based

Ion sensitive field effect transistors (ISFET) were developed on the basis of metal oxide silicon field effect transistor (MOSFET) with the gate electrode replaced by chemically sensitive membrane, solution and a reference electrode as presented in Figure 1.5.

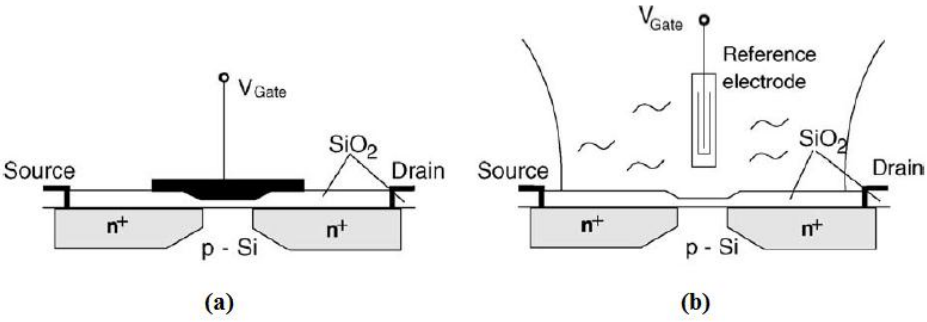


Figure 1.5 Schematic view of (a) MOSFET and (b) ISFET [15]

Charges from solution accumulate on top of this insulating membrane and do not pass through the ion-sensitive membrane. The dependence of the interfacial potential on the charge concentration can be explained with the well-known site-binding theory.

An anisotropic ion accumulation exists at the contact interface between an electrochemically active surface and a liquid electrolyte (Figure 1.6). Due to their different size and charge, the ions form a well-confined electric double layer close to the surface and, according to the Gouy–Chapman theory, a diffuse layer of outer charges exists between the Helmholtz planes and the neutral bulk of the solution. When $SiO_2$ is used as the insulator, the surface of the gate oxide contains –OH functionalities, which are in electrochemical equilibrium with ions in the solutions ($H^+$ and $OH^-$). The hydroxyl groups at the gate oxide surface can be protonated and deprotonated, and thus, when the gate oxide contacts an aqueous solution, a change of pH will change the $SiO_2$ surface potential.

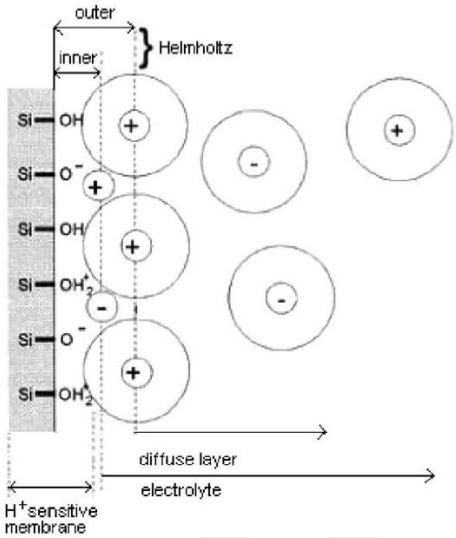


Figure 1.6 Electric double layer close to the $SiO_2$ surface [16]

A site-dissociation model describes the signal transduction as a function of the state of ionization of the amphoteric surface SiOH groups:

$$SiOH \leftrightarrow SiO^- + H^+ \quad (1.12)$$

$$SiOH + H^+ \leftrightarrow SiOH_2^+ \quad (1.13)$$

For silicon nitride ($Si_3N_4$) layer as insulator, the surface potential is determined by the $H^+$ ion exchange between the solution and the binding sites on the $Si_3N_4$ surface. Silicon nitride has two kinds of $H^+$ specific binding sites: silanol (SiOH) and primary amine ($SiNH_2$) groups that are responsible for the surface potential generation via the following reactions taking place at the dielectric interface:

$$SiOH \leftrightarrow SiO^- + H^+ \quad (1.14)$$

$$SiOH + H^+ \leftrightarrow SiOH_2^+ \quad (1.15)$$

$$SiNH_2 + H^+ \leftrightarrow SiNH_3 \quad (1.16)$$

The selectivity and chemical sensitivity of the ISFET are completely controlled by the properties of the electrolyte/insulator interface. For example, many different types of oxide coatings of inorganic materials (e.g., $SiO_2$, $Si_3N_4$, $Al_2O_3$ or $Ta_2O_5$) can be used for obtaining a pH response.

Protonation/deprotonation of the gate material is influenced by the pH at the gate area, which controls the surface potential. The sensor response obeys the Nernstian law (59.2 mV/pH). The response of an ion-selective electrode is given by

$$E = E_0 + \frac{RT}{zF} \ln[i] \tag{1.17}$$

where E is the measured potential (in volts), $E_0$ is a characteristic constant for the ionselective/ external electrode system, R is the gas constant, T is the absolute temperature (K), z is the signed ionic charge, F is the Faraday constant, and [i] is the molar concentration of the free uncomplexed ionic species [16].

## 1.2 Enzyme Immobilization

Biosensors require immobilization of biomolecules onto the surfaces of transducers. The success of biosensor mainly depends on the immobilization process. For this purpose, many immobilization strategies were developed. These methods can be grouped in four main groups such as adsorption, entrapment, covalent bonding and cross-linking. Each method has both advantages and disadvantages.

### 1.2.1 Adsorption

Physical adsorption of an enzyme onto a solid matrix is probably the simplest and fastest way to prepare immobilized enzymes (Figure 1.7-a). The method relies on a non-specific physical interaction based on weak forces, such as van der Waals or hydrophobic interactions between the enzyme and the surface of the matrix which is brought about by mixing a concentrated solution of enzyme with the solid. The

active site of the enzyme is normally unaffected and a nearly full activity is observed.

Many enzymes were immobilized using adsorption method. No reagent and only a minimum amount of activation step is necessary so this method is easy to perform, inexpensive and less disruptive to the enzyme compared to chemical attachment methods. The main disadvantage is the susceptibility of the immobilized enzymes to changes in temperature, pH and ionic strength that can result in desorption of the enzymes.

### 1.2.2 Entrapment

The entrapment method is based on the occlusion of an enzyme within a polymeric network that allows the substrate and products to pass through but retains the enzyme (Figure 1.7-b). The enzyme is not bound to the matrix or membrane. There are different approaches to entrapping enzymes such as gel, fiber entrapping and micro encapsulation. Nylon, cellulose nitrate, epoxy resins, collagen, polysulones, polyacrylates and polycarbonates are some examples. The practical use of these methods is limited by mass transfer limitations through membranes or gels.

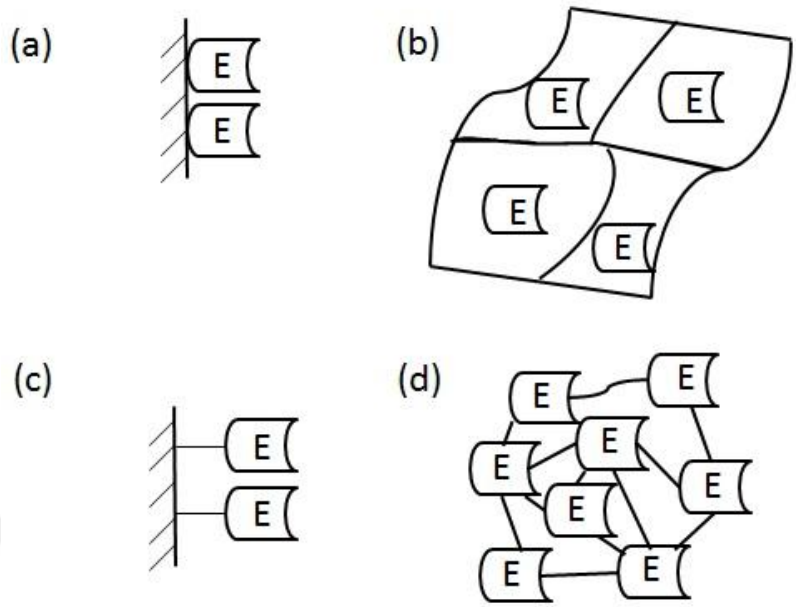


Figure 1.7 Schematic representation of the main enzyme immobilization methods; a) adsorption, b) entrapment, c) covalent bonding, d) cross-linking. E: Enzyme

### 1.2.3 Covalent Bonding

Covalent binding between the enzyme and support matrix is accomplished through funtional groups in the enzyme, which are not essential for its catalytic activity (Figure 1.7-c). The most frequently used reactions involve the following side chains of the amino acids: lysine (amino group), cysteine (thiol group) and aspartic and glutamic acids (carboxylic group). An advantage of this method is because of the stable nature of the bonds formed between enzyme and matrix, the enzyme is not released into the solution upon use. Nevertheless, the quantity of enzyme to be immobilized is usually higher and this method is also difficult to reproduce.

### 1.2.4 Cross-Linking

Enzymes can be cross-linked between sub-units or the domains of the protein using bifunctional reagents such as glutaraldehyde, dicarboxilic acid, diisocyanates, bisimidates or diamines (Figure 1.7-d). The method of protein cross-linking via the reaction of glutaraldehyde ($C_5H_8O_2$, GA) with reactive $NH_2$ groups on the protein surface, expecting to form Schiff bases with C=N group, is widely used in enzyme immobilization. Inert proteins like bovine serum albumin can also be mixed with the enzymes. However, GA is known to be as cytotoxic [17] and induces a partial denaturation of the biomolecules caused by the distortion of active enzyme confirmation and the chemical alterations of the active site during cross-linking [18-20]. Further, depending on the solution conditions, there can be different forms of GA as presented in Figure 1.8 due to the polycondensation and partial cyclization during its storage and use. This situation leads to less reproducible and predictable products [21,22].

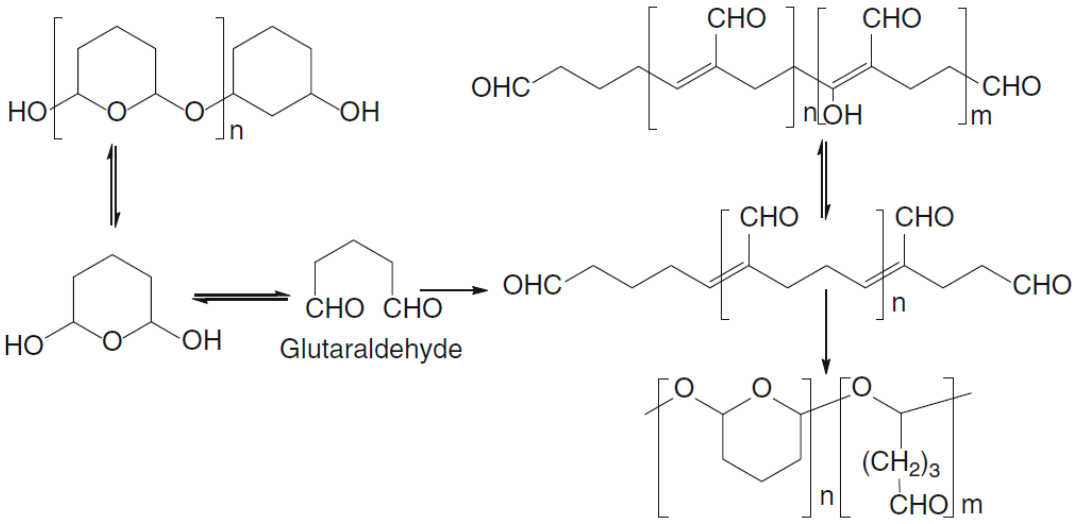


Figure 1.8 Possible forms of GA in aqueous solution [22]

Additionally, this technique had drawbacks such as low mechanical stability and difficulties in handling the gelatinous cross-linked enzymes. For fabrication of biosensors, this method is often used but it can induce the formation of diffusion barriers [23] leading to a higher response time of biosensor beside the other disadvantages described previously.

As an alternative to known enzyme immobilization methods nanomaterials such as; carbon nanotubes, copper, silver, gold nanoparticles and zeolites are used for developing enzyme immobilization. Among them, zeolites have potential use thanks to their stability, biocompatibility and adjustable hydrophilicity.

### 1.3 Zeolites

Zeolites are hydrated crystalline aluminosilicates, consisting of an anionic framework and charge-compensating cations. The primary building units of the framework are $TO_4$ tetrahedra where T atom is a silicon or aluminum atom. Each T atom is coordinated to four oxygen atoms with each oxygen shared between two T atoms as presented in Figure 1.9. These interconnected tetrahedra forms 3-dimensional frameworks with linked channel systems and well–defined micro- and mesopores. This high degree of open porosity leads to an exceptionally high surface area.

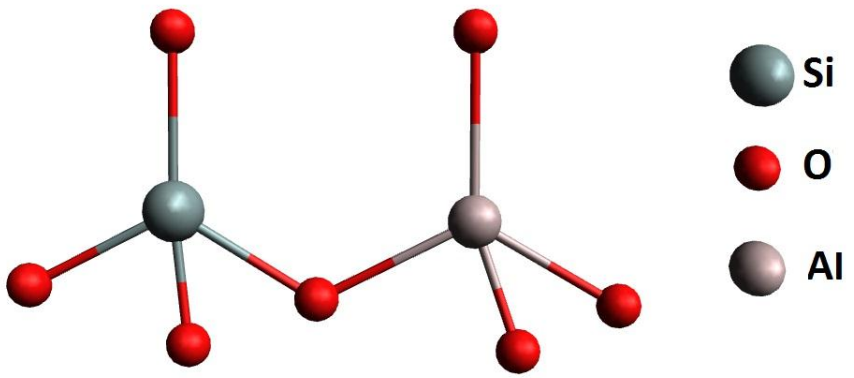


Figure 1.9 The binding of primary units of zeolites

Up to date, 232 types of synthetic zeolites with variable framework type structures with one-, two- and three-dimensional pore systems have been synthesized by linking these tetrahedra together in different combinations as presented in Figure 1.7 [24].

For example, two dimensional pore structure of silicalite-1 (MFI) is shown in Figure-1.10-a has straight channels with an estimated pore opening of 0.56 nm x 0.54 nm and sinusoidal channels with an estimated pore opening of 0.51 nm x 0.55 nm, whereas beta zeolites (BEA) presented in Figure 1.8-b have three dimensional channel system with pore diameters of 5.6 x 5.6 Å and 7.7 x 6.6 Å.

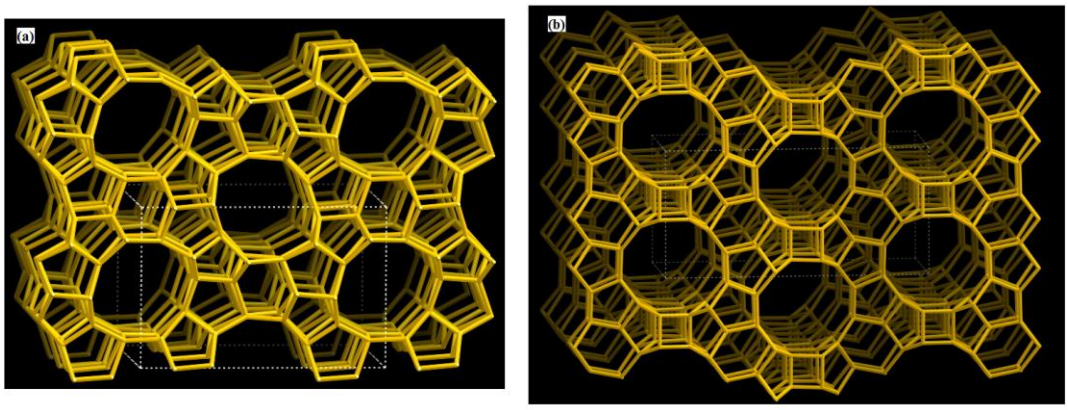


Figure 1.10 Pore structure of a) Silicalite (MFI), b) BEA [25]

In addition to the framework of one particular zeolite, the chemical composition is crucial in defining its specific properties. Generally, the following formula applies;

$$Me_{y/m}^{m+}[(SiO_2)_x \cdot (AlO_2^-)_y] \cdot zH_2O \quad (1.18)$$

Here, Me denotes a cation with the charge m. As shown in Eq. (1.18), the negative charge was introduced into the framework with $Al^{3+}$. This charge needs to be compensated by y/m cations $Me^{m+}$, which are electrostatically bound to the host framework and mobile along the channels. Consequently, zeolites with a high

aluminum content are highly polar materials, potential ion conductors, and excellent ion exchangers. Furthermore, the aluminum ions act as highly acidic sites that can catalyze a number of chemical reactions. An important parameter for zeolites is the ratio of Si/Al in the lattice, x/y, which indicates the content of mobile cations as well as the amount of acidic centers per unit cell. It is also used to denote the hydrophobicity, with higher ratios indicating a higher degree of hydrophobicity and lower ion exchange capacity [26]. In addition to their intrinsic components, zeolites can also be modified in a post-synthesis step by incorporating catalytically active metal clusters such as Pt, Fe, or Cu. Due to their large band-gap of several eV, no electronic conductivity is observed with zeolites in general. However, since mobile cations are present within the zeolite framework that may hop from one binding site to the next, zeolites exhibit ionic conductivity. The thermal activation energy of conduction and the specific conductivity depend on the nature of the mobile cation. In the dehydrated state, for example, highest conductivity values and lowest activation energies were observed for $Na^+$ compensated zeolites [27].

In general, the zeolites are mostly used in catalysis in order to ensure the easy diffusion of molecules and reaching the catalytic active sites in the zeolite pores. They are also used in sorption processes due to the molecular sieving effect. Furthermore, the materials with precise pore shapes are applied in systems where molecular recognition is needed such as shape-selective catalysis, selective adsorption, separation processes, chemical sensors and nanotechnology [28]. Currently, zeolites are being extensively explored for use in advanced biotechnological applications, such as supports for enzyme immobilization, biosensors, controlled drug delivery systems and biomedical implants. This is due to their structural/surface features, high surface area, biocompatibility, tailored ion exchange capabilities, well-defined cages/channels, high mechanical, thermal and chemical stability.

# CHAPTER 2

# LITERATURE REVIEW

## 2.1 Inorganic Materials as Support Materials for Biosensors

The global market for biosensors is expected to reach over $25 billion by 2020. Glucose-testing biosensors accounts for 85% of the gigantic world market [29]. Other commercial clinical biosensors are used for pregnancy, *Escherichia coli* O157, influenza A and B, *Helicobacter pylori*, human immunodeficiency virus (HIV), tuberculosis, and malaria detection in blood, serum, body fluids, and urine [30].

Short response time, sensitivity, ease of use, simplicity of preparation, possibility of mass production and low production costs, possibility of miniaturization and automatization are the major advantages of biosensors over traditional analytical methods. However, many biosensors explained in literature still have few drawbacks compared to other analytical methods. The main problems are the reduced stability, the lack of or low response reproducibility and limited lifetime of the biosensor [31].

By the development of nanotechnology, these problems are trying to be solved using different inorganic materials for support materials for enzyme immobilization in biosensor development. Some examples of these inorganic materials are clays, ZnO nanoparticles, carbon nanotubes, graphene and zeolites.

Clays are two-dimensional layered aluminosilicates that exhibit ion exchange capabilities and adsorption properties. They can be used in electroanalysis to preconcentrate target analytes (usually by ion exchange or organic compounds by adsorption) or to immobilize enzymes in biosensors as an alternative method [32,33].

Wang and Martinez reported the first clay-modified carbon paste electrode [34]. Montmorillonites, sepiolite, bentonites, kaolin and some other natural smectite clays (laponite) are some examples of clay-modified electrodes [35]. The existence of clays offers a favorable environment to enzyme activity and leads to improved analytical characteristics of the biosensors [20].

Shan et al. used laponite for immobilization of tyrosinase by entrapment, with GA cross-linking for detection of catechol [36]. Additionally, Azure B as an electron shuttle for the mediated detection of phenol was exchanged within the clay matrix. Laponite provided a hydrophilic immobilization matrix increasing the long term stability of the biosensor ( 93 % of its initial activity after two weeks and 47 % after 3 weeks) compared to the corresponding biosensors obtained by chemical cross-linking of tyrosinase with glutaraldehyde (63 % of its initial activity after two weeks and 36 % after 3 weeks). Azure B allowed the detection of phenol derivatives at applied potential closed to zero (−0.05 V). The detection limits obtained for catechol, p-cresol and phenol are 1, 1 and 17 nM, respectively.

ZnO nanoparticles have high surface to volume ratio, biocompatibility and fast electron transfer between the active sites of enzyme and electrode. These properties made the material preferred for enzyme immobilization matrix. Dai et al. prepared an amperometric biosensor for glucose detection based on direct electrochemistry of GOx immobilized by simple adsorption on tetragonal pyramid shaped porous ZnO (TPSP-ZnO) nanostructures. The prepared TPSP-ZnO had a large surface area and favorable biocompatibility providing a good matrix for protein immobilization and direct electron transfer. The biosensor had a linear response to glucose concentrations ranging from 0.05 to 8.2 mM with a low LOD such as 0.01 mM at

an applied potential of -0.50 V (versus a saturated calomel reference electrode) [37].

CNTs are composed of graphene sheets which are rolled into a cylindrical shape. They have $sp^2$ carbon units that comprise a seamless structure with hexagonal honeycomb lattices, being several nanometers in diameter and up to hundreds of microns long. There are two typical types of nanotubes, single-wall carbon nanotubes (SWCNT) and multiwall carbon nanotubes (MWCNT). SWCNTs represent a single graphite sheet rolled perfectly, demonstrating a tube diameter of 1 to 2 nm, whereas MWCNTs show concentric and closed graphite tubules with diameters ranging from 2 to 50 nm and an interlayer distance of 0.34 nm [38]. Due to their highly oriented structures, they have a high surface-volume ratio, a high conductivity, and a fast electron-transfer rate. Moreover, because of their hollow structure, enzyme loading can be substantially increased through immobilization on the outside and inside of the CNT. Furthermore, CNTs are able to act as electronic wires that shorten the electron transfer distance and enhance the electron transfer efficiency. Two major barriers for developing CNT-based devices are their spontaneous coagulation and insolubility in aqueous media due to their hydrophobic nature [39].

The first CNT-based sensor was reported by Britto et al., in 1996 [40]. Since then, CNTs have been incorporated into various electrochemical biosensors because these sensors tend to have higher sensitivities, faster response times and lower detection limits compared to conventional sensor designs with carbon electrodes.

Wang et al. used carbon nanotubes with immobilized GOx for detection of glucose. They observed that increasing the Nafion content from 0.1 to 5 wt% lead to enhancement of the solubility of both types of SWCNTs and MWCNTs, and thus use of Nafion as a solubilizing agent for CNTs overcomes a major obstacle for creating CNT-based biosensing devices [41]. The CNT/Nafion-coated electrode offered a highly selective low potential biosensing of glucose (−0.05 V vs. Ag/AgCl).

Graphene, which is also known as two dimensional carbon sheets, is the carbon structure with $sp^2$ hybridization in a densely packed honeycomb crystal lattice. Graphene has high stability and crystallographic quality with excellent electrical, mechanical and thermal properties due to the π conjugation.

Shan et al. [42] reported the first graphene-based glucose biosensor based upon graphene protected by polyvinylpyrrolidone that could thus be well dispersed in water. It has good electrochemical reduction toward $H_2O_2$. After the GOx is immobilized, the sensor achieved a direct electron transfer between GOx and electrode. A linear glucose response covered from 2 to 14 mM, with good reproducibility (3.2% for 10 successive measurements) was obtained [42] .

Zeolites are perspective nanomaterials for biosensor modification due to their controllable hydrophilic and hydrophobic properties, surface functional groups ready for further modifications, adjustable surface charge, high surface area, thermal and mechanical stabilities. The only restriction for this application was the powder form of zeolites and integration of these powder zeolites onto electrode surfaces. In literature, there are some studies to be able to have zeolite films.

## 2.2 Zeolite Thin Films

Walcarius classified methods for developing zeolite modified electrodes (ZME) reported up to date into four main categories [43]:

1. Dispersion of zeolites within electrode matrices
2. Compression of zeolite particles on conductive substrates
3. Zeolite coating embedded in polymeric films
4. Covalent binding of zeolites to electrode surfaces

In order to obtain a thinner zeolite film on electrode surfaces, further methods were proposed, such as secondary growth method. In this method, firstly nanozeolite seeds were adsorbed onto silane-modified surfaces. Then, inserting this surface into the zeolite synthesis solution for hydrothermal treatment in an appropriately

formulated solution leads to continuous and oriented zeolite thin films [44,45]. However, this method requires long time for modification of surfaces (18 h for only silanisation) and the high temperatures used for calcination of silanisation agent (300ºC) can damage electrodes.

Layer by layer deposition is another thin film fabrication method based on electrostatic interaction of zeolites and oppositely charged polyelectrolytes. Yoon et. al used linkers such as poly(sodium4-styrenesulfonate); $PSS^-$ and poly(diallyldimethylammoniumchloride); $PDDA^+$ in a sequence of [$Glass^+$/($PSS^-$/$PDDA^+$/$PSS^-$/$Zeolite^+$)$_5$] to fabricate five layers of zeolite on modified glass substrate. They obtained high degrees of coverage and alignment for 3 layers [46].

Direct attachment method is another method for zeolite thin film production. It was firstly used by Yoon et al. for the organized assembly of zeolite microcrystals with sizes between 500 nm and 12 µm on glass substrates [47]. Direct attachment method is rubbing of the zeolites on the surface with a finger. They claimed that due to the hydrogen bonds between the surface hydroxyl groups of bare zeolite crystals and bare glass substrates, high quality monolayers of calcined silicalite layers were formed (Figure 2.1-a). In addition to that polyethylenimine (PEI), a polymer having $–NH_2$ groups, was used between zeolite and substrate to enhance the number of hydrogen bonding as shown in Figure 2.1-b. Consequently, improved binding strength between microcrystals and substrates after usage of PEI was observed. Calcination was also thought to be useful after PEI modification.

By combining direct attachment method and secondary growth method, Pham et al. produced uniformly oriented MFI and BEA zeolite films [48].

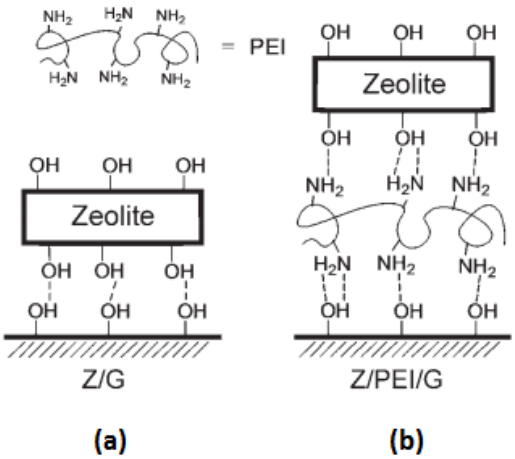


Figure 2.1 Types of bonding effective for the monolayer assembly of zeolite microcrystals on substrate, (a) hydrogen bonding between the surface hydroxy groups of zeolite and glass, and (b) PEI-mediated hydrogen bonding between the surface hydroxy groups of zeolite and glass [47]

Özturk et al. used direct attachment method to form submicron zeolite A monolayer with direct attachment on untreated silicon substrates [49]. The binding strength of the zeolite crystals were enhanced with baking process right after the monolayer formation in a conventional oven at 100°C for 30 min. By the combination of direct attachment and electron beam lithography, they produced oriented Zeolite A thin films of a single zeolite thickness (approximately 250 nm) on silicon wafers without using any chemical linkers on the substrates for the first time [49].

### 2.3 Protein Immobilization on Zeolites

Various methods were introduced for protein immobilization, such as physical adsorption, covalent bonding, entrapment and cross-linking. However, these methods may suffer from some limitations associated with diffusion barriers of the substrates or partial denaturation of enzyme. For this reason, the usage of zeolites

for protein immobilization has drawn a considerable amount of attention. The large specific surface formed by channels/or cavities linked by channels, a variety of shapes and pore sizes of molecular dimensions, adjustable surface charge and hydrophobic/hydrophilic properties together with ion-exchange capacity makes them prominent candidates for immobilization of biomolecules.

In literature, zeolites generally provided enhanced protein activity, increased storage and operational stability [50]. Zeolite parameters studied for protein immobilization are; the effect of zeolite structure, the composition of the zeolite framework, the amount of acidic sites (Si/Al ratio), hydrophilicity, counter ions, and particle size.

The influence of zeolite NaY (FAU) on the activity of horseradish peroxidase in the oxidation of phenol by co-immobilizing zeolite and enzyme in gelatin was studied [50]. They observed increases as large as 100% depending on the conditions of the experiments. They claimed that this result can be explained by the ion exchange of Na-ions of zeolite and protons of enzyme leading to some ionization of OH groups of the enzyme and the change in conformation of the enzyme due to the presence of zeolite.

The effect of zeolite acidity using adsorption of triglycine on Zeolite Y was investigated [51]. They concluded that the amount of acidic sites, which is determined by the amount of $Al^{3+}$, is a significant factor in triglycine adsorption. They showed that as the Si/Al ratio decreases, higher adsorption of enzyme can be obtained. This result was in accord with the results of Krohn and Tsapatsis, for adsorption of phenylalanine on zeolite beta [52].

The impact of zeolite NaY (FAU) on the immobilization of cutinase in sol-gel matrices was studied. They observed an increase in cutinase activity, which can be assigned to the substrate accessibility of enzyme due to presence of zeolite [53].

The influence of zeolite crystals on the immobilization of cytochrome c was also investigated. They used FAU, BEA and MFI framework type of zeolites. In their

study, it was shown that protein immobilization was strongly affected by electrostatic interactions depending on the pH of solution and the isoelectric point of the protein and Brønsted acidity was also effective when different frameworks were used [54].

Recently, pure zeolite membranes (BEA, MFI, FAU and MOR) were synthesized as functional scaffolds for adhesion and growing of fibroblasts. Zeolite membranes favored the cell growth for all zeolite types [55]. Several examples from literature are given below showing the improvement of zeolite modified electrodes in different biosensor applications.

### 2.4 Zeolite Modified Electrodes

The first example of zeolite modified electrode was prepared by Kotte et al. in 1995. In this study, phenolic compounds were detected by a secreen-printed sensor achieved by immobilized tyrosinase coated on a mediator modified carbon electrode containing zeolite particles. The effect of zeolite was explained as a host for positively charged mediator. The obtained electrode showed good sensitivity but long term stability was not achieved [56].

The integration of hydrophilic zeolites in carbon paste with glucose oxidase was investigated using amperometric biosensors. They obtained enhanced sensitivity, extended linear range and higher stability. These improvements in biosensor characteristics were assigned to the microstructure of zeolite providing higher diffusional limitations for the substrate [57].

Modified amperometric electrodes using de-aluminized Y zeolite for glucose oxidase immobilization resulted in high enzyme loading and sensitivity, long-term stability and reproducibility that were attributed to not only the large surface area but also the microenvironment provided by zeolite substrate [58].

An amperometric biosensor was constructed for detection of phenol using layer by layer assembly method. Indium tin oxide (ITO) electrodes were coated with

polycationic PDDA and negatively charged nanozeolite in cycles. When this cycle was repeated N times (nanozeolite/PDDA)$_N$ layers were fabricated. Tyrosinase enzyme was adsorbed by immersing the prepared electrode in enzyme solution. This biosensor displayed high sensitivity and good operational stability that was assigned to high immobilization capacity and biocompatibility of the zeolite assembled layers of enzyme [59].

Natural zeolite clinoptilolite was used for detection of urea using conductometric enzyme biosensors. The properties of high surface area, size and shape selectivity and ion-exchange capacity of clinoptilolite resulted in improved sensitivity and stability of the conductometric biosensor. This result was attributed to the closeness of the high surface area of zeolite to the sensitive electrode surface and the directed transportation of charged species to the electrode surface. Enzyme immobilization was conducted using GA cross-linking [60].

Zeolites for enzyme immobilization in conductometric biosensors based on urease and glucose oxidase was tested for the first time by Soy. et al [61]. Different framework structures of zeolites such as A, Y, silicalite and Beta were studied. Biosensor responses obtained from standard membrane transducer (SMT) involving only glutaraldehyde (GA) cross-linked enzyme and a new approach with zeolite membrane transducer (ZMT) involving both enzyme and zeolite cross-linked together using GA were compared. Using silicalite, all parameters such as zeolite concentration, immobilization time in glutaraldehyde, pH of carrier solution for immobilization of enzymes on zeolites were optimized. And finally they obtained the calibration curves for glucose oxidase and urease. The urease immobilized on silicalite had better performance than immobilized urease without zeolite. They showed that using different zeolites could be alternatives for enzyme immobilization in conductometric biosensor development. Additionally, they hypothesized that the optimum performance from a biosensor can be achieved upon choosing the right zeolite type and tuning its characteristic properties [61].

Urea and butyrylcholine chloride (BuChCl) biosensors were prepared by adsorption of urease and butyrylcholinesterase (BuChE) on heat-treated zeolite Beta crystals, which were incorporated into membranes deposited on ion-sensitive field-effect transistor (ISFET) surfaces. Soy et al. changed the heat treatment conditions of zeolite Beta to compare the Brønsted acid site effects on enzyme adsorption without affecting the size, morphology, overall Si/Al ratio, external specific surface area, and the amount of terminal silanol groups in zeolite crystals. They investigated the effect of Brønsted acid sites i.e., strongly acidic bridging hydroxyl Si–(OH)–Al groups associated with framework aluminum in tetrahedral coordination in enzyme adsorption and in the final biosensor responses. The results showed that the interactions between the enzymes and the Brønsted acid sites of a zeolite support can affect the actual biosensor performances. Zeolites with higher Brønsted acid sites gave better responses and in addition to that result they observed that zeolite membrane transducers always gave better sensitivities compared to standard membrane transducers (without zeolite). These results showed for the first time that it was possible to regulate the ISFET characteristics for two different enzyme- based biosensors by tailoring the electrode surfaces via a simple heat treatment procedure applied to the zeolite crystals incorporated into the electrodes [62].

Kirdeciler et. al used silicalite for producing a zeolite coated transducer (ZCT) and compared with standard membrane transducer (SMT) and zeolite membrane transducer (ZMT) for conductometric biosensor [63]. Different from SMT and ZMT as described before, for ZCT surfaces electrodes were modified by zeolites without any chemical, such as glutaraldehyde vapor. ZCT had fast responses than the others. This result was attributed to GA layer on top of the transducer, which may be considered as a diffusion barrier. In addition to this, enhanced effective spaces of the surface of modified electrodes for enzyme immobilization can be the reason for fast responding. This was the first study showing fabrication route of zeolite coated transducers without any cross-linker for conductometric biosensors for urea analysis. In their study they also showed that increasing Si/Al ratio in

zeolite Beta gave higher responses in both ZMT and ZCT due to increasing hydrophobicity and acid strength [63].

### 2.5 Gold Nanoparticles in Biosensors

Gold nanoparticles have different properties from its bulk size such as; biocompatibility, high surface area, high surface energy and high conductivity. Additionally, gold nanoparticles serve as excellent biocompatible surfaces for the immobilization of enzymes and proteins since the interaction between amino and cysteine groups of proteins with gold nanoparticles is as strong as that of the commonly used thiols [64]. Thus, amino acids and proteins may be directly immobilized on gold nanoparticles without any modification [65]. This makes them ideal choice for biosensors. Crumbliss et al. used colloidal gold as an immobilization matrix for the development of amperometric biosensor to detect glucose. They concluded that enzymes are tightly adsorbed onto gold nanoparticles and these nanoparticles provide a biocompatible surface that is suitable for immobilizing active enzymes onto electrodes. The same enzymes were shown to denature on planar surfaces of gold [66, 67]. Feng et. al expressed that gold nanoparticles can provide mild microenvironment and molecular freedom in orientation [68]. Additionally, gold nanoparticles (5-50 nm) can act as tiny conduction centers leading to a decrease in the electron transfer distance. These are both thought to facilitate electron transfer between the electrode surface and the prosthetic groups of enzyme [68–70]. Despite these advantages, there are only a few articles using gold nanoparticles in the field-effect transistor based biosensors [71-75].

The usage of gold nanoparticles with zeolites as an immobilizing matrix were studied previously for pepsin [76], hemoglobin [77] and recently for polyamine oxidase [78]. They demonstrated that gold nanoparticles and zeolite work synergistically and improve the performance of enzymes such as enhanced activity, pH and temperature stability.

## 2.6 Goal and Objectives

The most important part of a biosensor is its bioselective element. Accordingly, immobilization of biological material onto the transducer surface is the key stage in biosensor development. The goal of this work is to enhance and optimize the zeolite usage in immobilization of bioselective membrane and by this way improving the analytical characteristics of conductometric, amperometric and potentiometric (ISFET based) biosensors.

The main motivation of this thesis was to eliminate the classically used toxic chemicals (glutaraldehyde) and develop an enhanced method of bioselective interface using environmentally friendly and less costly zeolites for reusable, inexpensive, and portable biosensors. These biosensors aim to obtain sensitive, rapid, reliable, stable and reproducible data with respect to traditional glutaraldehyde cross-linking method.

To be able to use zeolites as enzyme adsorbents, two methods were developed and optimized for their specific use as bioselective element in all three biosensors. These methods are called as drop-coating and PEI coating. The developed methodologies enabled one to investigate the biosensor performances on well-organized and controlled zeolite mono/multilayer covered electrode surfaces for enzyme immobilization

In this thesis, firstly, drop-coating method for zeolites was optimized for improved analytical characteristics of urea sensitive conductometric biosensor such as reproducibility, inter-reproducibility and operational stability. The optimized drop-coating method was compared with other methods of immobilization, and the created biosensors were tested for urea analysis in real samples such as blood serum for the first time. Next, the zeolite thin films produced by PEI coating method were examined for the optimization of amperometric biosensors to determine glucose. ISFET based biosensors to determine urea were also optimized using PEI coating method. Furthermore, drop-coating method for zeolite usage as enzyme adsorbent

was adapted for ISFET based biosensors in creatinine determination. Moreover, zeolite coating methods; both drop-coating and PEI-coating were also compared. Additionally, effect of zeolite framework, particle size and the presence of gold on zeolites were investigated to improve the analytical characteristics of drop-coated zeolite modified ISFET based biosensors.

For all these studies, three enzymes were used in the development of biosensors: Urease for conductometric and ISFET biosensors, glucose oxidase (GOx) for amperometric biosensors and finally creatinine deiminase for ISFET based biosensors.

After all of this, the developed silicalite coated conductometric biosensor was tested in serum blood. By this way, developed biosensors found daily, real time application by these current studies.

# CHAPTER 3

# EXPERIMENTAL PROCEDURE

## 3.1 Synthesis of Zeolites and Zeolite Modified Electrodes

### 3.1.1 Zeolite Synthesis

#### 3.1.1.1 Silicalite

The gel composition for hydrothermal synthesis of silicalite crystals is 1TPAOH:4TEOS:350$H_2O$. The structure directing agent used was tetrapropylammonium hydroxide (TPAOH) and the silica source was tetraethyl orthosilicate (TEOS). TEOS was added to TPAOH solution under vigorous stirring. The mixtures were aged at room temperature for 6 hours. The gel was introduced into Teflon-lined autoclaves for crystallization. Static synthesis was carried out at 125°C for 24 hour. The crystals were centrifuged at 7500 rpm and dried overnight at 50°C.

The synthesized silicalite crystals (Sil) were calcined at 550°C for 6 hours at a rate of 1°C/min in air to remove the template and open the pores. After this procedure, it is referred as Cal-Sil.

#### 3.1.1.2 Beta (BEA)

Optimized molar composition of the gel used for the hydrothermal synthesis of zeolite beta (BEA) is 1.92 $Na_2O$ : 1 $Al_2O_3$ : 60 $SiO_2$ : 444 $H_2O$ : 4.6 $(TEA)_2O$. The mixture of sodium aluminate, sodium hydroxide, and distilled water was stirred for 40 min in a high-density polyethylene (HDPE) bottle, then placed in an oven at 100°C for 50 min to form alumina precursor solution. Tetraethyl ammonium

hydroxide (TEAOH) as structure directing agent was added to the cooled mixture and stirred for 15 min. Finally, Ludox HS-40 colloidal silica as source of silica was added into the prepared precursor solution and mixed for 15 min. The resulting mixture was introduced into Teflon-lined autoclaves for crystallization. Static synthesis was carried out for 7 days at 120°C. Product was centrifuged at 7500 rpm and dried overnight at 50°C. The synthesized BEA was calcined at at 550°C for 6 hours at a rate of 1°C/min in air atmosphere to remove the template and open the pores. After this procedure, it is referred as Cal-BEA.

#### 3.1.1.2.1 Ion Exchange of BEA with $Au^{3+}$

The ion exchange of BEA was done by slight modification of the procedure found in the literature [79]. The synthesized beta was calcined at 500°C in air for 6 hours before ion exchange procedure. 400 mg of calcined BEA was added to 2.33 mM Au(III)chloride solution for obtaining gold ion exchanged BEA samples (Au(III)BEA) according to maximum theoretical loading of 4 wt.% Au at 50°C with stirring. After 24 h, obtained Au(III)BEA samples were washed and centrifuged for four times at 7500 rpm. Following this, the samples were dried at 50°C under ambient air.

#### 3.1.1.2.2 Reduction of $Au^{3+}$-Ion Exchanged BEA

Gold ion reduction from Au(III)BEA was performed at 50°C in sodium borohydride (3.4mM) suspension and called as BEA-Gold. The reduction step was terminated when the hydrogen gas formation was finished. BEA-Gold samples were washed and centrifuged for four times at 7500 rpm and dried at 50°C.

### 3.1.1.3 Nano BEA

The aim of this synthesis was to obtain zeolite BEA with significant reduction in particle size (~100nm). Molar composition of the nano beta (nano BEA) is 0.25 $Al_2O_3$ : 25 $SiO_2$ : 490 $H_2O$ : 9 TEAOH [80]. Silica source was TEOS. Aluminum isopropoxide, TEAOH, and distilled water were used as the other reactants. Aging

was continued under static conditions for 4 hours with a clear solution. Crystallization was completed within 14 days under static conditions at 100°C in Teflon-lined autoclaves. Product was purified by using centrifugation at 7500 rpm. The synthesized nano BEA was calcined at at 550°C for 6 hours at a rate of 1°C/min in air to remove the template and open the pores. After this procedure, it is referred as Cal-Nano BEA.

### 3.1.2 Preparation of Zeolite Modified Electrodes

Conductometric, amperometric and potentiometric (ISFET based) biosensors were developed using zeolites as enzyme adsorbents and compared with the conventional method of enzyme immobilization; i.e., cross-linking using glutaraldehyde (GA) vapor. However, zeolites are in powder form upon synthesis. In order for them to be used in applications, it is of vital importance to coat them onto surfaces of interest in a controlled manner. Accordingly, for them to be tested as enzyme adsorbents in biosensor applications, the most efficient methodology was needed to be investigated to coat them onto the surface of transducers. For this purpose, two different procedures were applied to obtain zeolite coated electrodes; drop-coating of zeolites and zeolite attachment with polyethylenimine (PEI) coating.

#### 3.1.2.1 Drop-Coating

Before enzyme immobilization to electrodes, the gate areas of the transducers were coated with different types of zeolites using reported method [63] as illustrated in Figure 3.1. The transducers produced by drop coating method were named as drop-coated zeolite modified transducer (DZMT).

As seen from Figure 3.1, in the case of drop coating, 10 % (w/w) zeolite suspension in 5 mM phosphate buffer, pH 6.5 was used for urea and GOx biosensors while pH 7.4 was used for creatinine deiminase biosensor. This suspension was ultrasonicated for at least 20 min. Then about 0.2 µl of suspension was deposited onto the active zone of working and reference electrodes, whereas 0.4 µl of suspension was deposited onto all active zones of amperometric multitransducer. Afterwards they were heated to 200°C and kept at that temperature for 6 min to assemble conductometric biosensors, whereas 150°C and 3 min were chosen for amperometric biosensors. ISFET based biosensors were fabricated using 120°C and 15 min duration. The temperature and duration were optimized according to the used electrodes; since exceeding mentioned conditions damaged the electrodes. The procedures resulted in coating transducer surfaces with a layer of zeolite particles.

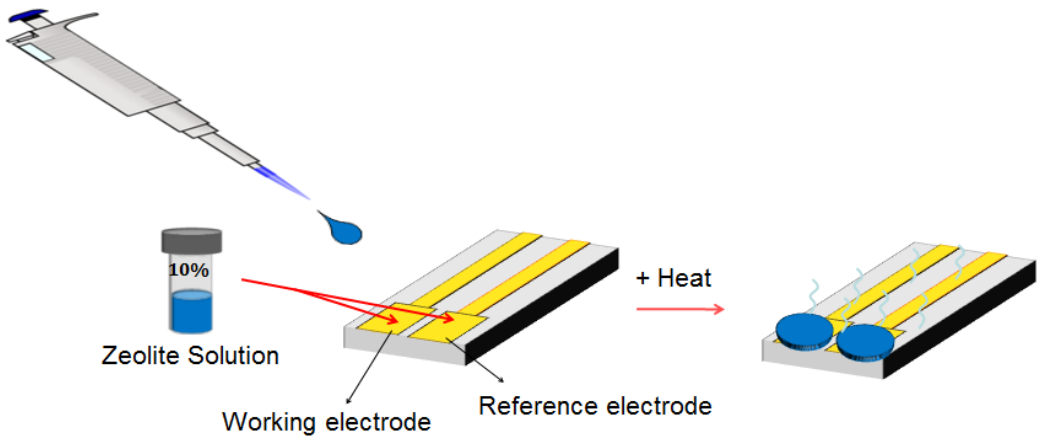


Figure 3.1 Creation of drop-coated zeolite modified transducer, DZMT

#### 3.1.2.2 Polyethylenimine (PEI) Coating

Polyethylenimine (PEI) is a positively charged polymer, which is composed of amino groups. Depending on the synthesis and modification methods which change their physical and chemical properties; they can have different architectures such as linear, branched, comb, network and dendrimer [81]. In this study, a branched PEI (MW ~ 800) was used as a linker between zeolite and transducer surface before zeolite attachment. In this way, it was aimed to control the thickness of the zeolite layer. For optimization of PEI coating conditions, silicon wafers were used instead of transducer surfaces.

The effect of PEI solvent (hot distilled water or ethanol), PEI concentration (10%, 6%, 1% (v/v) PEI in ethanol), spin coating time (15s, 7s) and calcination temperature (150°C, 100°C, 50°C) on direct attachment of zeolites on silicon wafer were investigated. In order to solve the homogeneity problem, mucasol, which is generally used to alter the surface hydrophobicity, was used before the PEI modification step. For that purpose, the surfaces were drop-coated with mucasol (1/6, v/v) in distilled water for 15 min. Afterwards, mucasol treated surfaces were rinsed with copious amount of water and dried in air. After mucasol treatment, 0.5% (v/v) PEI was spin coated to silicon wafers at the optimized conditions such as 3000 rpm for 15 s and calcination at 90°C for 30 min. Finally, the synthesized zeolites were directly attached to the obtained surfaces simply by rubbing zeolites with a finger, a technique called direct attachment. These methods were used on electrode surfaces to develop zeolite coated transducers to use in further biosensor studies. The transducers produced by this method were named as PEI-coated zeolite modified transducer (PZMT).

#### 3.1.2.3 Enzyme Immobilization on Zeolite Modified Electrochemical Transducers

Enzyme immobilization was achieved by physical adsorption of enzymes onto the zeolite modified transducer surfaces by either of the methods described above; i.e.,

DZMT or PZMT. The only other method used frequently is the covalent attachment method, which involves the usage of GA as a cross-linker. The transducers developed using GA as a cross-linker were called as standard membrane transducers (SMT). General scheme of produced electrodes are given in Figure 3.2.

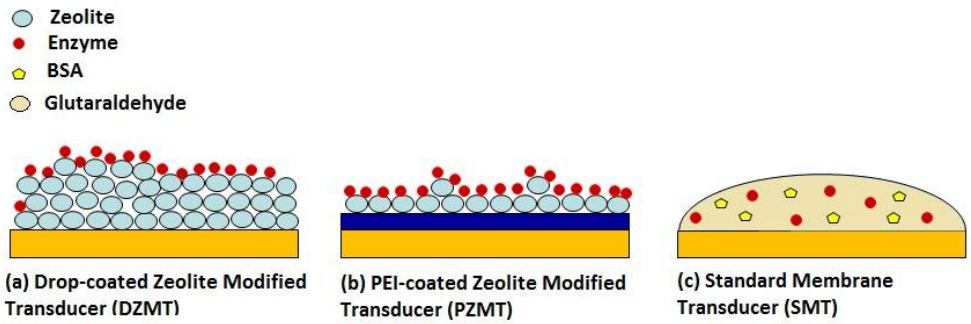


Figure 3.2 Schematic representation of transducers; (a) Drop-coated Zeolite Modified Transducer (DZMT)), (B) PEI-coated Zeolite Modified Transducer (PZMT), (C) Standard Membrane Transducer (SMT)

To produce the enzyme membrane on zeolite modified transducers, 5% (w/w) enzyme solution in 20 mM phosphate buffer (pH 6.5 was used for conductometric and amperometric biosensors while pH 7.4 was used for ISFET based biosensors) was prepared. To obtain the reference membrane for conductometric and ISFET based biosensors 5% BSA solution in 20 mM phosphate buffer was prepared, for holding the protein amount constant. A constant amount of enzyme solution was deposited onto the working electrode, which is covered with zeolite; whereas BSA solution without enzyme was deposited onto the reference electrode. After immobilization, the transducers were dried in air and washed in buffer for 10-15 min to discard the unbounded enzymes. Before measuring, the sensors with deposited biomaterial were kept in the working buffer until a stable signal baseline

is obtained. In this procedure of enzyme adsorption, neither glutaraldehyde nor other auxiliary compounds were used as in the case of GA cross-linking.

As a distinction from the above procedure for creatinine deiminase biosensors, working solution was containing 10% CD (w/w) solution in 20 mM phosphate buffer with 10% glycerol, 4% lactitol, 0.4 % DEAE-Dextran and the reference solution was containing 10% BSA instead of CD at a pH of 7.4. The rest of the previously mentioned procedures were the same.

After experiments, surfaces of transducers were cleaned from zeolite particles and adsorbed enzyme using ethanol-wetted cotton.

## 3.2 Biosensor Set up

### 3.2.1 Conductometric Biosensors

#### 3.2.1.1 Materials

Enzyme urease (EC 3.5.1.5) with specific activity of 66.3 U/mg from Fluka was used in conductometric biosensor studies. Glycerol, bovine serum albumin (BSA, fraction V), 50% aqueous solution of glutaraldehyde solution and urea were provided from Sigma-Aldrich Chemie. All chemicals were of analytical grade and used as received without additional purification.

#### 3.2.1.2 Enzymatic Reaction

The conductometric biosensor based on urease immobilization function according to the enzymatic reaction as shown below:

$$\begin{matrix} H_2N \diagdown \\ \\ H_2N \diagup \end{matrix} C = O + 2H_2O + H^+ \xrightarrow{\textit{Urease}} 2NH_4^+ + HCO_3^- \qquad (3.1)$$

Urease decomposes urea to ammonium and bicarbonate. This reaction results in changes of the conductivity in the near electrode layer of the solution that can be

registered by conductometric transducer. These changes and consequently the responses of biosensor are proportional to the urea concentration.

#### 3.2.1.3 Sensor Structure and Data Measurement

Conductometric transducers were manufactured in V. Lashkaryov Institute of Semiconductor Physics of National Academy of Science of Ukraine (Kyiv, Ukraine). They consisted of two identical pairs of gold inter-digitated electrodes deposited onto a ceramic support obtained by vacuum deposition as presented in Figure 3.3-a. They were 5 x 30 $mm^2$ in size and the sensitive area of each electrode was about 1.0 x 1.5 $mm^2$. The width of each digit and the interdigital space was 20 μm.

A portable conductometric analyzer (Figure 3.3-b) developed in the Institute of Electrodynamics of National Academy of Science of Ukraine (Kyiv, Ukraine) was used to determine changes in conductivity in the near electrode buffer layer with a pair of electrodes (working and reference) of each conductometric transducer. This device applied a sinusoidal potential with a frequency of 36.5 kHz and amplitude of 14 mV, avoiding such effects as faradaic processes, double-layer charging, and polarization of the microelectrodes. The nonspecific changes in the output signal induced by the fluctuations of temperature, medium pH, etc. were decreased due to the usage of differential mode of measurement. Conductivity of solution measured by the reference electrode was subtracted from the conductivity measured by the electrode with biorecognition element (working electrode). Illumination and temperature variations had practically no influence on the biosensor characteristics.

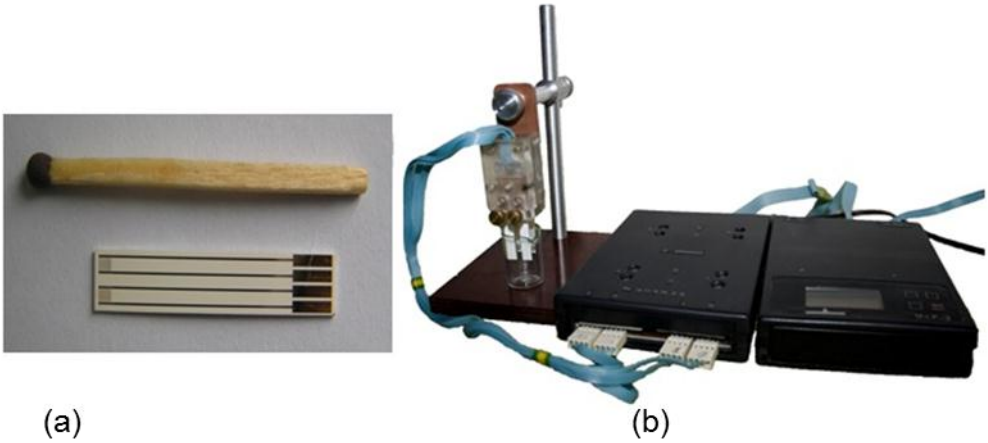


Figure 3.3 Overall view of a) conductometric transducer and b) portable conductometric analyzer

The measurements were carried out in a glass cell filled with 5 mM phosphate buffer at pH 6.5 under vigorous magnetic stirring. The substrate concentration in the cell was specified by the addition of different aliquots of the substrate stock solutions to the working buffer solution. Experiments were performed for at least three repetitions.

Drop-coated zeolite modified transducers (DZMT) were developed as described in Chapter 3.1.2.1 and urease was immobilized onto these DZMT as it was explained in Chapter 3.1.2.3 Obtained transducers were compared with the other methods of urease immobilization in biosensorics such as: GA vapor (SMT) GA drop, urease adsorption on nitrocellulose and photopolymerization in PVA/SbQ. These methods were applied to be able to find the most appropriate method for enzyme immobilization to improve the analytical characteristics of the obtained biosensors.

#### 3.2.1.4 Urease Immobilization in GA vapor

5% (w/w) urease, 5% BSA and 10% glycerol in 20 mM phosphate buffer at a pH of 6.5, was used for urease immobilization on working electrode surface. Urease was replaced by BSA for the preparation of reference membrane for which the rest of the conditions were kept identical. After deposition of 0.15µl of both solutions

onto the working and reference electrode seperately, surfaces were placed in saturated GA vapor as illustrated in Figure 3.4 for 30–35 min and then dried for 15 min in air at room temperature. Afterwards, the transducers were submerged into the working buffer for 20–30 min to wash off the unbounded enzyme and GA excess. By this way standard membrane transducers (SMT) were developed.

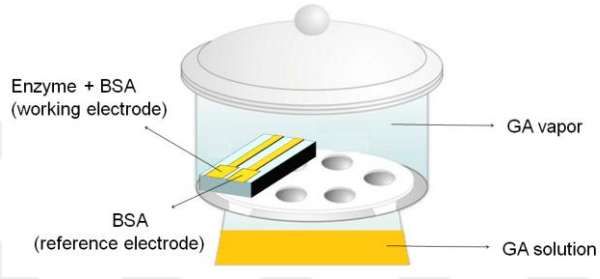


Figure 3.4 Schematic representation of enzyme immobilization in GA vapor

### 3.2.1.5 Urease immobilization in GA drop

To prepare working membranes by immobilization in GA drop, urease (10%, w/w) and BSA (10%) in 20 mM phosphate buffer at a pH of 6.5, which is mixed with 20% glycerol was used. The mixture for reference membrane was prepared in an analogous way, except that urease was replaced by BSA (20%). Both solutions were mixed with 2% (w/w) aqueous solution of glutaraldehyde at ratio of 1:1, prior to the deposition onto the surface of transducer. Immediately, 0.15 µL of the prepared mixtures was deposited onto the transducers by using a pipette to let a full coverage of the working surfaces of conductometric inter-digitated electrodes and dried for 45 min in the air at room temperature. Dry membranes were submerged in the working buffer for 30 min to wash-out the unbounded enzyme and excess GA.

#### 3.2.1.6 Urease immobilization on Nitrocellulose

The method of urease adsorption on nitrocellulose was elaborated and described in detail in [82]. For my experiments, the concentration of nitrocellulose in source solution was taken as 1% instead of 5% as suggested by Yin et al. [82], since substantial decrease in transducers sensitivity was observed at 5% concentration.

For this method, nitrocellulose (1%, w/v) and 3-glycidoxypropyltrimethyoxy-silane (GPTS) (4%, v/v) were dissolved in acetone. Distilled water was added to this mixture of nitrocellulose and GPTS, after nitrocellulose had completely dissolved in the solution overnight upon shaking. The mixture was spin-coated after 2 hours of shaking. Finally, the sensor was carefully dried at 60ºC for 30 min.

After the modification of the surface of transducer with nitrocellulose, 0.15 µL of enzyme solution (5% urease in 20 mM phosphate buffer, pH 6.5) was dropped on one pair of electrode, while the other electrode was coated with 0.15 µL of reference solution (5% BSA in 20 mM phosphate buffer, pH 6.5). Next, the transducers were dried and washed in working buffer.

#### 3.2.1.7 Urease Photopolymerization in PVA/SbQ

Immobilization of urease by photopolymerization in PVA/SbQ (poly(vinyl alcohol) containing styrylpyridinium) was conducted in accordance with the procedure presented in [83]. To form the bioselective membrane, one of the electrodes was drop-coated with 0.3 µl of 5 mM PBS at a pH of 6.5, which contained 2.5% of urease, 25% of PVA/SbQ, and 10% of glycerol; while 0.3 µl of the identical solution with the exception of 2.5% of BSA instead of urease was drop-coated onto the reference electrode. Then, the transducer was exposed to irradiation with UV lamp for 30 min for allowing the membrane formation.

### 3.2.2 Amperometric Biosensors

#### 3.2.2.1 Materials

Glucose oxidase (GOx, EC 1.1.3.4) from Aspergillus niger with an activity of 272 U/mg (Genzyme, UK) was used in bioselective element of biosensors. Bovine serum albumin (BSA, fraction V), glucose, glycerol, ascorbic acid, HEPES, and 50% aqueous solution of glutaraldehyde (GA) were received from Sigma-Aldrich Chemie (Germany). All other chemicals were of analytical grade.

#### 3.2.2.2 Enzymatic Reaction

The operation of amperometric biosensor for glucose determination is based on the enzymatic reaction with consequent hydrogen peroxide oxidation on the working electrode, which occurs upon applying necessary potential and direct registration of this data by the amperometric transducer. The biosensor response is proportional to the glucose concentration. In the presence of glucose, the reaction taking place on the electrode surface is as follows:

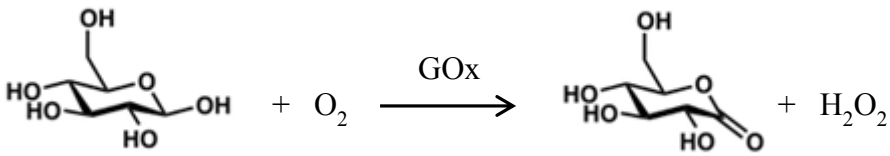


(3.2)

β-D-glucose D-glucono-1,5 -lactone

$$H_2O_2 \xrightarrow{+1000\ mV} 2H^+ + 2e^- \qquad (3.3)$$

The obtained biosensor response using immobilized glucose oxidase is proportional to the glucose concentration.

#### 3.2.2.3 Sensor Structure and Data Measurement

A three-electrode scheme of amperometric analysis was used. The working amperometric transducers were developed, which were connected to the PalmSens potentiostat (Netherlands) along with the auxiliary nickel electrode (with a much larger area of the nickel surface compared to the working electrode) and the Ag/AgCl reference electrode as presented in Figure 3.5. Each electrode has its own function in the amperometric analysis. When positive potential is applied to the working electrode, all the solution molecules on the electrode surface are oxidized and an electron transition from the solution to the electrode takes place. If there was no additional electrode, a large potential difference would be generated due to the stoichiometric imbalance. The function of the auxiliary electrode is to form the external circuit providing the electrons their pathway back to the solution. Obviously, this results in the reduction process on the auxiliary electrode, equivalent to the oxidation process on the working electrode. This flow of electrons generates a current in the amperometric sensor. The third electrode is a reference electrode, which should contain a known chemical compound that includes both forms of the redox pair. Usually it is either $Hg/HgCl_2$ (saturated calomel electrode) or Ag/AgCl (chloro-silver electrode). Since the applied potential is fixed, the reference electrode has a stable point, which can be used by the working electrode for measurement. That is, the applied potential is controlled between the working and reference electrodes, whereas the current is measured between the working and auxiliary electrodes [11]. For the development of planar amperometric multisensor, the design having four working electrodes, one reference and one auxiliary electrode was chosen as presented in Figure 3.5.

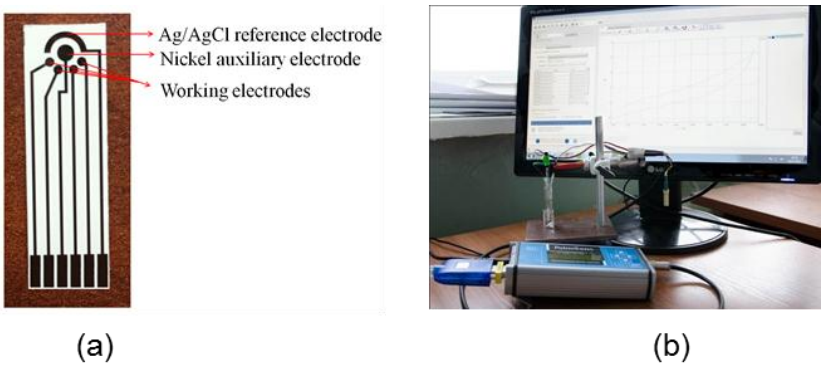


Figure 3.5 The photograph of (a) amperometric transducer and (b) measuring device

Measurements were carried out in 20 mM HEPES at a pH of 7.4, using voltamperometric mode at a constant potential of +1 V vs Ag/AgCl reference electrode in an open cell under vigorous stirring. The substrate concentration in the measuring cell was specified by the introduction of aliquots of the substrate standard stock solution to the working buffer. All experiments were performed for at least three series.

Drop-coated zeolite modified transducers (DZMT) were developed as described in Chapter 3.1.2.1 and PEI-coated zeolite modified Transducers (PZMT) were developed for glucose determination according to Chapter 3.1.2.2. GOx was immobilized on these transducers as it was explained in Chapter 3.1.2.3. Standard Membrane Transducers (SMT) were also developed and explained in the following chapter.

### 3.2.2.4 Glucose oxidase immobilization in GA vapor

5% (w/w) GOx, 5% BSA, 10% glycerol was prepared in 20 mM phosphate buffer at a pH of 7.2. This mixture was deposited onto the transducer until the working surface was covered completely. All membrane mixture contained the same total amount of protein for which the volume of each membrane was about 0.05µl.

### 3.2.3 ISFET based Biosensors

#### 3.2.3.1 Urea Determination

##### 3.2.3.1.1 Materials

Enzyme urease (EC 3.5.1.5) with specific activity of 66.3 U/mg from Fluka was used in conductometric biosensor studies. Glycerol, bovine serum albumin (BSA, fraction V), 50% aqueous solution of glutaraldehyde solution and urea were provided from Sigma-Aldrich Chemie. Potassium-phosphate buffer solution ($KH_2PO_4$-$Na_2HPO_4$) was used for working buffer. All chemicals were of analytical grade and used as received without additional purification.

##### 3.2.3.1.2 Enzymatic reaction

The functioning of ISFET-based urea biosensor using urease is based on the reaction of urea cleavage to ions $NH_4^+$ with the consumption of protons as shown in Chapter 3.2.1.2, equation 3.1. This reaction results in the change of the pH inside the selective membrane, which can be recorded by pH-sensitive field effect transistors.

##### 3.2.3.1.3 Sensor Structure and Data Measurement

pH-sensitive field-effect transistors and the measuring device used in the current study presented in Figure 3.6 were fabricated at Lashkarev Institute of Semiconductor Physics of National Academy of Sciences of Ukraine (Kyiv, Ukraine) and the detailed information can be found in [15] and [84] respectively.

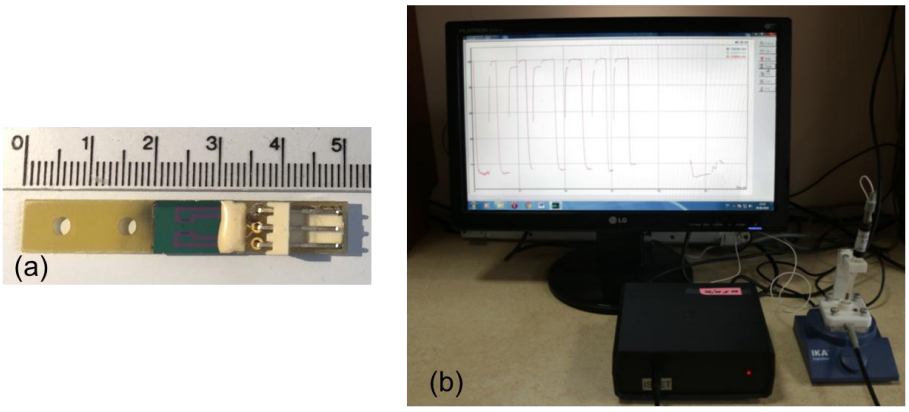


Figure 3.6 The photograph of (a) pH- sensitive field effect transistor and (b) measuring device

Basically, the potentiometric biosensor has a differential pair of two identical p-channel field-effect transistors placed on a single crystal with the total area of 8 x 8 $mm^2$. Usage of two transistors provides being able to work in differential mode to avoid the changes associated with the fluctuations in temperature, environmental pH, and electrical noise. The gate of the dielectric layer was formed from $SiO_2$ and $Si_3N_4$ films. The transconductance of the ISFETs measured in phosphate buffer with Ag/AgCl reference electrode was 400-500 μA/V and pH-sensitivity of the transistor was approximately 40 mV/pH, thus providing pH-sensitivity of the transistor channel current of 15-20 μA /pH.

Measurements were conducted in 5 mM phosphate buffer at a pH of 7.4 under stirring at room temperature. The substrate concentration in the cell was specified by the addition of different aliquots of the substrate stock solutions to the working buffer.

Non-specific changes in the output signal associated with fluctuations of temperature, medium pH, and applied voltage were compensated by using differential mode, i.e. measurement of the difference between the signals from two

pH-FET electrodes (with enzyme and reference membranes), placed onto the same transducer. All experiments were performed for at least three times.

The development of PEI-coated zeolite modified transducers (PZMT) for urea determination and the immobilization technique of urease onto these transducers were explained in Chapter 3.1.2.2 and 3.1.2.3, respectively. Standard membrane transducers (SMT) were also developed and explained in the following chapter.

#### 3.2.3.1.4 Urease immobilization in GA vapor for ISFET based biosensor

The enzyme membrane consists of 5% (w/w) urease, 5% BSA and 10% glycerol in 20 mM phosphate buffer at a pH of 7.4 for urease immobilization on working electrode surface. Urease was replaced by BSA for the preparation of reference membrane for which the rest of the conditions were kept identical. After deposition of 0.15µl of both solutions onto the working and reference electrode seperately, surfaces were placed in saturated GA vapor for 30–35 min and then dried for 15 min in air at room temperature. Afterwards, the transducers were submerged into the working buffer for 20–30 min to wash off the unbounded enzyme and excess GA.

### 3.2.3.2 Creatinine Determination

#### 3.2.3.2.1 Materials

Creatinine deiminase (EC 3.5.4.21) with an activity of 36 U/mg was purchased from Sigma-Aldrich; bovine serum albumin (BSA) (fraction V), 25 % aqueous solution of glutaraldehyde and creatinine were purchased from Sigma–Aldrich Chemie; DEAE-Dextran and lactitol were purchased from Fluka. The working phosphate buffer ($KH_2PO_4$-NaOH), was prepared at a pH of 7.4 from reagents obtained from Helicon. Other non-organic compounds used were of analytical grade.

The samples of blood serum for the measurements of creatinine content were obtained from Kiev municipal scientific and practical center of nephrology and hemodialysis.

#### 3.2.3.2.2 Enzymatic reaction

When elaborating biosensors for creatinine determination, the enzyme creatinine deiminase (CD) was used. These biosensors function due to the enzymatic reaction of:

$$\text{Creatinine} + H_2O \xrightarrow{\text{Creatinine deiminase}} \text{N-methylhydantoine} + NH_4^+ \qquad (3.4)$$

The pH changes induced due to creatinine hydrolysis are proportional to the substrate concentration in the tested solution and are registered by the pH-sensitive field-effect transistors with corresponding enzymatic membranes.

#### 3.2.3.2.3 Sensor Structure and Data Measurement

pH-sensitive field-effect transistors and the measuring device for urea determination described in Chapter 3.2.3.1.3 were also used in this study to measure creatinine concentration.

Measurements were conducted in 5 mM phosphate buffer at a pH of 7.4under stirring at room temperature. The substrate concentration in the cell was specified by the addition of different aliquots of the substrate stock solutions to the working buffer.

The development of drop-coated zeolite modified transducers (DZMT) for creatinine determination and the immobilization technique of creatinine deiminase onto these transducers were explained in Chapter 3.1.2.1 and 3.1.2.3, respectively. Standard membrane transducers (SMT) were also developed and explained in the following chapter.

#### 3.2.3.2.4 Creatinine deiminase immobilization in GA vapor

Working solution was prepared using 10% CD and 10% BSA in 20 mM phosphate buffer (pH 7.4) containing 10% glycerol, 4% lactitol, 0.4% DEAE-Dextran. In reference solution, instead of enzyme, 20% BSA was used to hold the protein concentration constant. BSA was used both for providing amino groups for crosslinking and also for stabilization of enzymes. Lactitol and DEAE-Dextran were used as enzyme stabilizers. The latter and glycerol were also used to prevent the membrane from being cracked which was believed to provide better adhesion to ISFET surfaces.

0.1µl of working solution was deposited to one fragment of the transducer and 0.1 µl of reference solution was deposited on the other side of the transducer. These transducers were exposed to saturated glutaraldehyde vapor for 15 min and dried at ambient air for 15 min. Finally, they were washed with buffer solution to remove the unbound protein and excess glutaraldehyde.

## 3.3 Material Characterization

Synthesized and calcined zeolites were characterized by using X-Ray Diffraction (XRD), Scanning Electron Microscopy (SEM), Multipoint BET and Zeta potential analysis. Scanning Transmission Electron Microscopy (STEM), Inductively Coupled Plasma Optical Emission Spectrometry (ICP-OES), X-ray photoelectron spectroscopy (XPS) analysis were conducted on ion exchanged and reduced BEA-Gold samples. Atomic Force Microscopy (AFM) and cross sectional SEM images were taken from zeolite coated silicon wafers. All characterization studies were done at METU Central Laboratory.

### 3.3.1 X-Ray Diffraction (XRD)

X-ray diffraction measurements for phase identification were obtained by a Rigaku Ultima IV X-Ray diffractometer using Cu-Kα radiation. The voltage and current of the X-ray beam were 40 kV / 30 mA, respectively. The diffraction peaks were

scanned between 5-40° 2θ degrees with a scan speed of 1°/min. Time constant was 1s, and slit was 0.2 mm.

### 3.3.2 Scanning Electron Microscopy (SEM)

Morphological properties and particle sizes of synthesized zeolites were examined by FEI Quanta 400F field emission scanning electron microscope, operated at 30 kV. The energy dispersive X-ray spectroscopy (EDX) analysis of all samples was carried out to determine crystal Si/Al ratios utilizing a Phoenix EDAX X-ray analyzer equipped with Sapphire super ultrathin window detector attached to the Hitachi S-4700 FE-SEM (accelerating voltage 12 kV, beam current 10 μA.

### 3.3.3 Scanning Transmission Electron Microscopy (STEM)

High-angle annular dark-field (HAADF) STEM images of gold-BEA zeolite was obtained with a JEM JEOL 2100F electron microscope equipped with a field emission gun and operated at 200 kV with a STEM detector. This observation was coupled with EDX investigations for elemental analysis using Oxford EDS. The sample was added to ethanol solution and sonicated before dropping onto the copper grid.

### 3.3.4 Particle Size Analysis

Particle size analysis of zeolite BEA was performed by Malvern Mastersizer 2000. The powder sample was dispursed in distilled water and sonicated during analysis. The particle size of other zeolites were measured from SEM images.

### 3.3.5 Surface Area Analysis

The nitrogen adsorption/desorption experiments were carried out at by Autosorb 6 series (Quantachrome Instruments) instrument. The surface area of the samples was obtained by Multipoint BET method, while external surface area was obtained by t-plot method. Sample preparation method includes outgassing samples under vacuum at 300°C for 4 h before analysis.

### 3.3.6 Zeta Potential

The zeta potential of zeolites were obtained by Malvern, Nano ZS90 at 25°C. The particles were dispersed in buffer solution at pH 7 (solid loading was 1 wt %) and ultrasonicated for 1 h before measurement.

### 3.3.7 Inductively Coupled Plasma Optical Emission Spectrometry (ICP-OES)

Inductively Coupled Plasma Optical Emission Spectrometry (ICP-OES) was used for elemental analysis of BEA and BEA-Gold using Perkin Elmer Optima 4300DV.

### 3.3.8 X-ray Photoelectron Spectroscopy (XPS)

X-ray photo-electron spectroscopy (XPS) analysis was carried out on a PHI 5000 VersaProbe spectrometer with an Al-Kα radiation source. The binding energies were referenced to the internal standard C 1s binding energy at 284.5eV.

### 3.3.9 Contact Angle Measurement

Contact angles, Θ, were measured from electrode surfaces using static sessile water drop method with an Attension Theta goniometer. At least 5 measurements were made for each sample and the measurements were taken immediately after the drop had been deposited onto the surface. The average angle was calculated by using the OneAttension software from both the left and right sides of the droplet. The standard error in Θ was approximately ±2°.

### 3.3.10 Atomic Force Microscopy (AFM)

Atomic force microscopy was performed in air on a Veeco MultiMode V AFM operated in tapping mode. A silicon tip was used with a scan rate of 1-2 Hz. For AFM measurements, zeolite coated silicon wafers were used.

# CHAPTER 4

# RESULTS AND DISCUSSIONS

## 4.1 Synthesis and Characterization of Zeolites

Different types of zeolites were used for different types of biosensors, since each biosensor type was operating based on different mechanisms. Thus, their effect on biosensor responses were investigated separately. The two major zeolite types used for developing zeolite modified electrochemical biosensors in this study were silicalite and zeolite beta. The reason for this choice is based on the fact that silicalite has no $Al^{3+}$ whereas zeolite beta contains $Al^{3+}$ in their framework. This creates an imbalance in the overall electronegativity and hydrophilicity of the zeolite structures, which was thought to have an effect on biosensor performances. The results are explained as follows:

### 4.1.1 Silicalite

XRD patterns of silicalite and Cal-Sil are shown in Figure 4.1. The characteristic diffraction peaks of silicalite at 7.8, 8.8 and 23.1º 2θ, correspond to (101), (020) and (501) reflections, respectively. These were found to be in accordance with the literature data [85], (JCPDS #48-0136 card) indicating successful formation of silicalite crystals. Accordingly, silicalite was the unique crystalline phase and XRD analysis of calcined silicalite particles indicate no change in phases upon calcination.

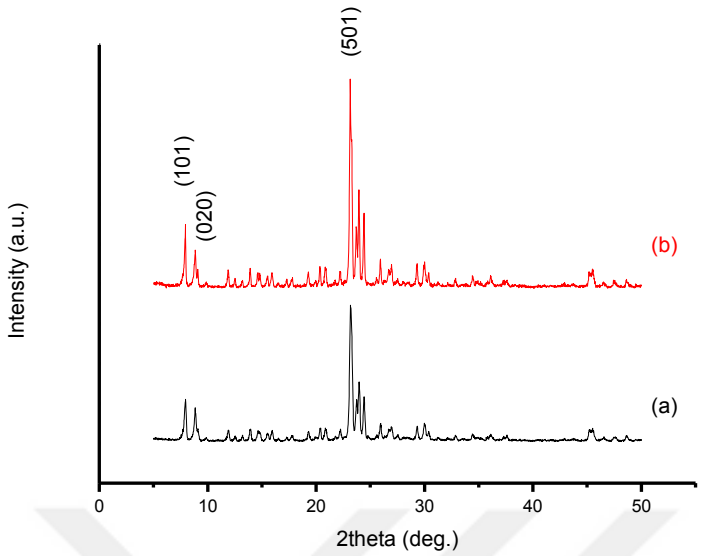


Figure 4.1 XRD patterns of synthesized Silicalites: a) Silicalite and b) Cal- Sil

The particles were also examined by scanning electron microscopy to obtain information about the morphology and particle sizes as shown in Figure 4.2. The crystal morphology for silicalite was shown to be more of a round plate shape of around 470 nm length and 250 nm thickness with smooth surface morphology. Additionally, it was observed that the calcination procedure has no effect on the morphology of silicalite crystals (Figure 4.2-b).

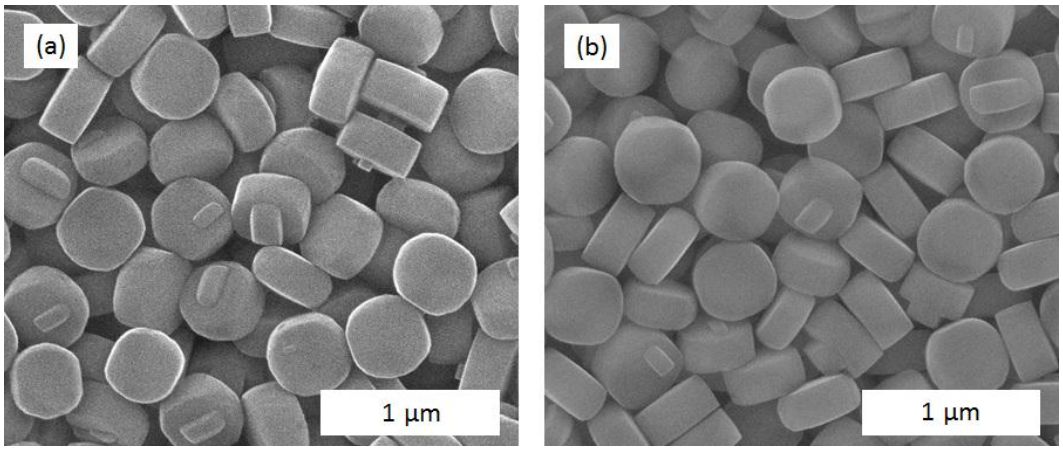


Figure 4.2 SEM images of silicalite crystals a) Silicalite, and b) Cal-Sil

The measured physical properties of silicalite samples are tabulated in Table 4.1. Accordingly, a variation in surface area and pore volume along with particle size could be achieved by using calcination procedure. The surface area of silicalite was determined to be 185 $m^2/g$, external surface area was found as 52 $m^2/g$ while pore volume was 0.08 cc/g. There was an increase in the surface area, external surface and pore volume after calcination of silicalite due to the removal of template.

Table 4.1 Physical properties of silicalite crystals

| Sample Name | Si/Al[a] | Part.size[b] (nm) | $S_{BET}$ [c] ($m^2/g$) | $S_{EXT}$[d] ($m^2/g$) | Pore Volume[e] (cc/g) |
|---|---|---|---|---|---|
| Silicalite | ∞ | 470 | 185 | 52 | 0.08 |
| Cal-Sil | ∞ | 470 | 447 | 96 | 0.18 |

a Measured by EDX
b Measured by SEM
c Measured by Multipoint BET .
d Measured by t-plot Method.
e Measured by Saito-Foley (SF) Method

### 4.1.2 BEA

XRD patterns of BEA, calcined form of BEA (Cal-BEA), nano BEA and calcined form of nano BEA (Cal-Nano BEA) are presented in Figure 4.3. Two characteristic diffraction peaks of BEA at Bragg angles of 7.6 and 22.6º 2θ that correspond to (101) and (302) reflections, respectively confirmed that all BEA crystals synthesized were of pure material (JCPDS #48-0074 card) and calcination procedure had no negative effect on BEA-type framework [80, 86]. Additionally, there was a decrease in the peak intensity of nanosized BEA compared to BEA. This result can be attributed to the formation of smaller crystallites as also suggested by literature [80, 87].

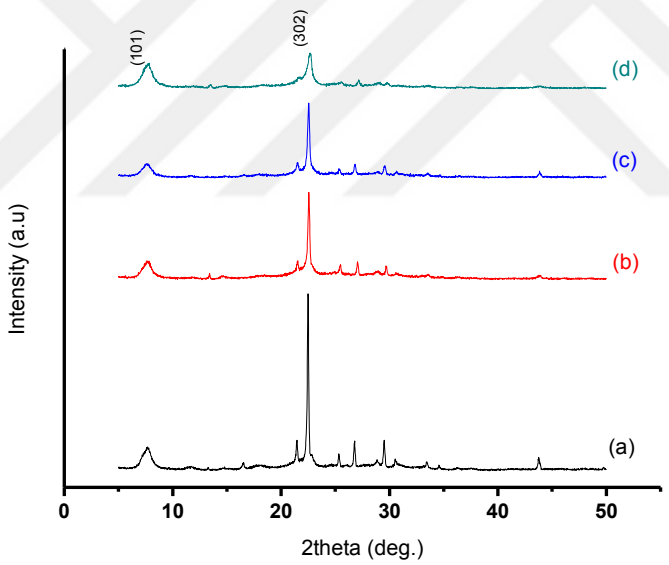


Figure 4.3 The X-ray diffraction patterns of (a) BEA, (b) Cal-BEA, (c) Nano BEA, (d) Cal-Nano-BEA

Representative SEM images of the samples used in the studies of zeolite modified electrochemical biosensors are shown in Figure 4.4 for (a) Cal-BEA and (b) Cal-Nano BEA.

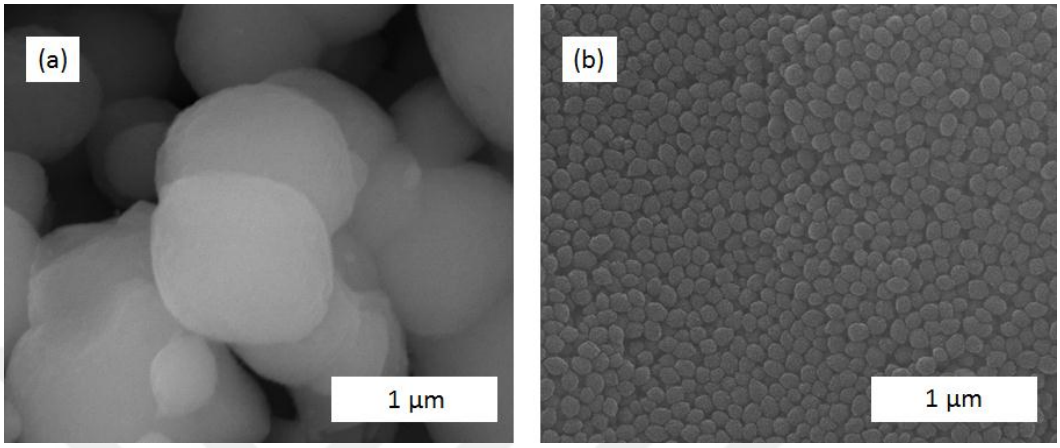


Figure 4.4 SEM images of BEA crystals a) Cal-BEA, and b) Cal-Nano BEA

BEA samples were around 1200 nm with typical truncated bipyramidal morphology (Figure 4.4-a) and nano BEA crystals were around 100 nm with more of a spherical morphology (Figure 4.4-b). The morphology of nano BEA remained the same after calcination procedure , in agreement with the given XRD patterns (Figure 4.3).

As shown in Table 4.2, the surface area of Cal-BEA is 743 $m^2/g$ whereas nano BEA and Cal-Nano BEA have surface areas 472 $m^2/g$ and 696 $m^2/g$, respectively. The removal of template lead to increase in surface area and pore volume of nano BEA from 472 $m^2/g$ to 696 $m^2/g$ and 0.20 cc/g to 0.29 cc/g, respectively. Additionally, external surface area of the Cal-BEA zeolite was 128 $m^2/g$ whereas Nano-BEA has 190 $m^2/g$ and the particle sizes of the zeolites were changing from 1200 nm to 100 nm, respectively.

Table 4.2 Physical properties of BEA crystals

| Sample Name | Si/Al[a] | Average Part.size[b] (nm) | $S_{BET}$ [c] ($m^2/g$) | $S_{EXT}$[d] ($m^2/g$) | Pore Volume[e] (cc/g) |
|---|---|---|---|---|---|
| Cal-BEA | 21.5 | 1200 | 743 | 128 | 0.30 |
| Nano BEA | 26.54 | 100 | 472 | 190 | 0.20 |
| Cal-Nano BEA | 20.8 | 100 | 696 | 183 | 0.29 |

a Measured by EDX
b Measured by SEM
c Measured by Multipoint BET
d Measured by t-plot Method.
e Measured by Saito-Foley (SF) Method

#### 4.1.2.1 Modification of BEA

BEA-Gold was obtained by reduction of ion-exchanged BEA as described in Chapter 3.2. The influence of formation of Au nanoparticles on BEA framework was investigated by XRD and SEM analysis.

XRD spectra of Cal-BEA and BEA-Gold are given in Figure 4.7-a and b respectively. It was seen that all peak positions matched well with the literature data. Two characteristic diffraction peaks of zeolite BEA at Bragg angles of 7.6 and 22.6º 2θ were observed, which correspond to (101) and (302) reflections, respectively. As seen from the figure, there is no noticeable change in the positions of the Bragg peaks indicating that the unit cell of the samples was not altered after ion exchange and reduction procedures. $Au^0$ phase at 38.1° 2θ in Figure 4.7-b, indicates the presence of gold nanoparticles on Cal-BEA [88].

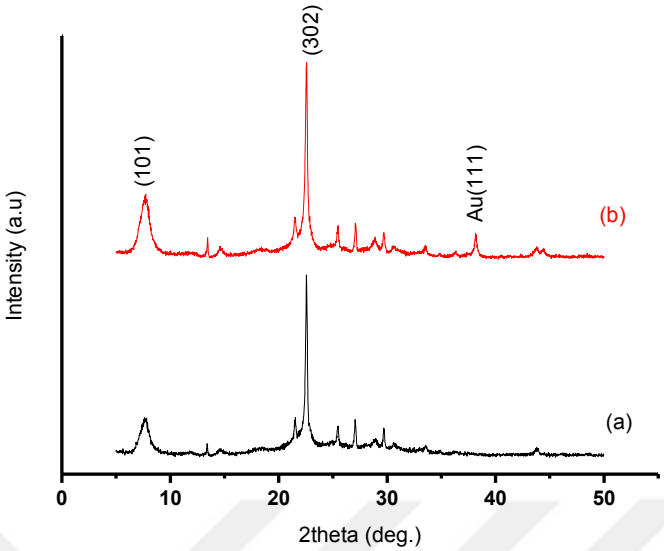


Figure 4.5 X-ray diffraction patterns of (a) Cal-BEA and (b) BEA-Gold

The results of the XRD were in accordance with the SEM images presented in Figure 4.4-a and Figure 4.6, which show successful synthesis of Cal-BEA and BEA-Gold, respectively. It can be seen that the typical truncated bipyramidal morphology of BEA remained the same after reduction procedure in BEA-Gold.

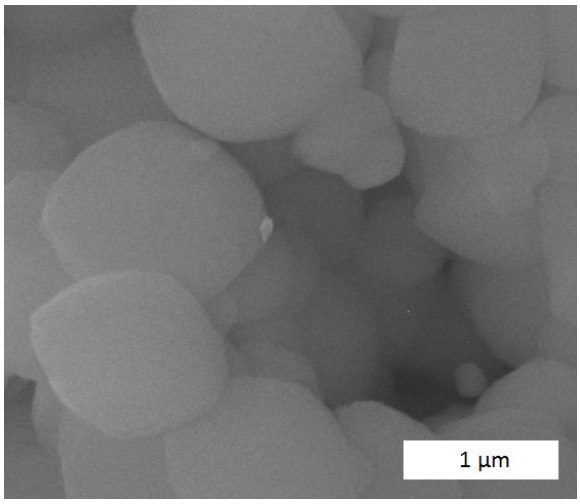


Figure 4.6 SEM image of BEA-Gold

Additional insight for gold characterization in zeolite BEA was investigated by ICP-OES, STEM, STEM-EDX, and XPS. According to ICP-OES, BEA-Gold contains 0.65% gold, whereas zeolite BEA has no gold inside. In Table 4.3, it can be noticed that Si/Al ratio of the zeolite remains approximately the same after ion-exchange and reduction procedures, which suggests that the local structure of zeolite BEA did not collapse.

Table 4.3 ICP-OES results of Cal-BEA and BEA-Gold

| ICP | Cal-BEA | BEA-Gold |
|---|---|---|
| Si(%) | 35.80±1.6 | 34.70±0.7 |
| Al(%) | 1.52±0.03 | 1.52±0.02 |
| Na(%) | 0.45±0.01 | 0.03±0.01 |
| Au(%) | - | 0.65±0.02 |
| Si/Al (mole) | 23.55 | 22.83 |

The presence of gold nanoparticles can be seen in STEM images presented in Figure 4.9. The heavy Au atoms clearly stand out on the light background of zeolite BEA. Additionally, STEM-EDX at the shown point of Figure 4.9-a can be shown as additional evidence for the existing gold nanoparticles. The average size of gold nanoparticles produced was 10 nm according to the taken STEM images. This result showed that gold nanoparticles were on the zeolite surface rather than in the pores of zeolite since the pore diameters are 5.6 x 5.6 Å and 7.7 x 6.6 Å for zeolite BEA.

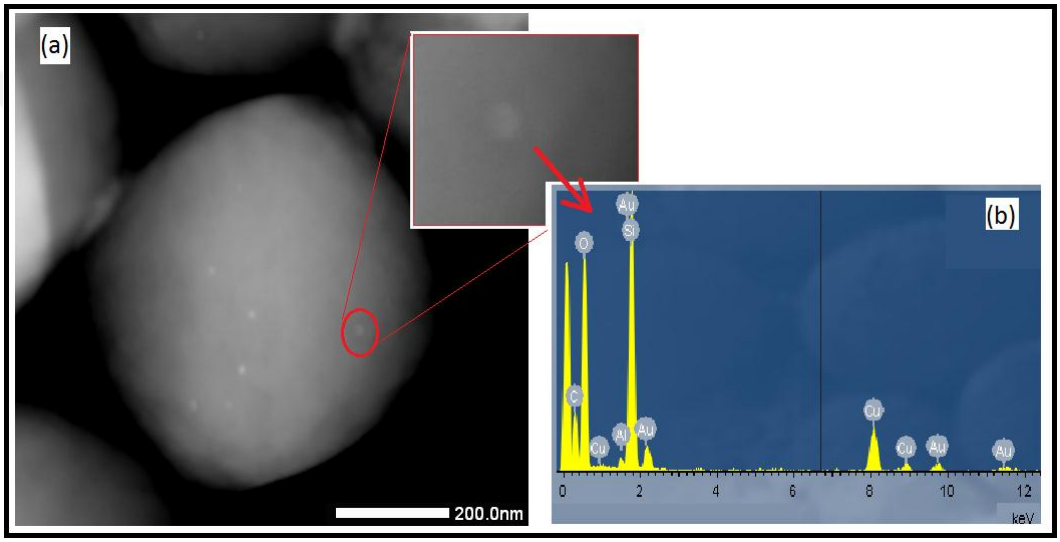


Figure 4.7 (a) STEM dark field image of gold nanoparticles and (b) STEM-EDX spectra of gold nanoparticle selected in (a)

The XPS spectrum of BEA-Gold given in Figure 4.10 shows two bands at 83.8 and 87.4 eV, which corresponds to $Au4f_{7/2}$ and $Au4f_{5/2}$, respectively. The band positions show good correspondence with the literature [79, 89].

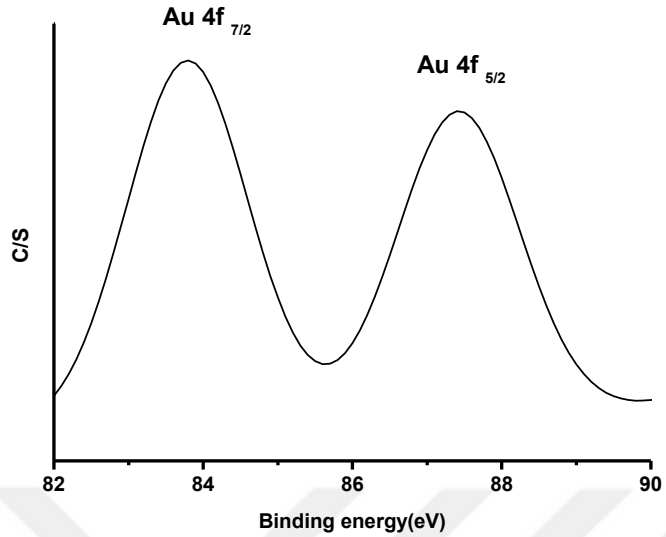


Figure 4.8 XPS Au 4f core-level spectrum of BEA-Gold

Table 4.4 gives a list of different types of synthesized zeolites that were used in the current zeolite modified electrochemical biosensor study.

Table 4.4 The summary of zeolite, the type of biosensors and enzymes used in bioselective elements

| Zeolite Type | Biosensor Type | Bioselective Element |
|---|---|---|
| Silicalite | Conductometric | Urease |
| | Amperometric | GOx |
| | ISFET | Urease |
| Cal-Sil | ISFET | CD |
| Cal-BEA | ISFET | CD |
| BEA-Gold | ISFET | CD |
| Nano BEA | Amperometric | GOx |
| | ISFET | Urease |
| Cal-Nano BEA | ISFET | CD |
| | ISFET | Urease |

## 4.2 Surface Modification for Zeolite Modified Electrochemical Biosensors

The primary purpose of surface modification was to form controlled and well-organized zeolite layers on electrode surfaces for enzyme immobilization in biosensors. For this purpose two methods were optimized; drop-coating and PEI coating.

### 4.2.1 Drop-Coating

Drop-coating method was applied directly on conductometric transducers as described in Chapter 3.3.1.2. The obtained DZMTs using Silicalite were investigated using SEM as presented in Figure 4.9.

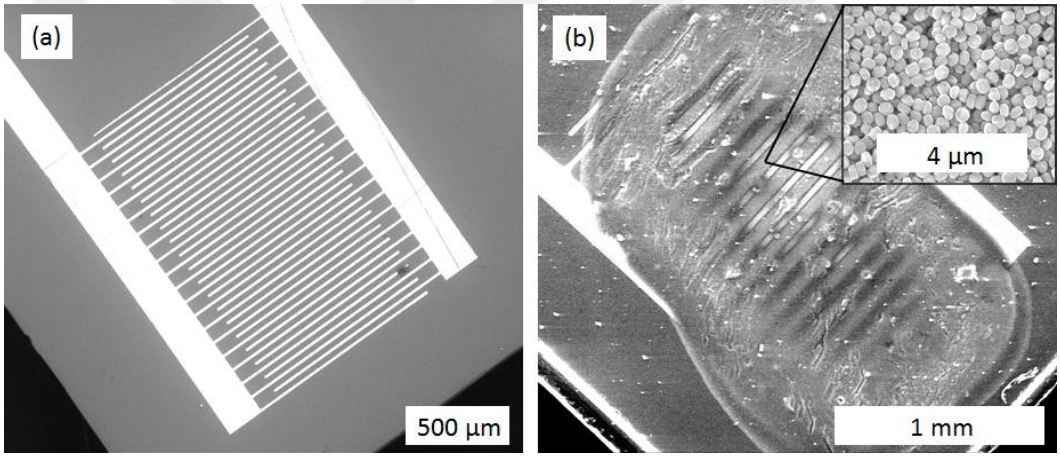


Figure 4.9 SEM image of conductometric transducer a) Bare and b) Drop-coated zeolite modified electrode using silicalite

According to Figure 4.9-b, silicalite was coated successfully onto the transducer surface with a simple method in agreement with Kirdeciler et al. [63]. Further studies were conducted to optimize the method in biosensor studies.

### 4.2.2 PEI Coating

Electrode surfaces are made up of gold on ceramic substrate. In order to achieve a reproducible way to modify any surface with the potential of being used in the current study, PEI was investigated as a means to make such well-formed zeolite coated surfaces. According to Lee et al., PEI increased the number of hydrogen bonds and strengthened the interactions between microcrystals and subtrates [47]. For that purpose, PEI was coated on silicon wafers using a spin coater. It is known that PEI concentration can be an important factor in the quality of the formed modified surfaces. Accordingly the effect of PEI concentrations, i.e., 0.5, 1, 3, 6, 10 % (v/v) PEI in ethanol, on Si wafer was investigated using spin coating. Spin coating rate was optimized as 3000 rpm and 15 s. The main goal was to see which concentration would result in a homogeneous distribution of silicalite on Si wafer. Silicalite crystals were attached to PEI-coated silicon wafers by direct attachment.

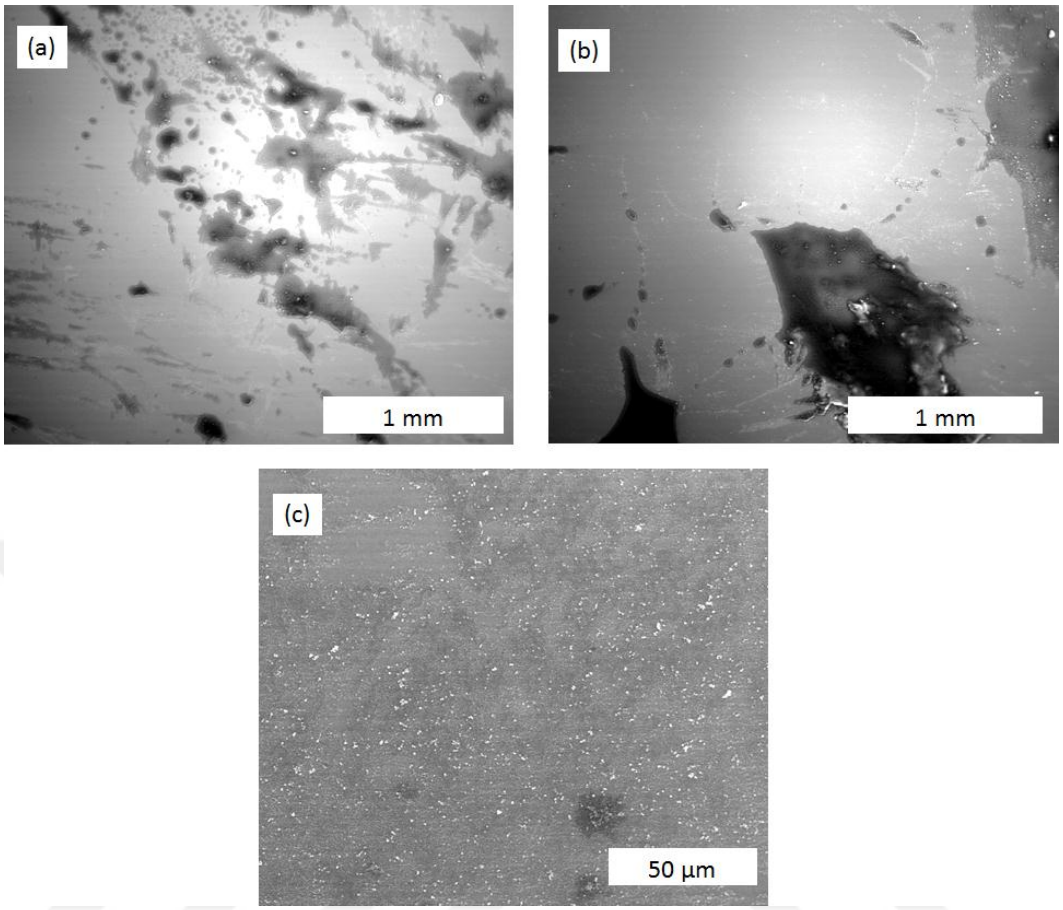


Figure 4.10 SEM images of PEI modified silicon wafers with silicalite using varying concentrations of PEI; a) 10%, b) 6% and c) 1%

Figure 4.10, presents the SEM images of silicalite coated silicon wafers with varying PEI concentration such as: 10%, 6% and 1%. It was observed that relatively lower concentrations of PEI resulted in a better, more homogeneously distributed film formation with respect to higher concentrations.

In addition to using PEI, mucasol cleaning step, which is generally used to alter the surface hydrophobicity, was used before the PEI modification step. It was believed that this additional step could enhance the homogeneity of zeolite distribution on the surface. For that purpose, the surfaces were ultrasonicated in Mucasol (1/6 v/v)

in distilled water for 30 min. Afterwards, mucasol treated surfaces were rinsed with water and dried under air. After mucasol treatment, PEI was again spin coated at 3000 rpm for 15 s. The obtained silicalite modified surfaces using different concentration of PEI with mucasol pretreatment were presented in Figure 4.11.

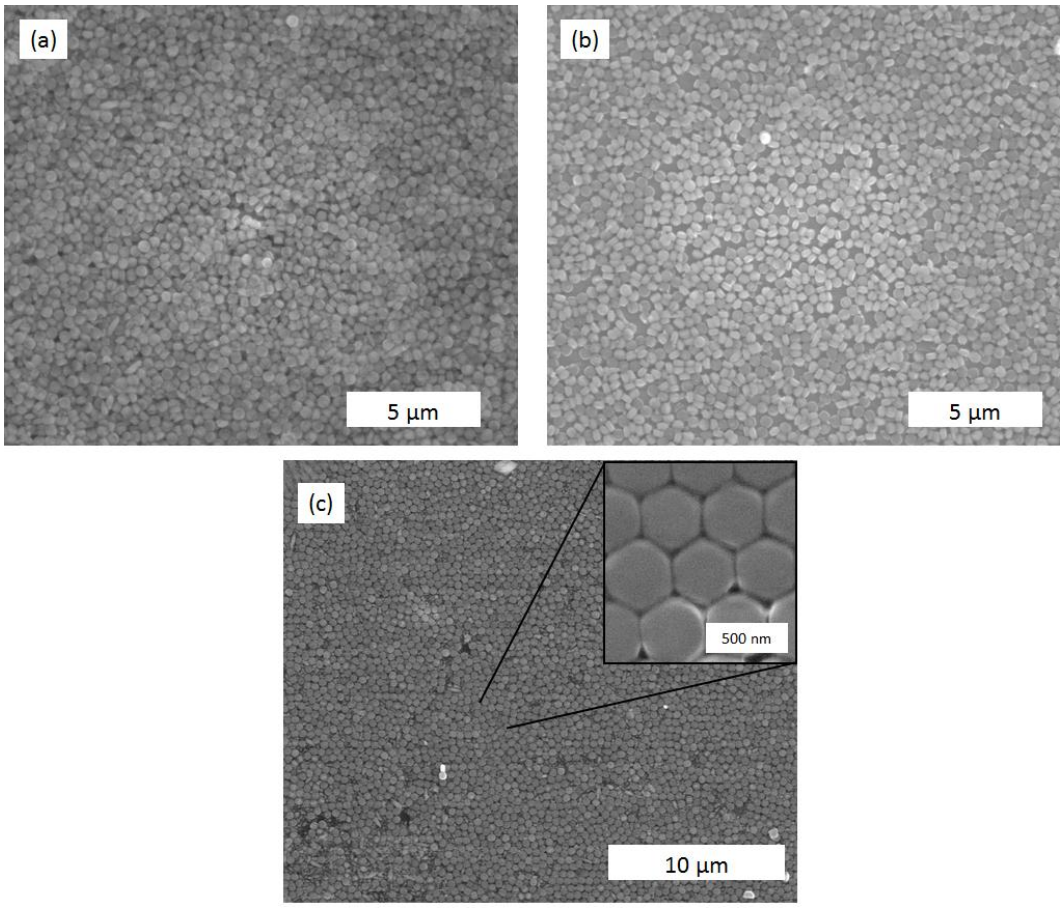


Figure 4.11 SEM images of Mucasol-PEI modified silicon wafers with silicalite using a) Mucasol -3% PEI, b) Mucasol -1% PEI c) Mucasol -0.5 % PEI

As shown in Figure 4.11, mucasol pretreatment provided significant improvement in surface modification with PEI and 0.5% PEI concentration was observed to lead to form monolayers of silicalite on Si wafer.

After optimization of modification of silicon wafer these studies were adapted to conductometric, amperometric and ISFET based biosensor surfaces for being able to obtain homogeneous and reproducible zeolite films to be used in immobilization of bioselective elements in amperometric biosensors and ISFET based urea biosensors.

## 4.3 Zeolite Modified Electrochemical Biosensors

### 4.3.1 Conductometric Biosensors

In literature, it was shown that urease adsorption on zeolite thin film produced by drop-coating method gave better results than standard GA membrane (SMT) [62], so the goal of this study was to prove an efficiency of this method by optimizing the conditions for urease immobilization using drop-coating method and comparing the results with other methods of immobilization. Furthermore, created conductometric biosensors were tested in real blood samples for urea determination.

#### 4.3.1.1 Preparation of Silicalite-Based Electrodes

A silicalite layer synthesized according to the procedure described in Chapter 3.1.1.1 was formed on the surface of transducer by drop-coating as described in Chapter 3.1.2.1. The obtained active region of silicalite-coated transducer is shown in Figure 4.12.b-c and the transducer without zeolite were presented in Figure 4.12-a for comparison. As can be seen, the procedure resulted in formation of a thin silicalite layer on the active zones of electrodes.

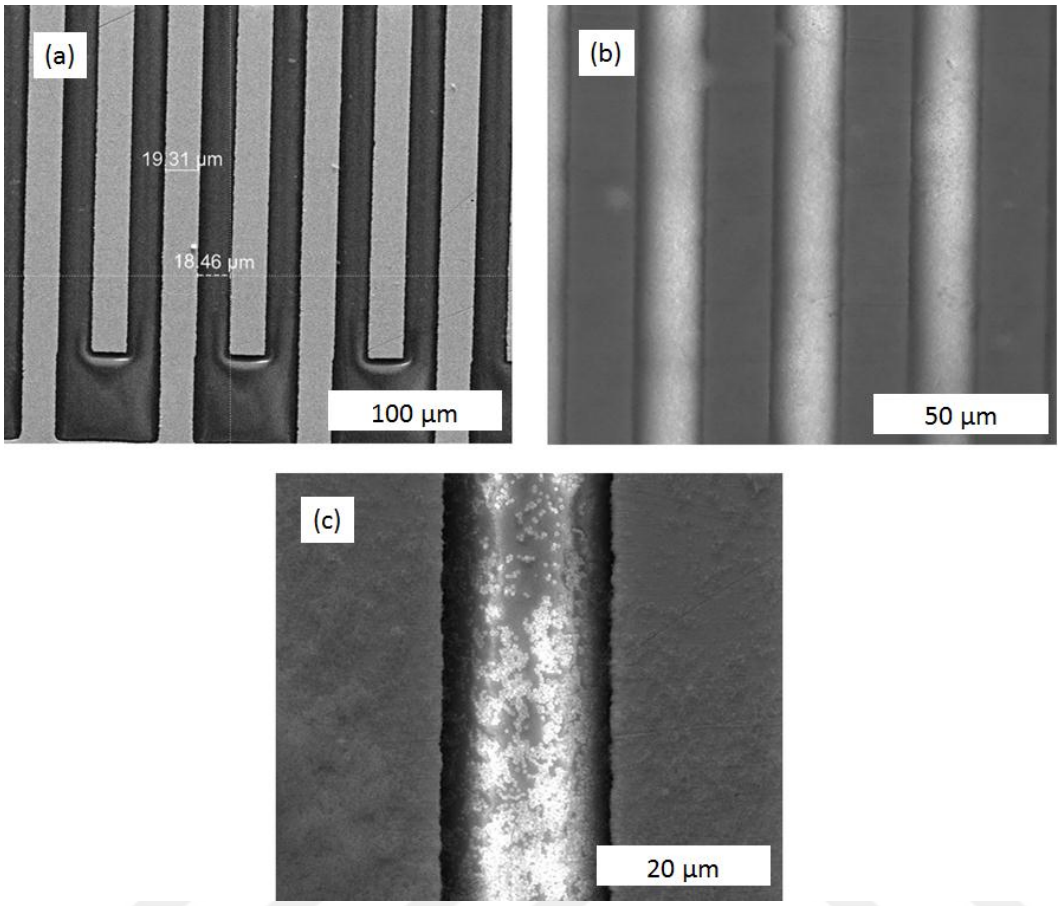


Figure 4.12 SEM images of the active region of conductometric transducer showing (a) bare electrode, (b) with silicalite layer and (c) higher magnification of the electrode with silicalite

For bioselective element, urease was immobilized on drop-coated zeolite modified transducer (DZMT) as described previously in Chapter 3.1.2.3 by only dropping 0.2 µl of 5 % urease solution in 20 mM PBS, pH 6.5 to working electrode and 0.2 µl of 5 % BSA solution in 20 mM PBS, pH 6.5 to reference electrode of the transducer without using any GA, which is known to induce partial denaturation of the enzymes [90].

#### 4.3.1.2 Effect of Silicalite Amount on Transducer

At the first stage, it was necessary to determine the optimal amount of silicalite on the surface of transducer for enzyme adsorption. Zeolite amount was increased by repeating the drop-coating step.

The procedure of drop-coating of the transducer with silicalite (5%, w/w in PBS) was repeated several times and then urease was adsorbed for 17 min. Dependence of biosensor responses on silicalite amount is shown in Figure 4.13. Accordingly, two-times drop-coating resulted in significant higher activity of bioselective element compared to one-time procedure, however further repeat of drop-coating gave no appreciable effect. Thus, two-times of drop-coating procedure was used for further experiments.

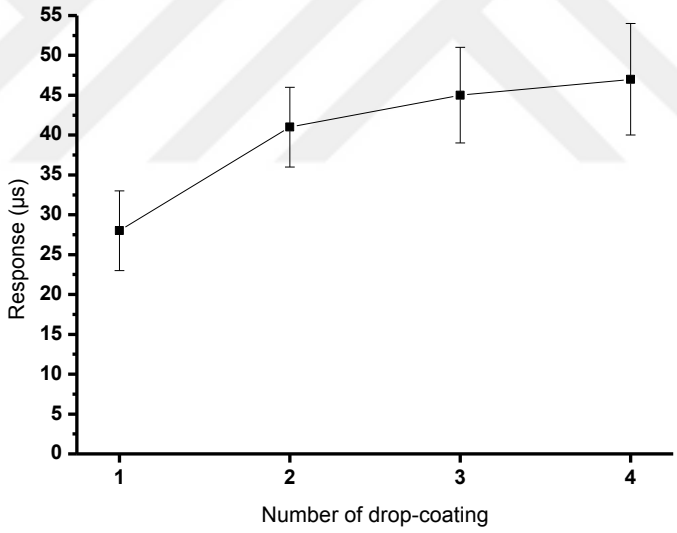


Figure 4.13 Response dependence of conductometric based urea biosensor on silicalite amount

#### 4.3.1.3 Effect of Adsorption Time

Urease immobilization is the key point of biosensor development. To be able to obtain the optimized immobilization amount time of immobilization on zeolite-coated surfaces was investigated. The duration time of urease adsorption on silicalite was optimized according to the obtained biosensor responses. It was observed that within the range of adsorption time of 5–30 min, the responses were of about the same value as presented in Figure 4.14. Accordingly, 17 min of adsorption was accepted as an optimal value, because during this time an enzyme-containing drop deposited on the transducer becomes completely dry after this time interval.

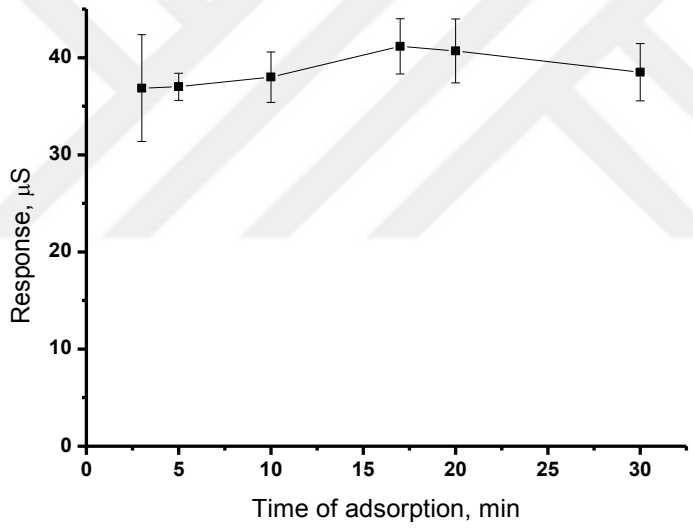


Figure 4.14 Response dependence of conductometric based urea biosensor on urease adsorption time

#### 4.3.1.4 Effect of Solution Properties

The performance of the enzyme based biosensors depends on the activity of an immobilized enzyme, which is strongly affected by the environmental conditions,

especially by the pH value of the aqueous measurement medium. The measurements were conducted in a polymix buffer (such a buffer solution allows a stabilized buffer capacity in a wide pH range). It was composed of 5 mM tris, monopotassium phosphate, citric acid and sodium tetra borate. Polymix buffer was used to exclude any influence of buffer capacity changes on the sensor response. The response dependence of the biosensor on pH of working solution based on adsorbed urease was compared to the results of the biosensor based on urease immobilized in GA vapor.

As shown in Figure 4.15, the sensor responses are alike for both methods (pH 6 for adsorbed urease, pH 5.5. for GA vapor). Accordingly, pH of 6.5 was decided to be used since it is closer to real samples (blood pH 7.4).

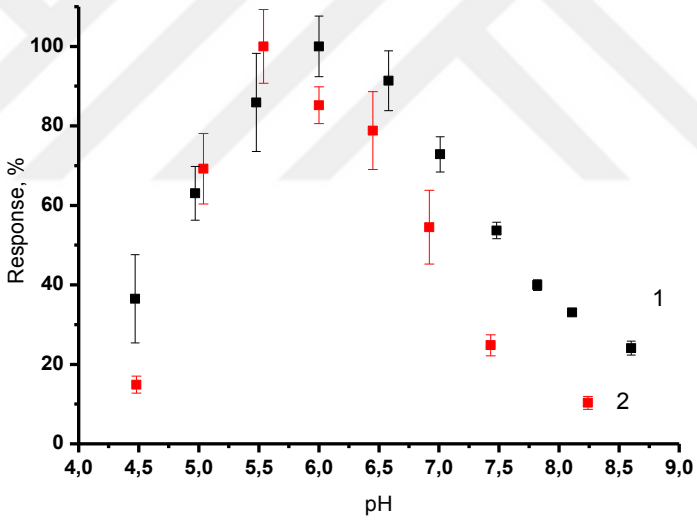


Figure 4.15 Response dependence of conductometric based urea biosensor on pH based on urease, (1) adsorbed on silicalite and (2) immobilized in GA vapor Measurements were conducted in 2.5 mM polymix buffer at room temperature, urea concentration was 2 mM

It is known that the response of conductometric biosensor considerably depends on ionic strength of the solution, in which the response is measured. The influence of ionic strength (KCl concentration) on the value of responses of the biosensor based on adsorbed urease was also studied and compared with that for the biosensor based on urease immobilized in GA vapor and shown in Figure 4.16.

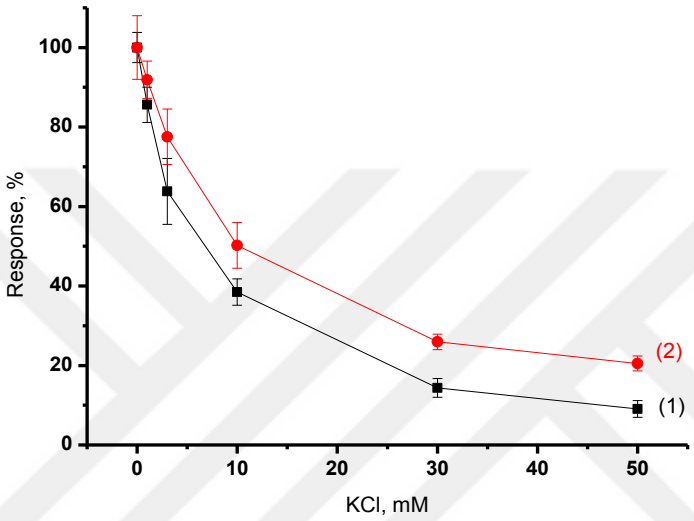


Figure 4.16 Dependence of biosensor's responses on ionic strength, (1) adsorbed on silicalite and (2) immobilized in GA vapor, measurements were conducted in 2.5 mM polymix buffer at room temperature, urea concentration was 2 mM

The responses of both types of biosensors decreased significantly while increasing ionic strength, i.e. at 50 mM concentration of KCl, biosensor responses (to a saturating concentration of substrate) were decreased in comparison with the same responses without KCl. Thus, it is necessary to control ionic strength in order to decrease the measurement error while working with real samples.

#### 4.3.1.5 Sensitivity

The calibration curves of silicalite based biosensor and SMT were presented in Figure 4.17. The response of silicalite based biosensor to 2 mM urea was 41µs whereas standard membrane transducer gave 30µs. From the calibration curve of silicalite based urea biosensor, the linear detection range was up to 0.75 mM for silicalite based biosensor whereas it was 0.9 mM for SMT.

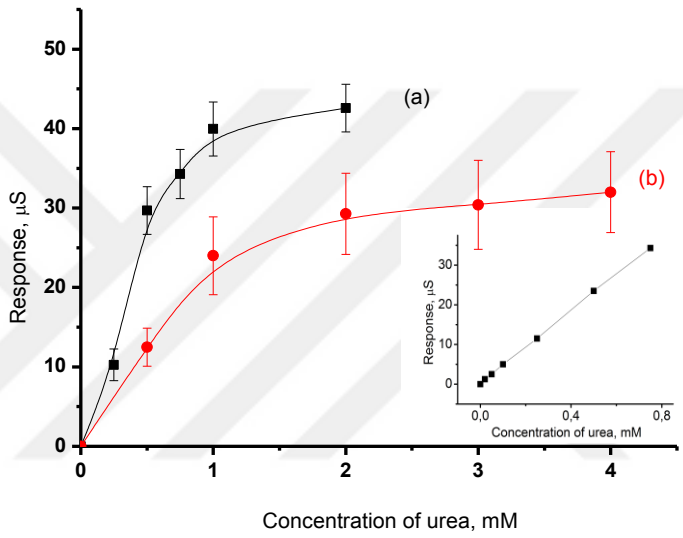


Figure 4.17 Calibration curves for urea detection by biosensors, based on urease, (a) adsorbed on silicalite (b) urease immobilized in GA vapor in 5 mM phosphate buffer, pH 6.5 and inset of the figure shows the linear range of calibration curve of silicalite coated biosensor

#### 4.3.1.6 Comparison of Urease Adsorption on Silicalite with Other Methods of Immobilization

An efficiency of urease adsorption on drop-coated silicalite was compared with other methods of urease immobilization. These methods were urease immobilization in GA vapor, in GA drop, on nitrocellulose and

photopolymerization in PVA/SbQ described in Chapter 3.2.1.4, 3.2.1.5, 3.2.1.6 and 3.2.1.7, respectively.

In particular, important working analytical characteristics of the biosensors based on these methods can be given as the response obtained for the saturated substrate concentration (2 mM), entire response time and linear working range. As seen from Table 4.5, the results of adsorption on silicalite are no worse, sometimes even better, than the results of enzyme immobilization by other methods. As seen, the closest to urease adsorption were the results of enzyme immobilization in GA vapor; so this method was used for further comparisons.

Table 4.5 Comparison of conductometric urease biosensors based on different methods of immobilization.

| Type of urease Immobilization | Biosensor response to 2mM urea (μs) | Response time (min) | Linear working range (μM) |
|---|---|---|---|
| Adsorption on silicalite | 41 | 3-4 | 3-750 |
| GA vapor | 30 | 4 | 8-900 |
| GA drop | 34 | 5-6 | 4-850 |
| Adsorption on nitrocellulose | 18 | 3-4 | 8-900 |
| Photopolymerization in PVA/SbQ | 13 | 4 | 9-650 |

#### 4.3.1.7 Signal Reproducibility and Operational Stability

Reproducibility and operational stability are important working characteristics of biosensors. To determine the signal reproducibility, the biosensors responses to the saturation concentration of urea (2 mM) were measured during one working day with 10–15 min intervals but keeping the sensors continuous stirring of buffer. Relative standard deviation (RSD) of urea measurement was about 4% for both the biosensor based on adsorbed urease and biosensor based on urease immobilized in GA vapor.

A common disadvantage of biosensors with adsorbed enzymes is gradual wash-out of the latter into working solution due to weak binding between enzyme and adsorbent. An important stage in our work was investigation of the stability of the developed biosensor during several days. For comparison, the biosensors based on urease immobilized in GA vapor were used.

During the stability experiments, the transducers with adsorbed and cross-linked urease were stored dry at 4°C. The relative standard deviation of response was 4.5% for both the biosensors as presented in Figure 4.18. During 10 days the responses decreased to 90% of initial value; thus, biosensor stability is the same or better than reported in previous works on conductometric urease biosensors. For example, Lee et al. developed a conductometric biosensor using urease immobilization in a silica sol-gel matrix with response time of 16.5 min and detection limit of 30 μM. The reproducibility of the biosensor was 4 % and 70% of its original activity retained after 10 days [91].

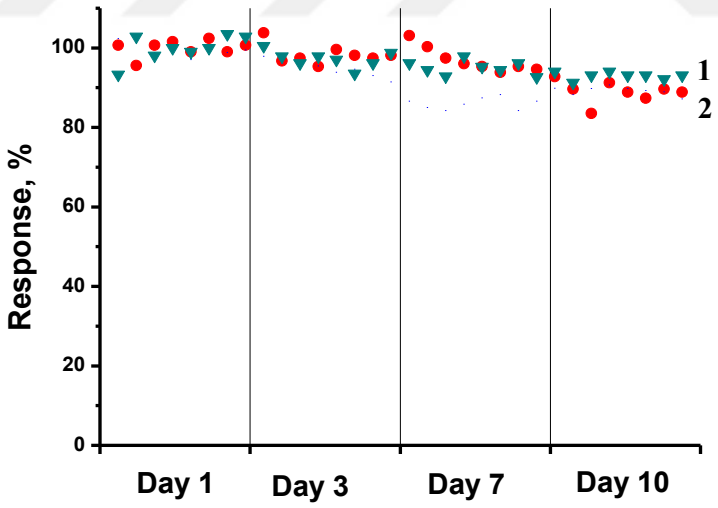


Figure 4.18 Operational stability of biosensors based on urease, adsorbed on silicalite (1) and immobilized in GA vapor (2). Measurements were conducted in 5 mM phosphate buffer, pH 6.5, urea concentration was 2 mM

#### 4.3.1.8 Biosensor Inter-Reproducibility

Inter-reproducibility of preparation of biosensors is important for biosensor standardization, therefore, this parameter was checked for the biosensor based on adsorbed urease and compared with that of biosensor based on urease immobilized in GA. The experiments were carried out as follows: several clean electrodes were two-times drop-coated with silicalite, then urease was adsorbed and responses to the substrate (saturation concentration) were measured three times. Next, enzyme and silicalite were removed from the transducers with spirit-wetted cotton, and entire procedure was repeated 5–8 times. In analogous way inter-reproducibility of biosensors based on urease, immobilized in GA saturated vapor according to the described technique was studied. A similar approach was conducted for immobilization in GA vapor and the results are shown in 4.19. The relative standard deviation in inter-reproducibility for biosensors based on adsorbed urease was 9% while for biosensors with covalently immobilized urease was 22%.

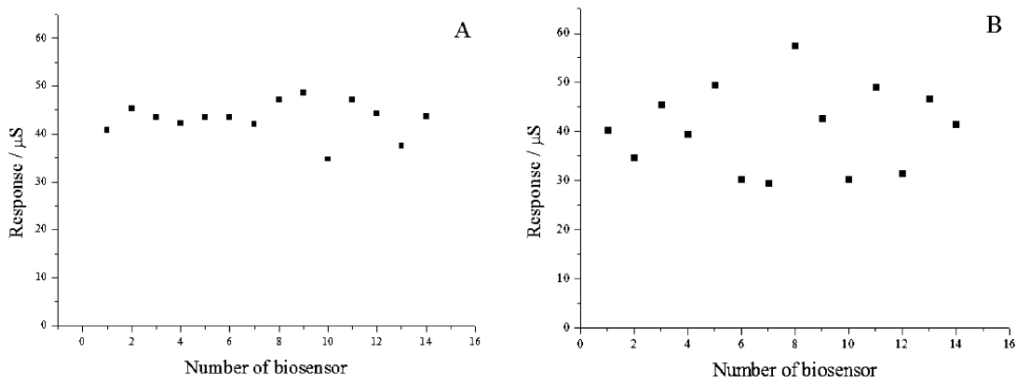


Figure 4.19 Inter-reproducibility of biosensors based on urease, adsorbed on silicalite (A), and immobilized in GA saturated vapor (B). Measurements were conducted in 5 mM phosphate buffer, pH 6.5, urea concentration: 2 mM

The reason of substantially lower dispersion of responses at adsorption can be due to considerably weaker dependence of enzyme adsorption on environmental conditions, with respect to immobilization in GA vapor. Besides, the procedure of adsorption is more controllable than immobilization in GA vapor [92].

#### 4.3.1.9 Application of Developed Biosensor in Serum

After obtaining the optimal conditions for drop-coated silicalite based biosensor, it was tested with real samples. Five blood serum samples with excessive urea concentration taken from patients with renal failure along with two samples taken from healthy people were analyzed and the results were compared with diacetyl monoxime reaction.

The urea concentration in blood assays were performed by the method of standard additions at 500-fold sample dilution. This amount of dilution was used to be able to neglect the influence of solution properties such as pH and ionic strength since the concentration of added interfering substances will be too low to change the biosensor characteristics. The example of experiments is shown in Figure 4.20. First, the biosensor response to the insertion of the blood serum aliquot into the measuring cell was obtained and plotted on the ordinate axis. Next, three responses were obtained respect to three injections of 0.025 mM urea into the same cell. Plotting these results, lead to a straight line of which its intersection with the abscissa axis corresponded to the urea concentration in the tested sample of blood serum (considering 500-fold dilution). Total time of analysis of one sample was about 10 min.

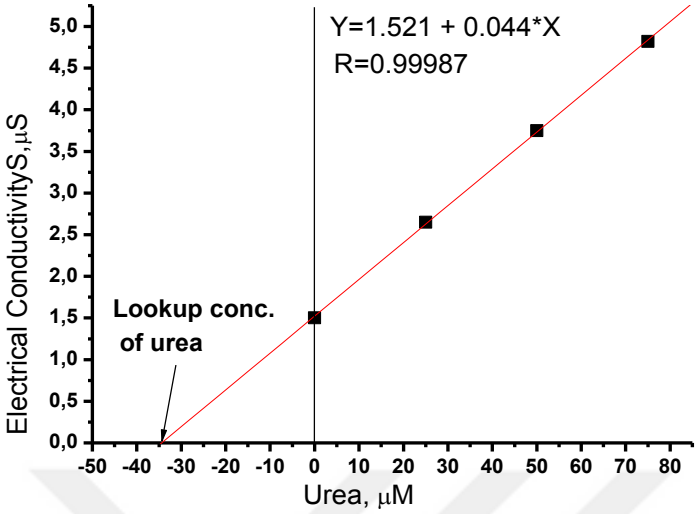


Figure 4.20 Real experiment on urea determination by the developed biosensor using the method of standard additions in 5mM, pH 6.5

For each addition, three to five repetitive measurements were carried out and then a mean value and standard deviation were calculated. As seen from Figure 4.21, sensitivity and accuracy of the biosensors were quite sufficient for precise differentiation of the serum samples taken from patients and healthy people.

The traditional method of diacetyl monoxime reaction was used as a control method of urea determination [93]. The working principle of diacetyl monoxime reaction is that (in the presence of thiosemicarbazide and iron(III) ions) urea forms a complex with diacetyl monoxime, whose color intensity that is measured at 540 nm is directly proportional to the urea content in the biosamples tested. 15-20 min is required for each test. The main disadvantages of the reaction are sensitivity of the urea-diacetyl monoxime complex to light and quick loss of color. Furthermore, reagents for the reaction are toxic.

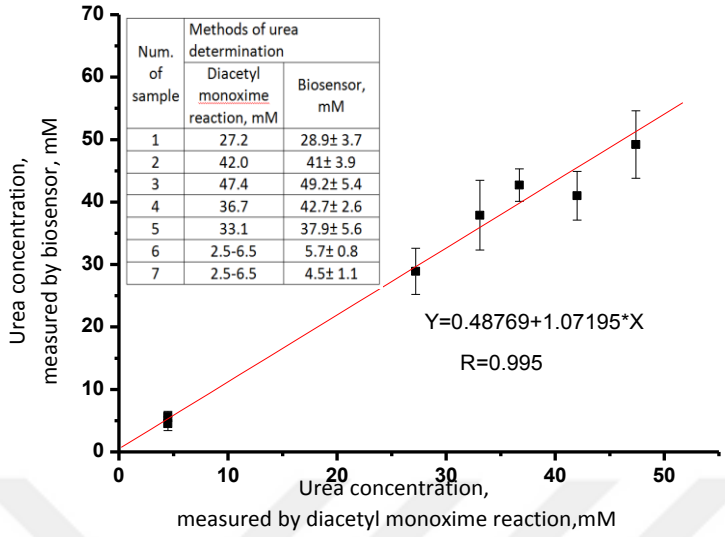


| Num. of sample | Methods of urea determination | |
|---|---|---|
| | Diacetyl monoxime reaction, mM | Biosensor, mM |
| 1 | 27.2 | 28.9± 3.7 |
| 2 | 42.0 | 41± 3.9 |
| 3 | 47.4 | 49.2± 5.4 |
| 4 | 36.7 | 42.7± 2.6 |
| 5 | 33.1 | 37.9± 5.6 |
| 6 | 2.5-6.5 | 5.7± 0.8 |
| 7 | 2.5-6.5 | 4.5± 1.1 |

Figure 4.21 Comparison of measurement by biosensors based on silicalite-adsorbed urease and by the method of diacetyl monoxime reaction. Measurement in 5 mM phosphate buffer, pH 6.5

A good correlation between the values of urea concentration in the samples of blood serum measured by the biosensor based on silicalite-adsorbed urease and those obtained by diacetyl monoxime reaction was found and presented in Figure 4.21. The correlation coefficient was 0.995.

Reproducibility of the biosensor was measured by using two different concentrations of urea in serum; a serum sample with a higher urea and normal urea concentrations. These serums were sequentially tested by the same biosensor 10 times during one working day. The results are given in Figure 4.22. The RSD between measurements was 9%. Certainly, in this case, reproducibility was lower than the case in model solution, however this is a common case for impure real assays [94].

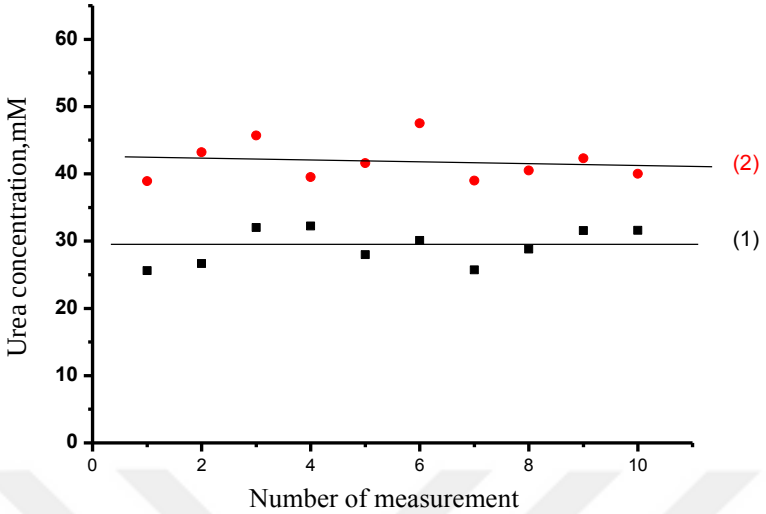


Figure 4.22 Reproducibility of the results of measurement of two serum samples: (1) sample with 42 mM of urea, and (2) sample with 29 mM of urea by the biosensor based on silicalite adsorbed urease. Measurement in 5 mM phosphate buffer, pH 6.5, by using the method of standard additions (500-fold dilution)

### 4.3.2 Amperometric Biosensors

In this study, silicalite and nano BEA zeolites were used for creation of amperometric glucose biosensor with enhanced analytical characteristics. For the first time thin zeolite layers were produced using PEI on the amperometric transducers to immobilize glucose oxidase (GOx) and compared with drop-coating method which was used in previously conductometric biosensor application and by GA vapor immobilization.

#### 4.3.2.1 Preparation of Zeolite Modified Electrode

Silicalite and nano BEA were synthesized as described in Chapter 3.1.1. and 3.1.3, respectively. To produce zeolite modified electrodes for GOx detection both drop-coating and PEI methods were used.

Firstly, zeolite layer was formed on the transducer surface by drop-coating method as described in Chapter 3.1.2.1. 10 % zeolite solution in 5 mM PBS at a pH of 6.5 was used. 0.4µl of the solution was deposited onto all active zones of multi-transducer, then it was heated at 150 °C for 3 min. This temperature had no effect on silicalite and did not influence the transducer working parameters.

For PEI coating described in Chapter 3.1.2.2, the suitable conditions for thin zeolite layer production were chosen as follows: samples were spin coated with 0.5 % PEI in ethanol at 3000 rpm for 15 s, and calcined at 90 °C for 30 min. The synthesized zeolites were directly attached onto the obtained electrode surfaces simply by direct attachment technique [47], which is composed of rubbing zeolites. These electrodes were used in further studies.

Then to achieve the bioselective membranes on zeolite coated electrodes, 0.1µl of 5% GOx solution in 20 mM phosphate buffer with a pH of 6.5 was deposited onto the silicalite coated active zones of multi-transducer, after which they were exposed to complete air-drying for 20 min (Chapter 3.1.2.3). During this study, neither GA nor any other auxiliary compounds was used. Next, the transducers were submerged into the working buffer for 20–30 min to wash off the unbound enzyme. After experiments, the transducer surface was cleaned from enzyme with ethanol-wetted cotton.

The analytical characteristics of zeolite-coated amperometric biosensors were compared with the biosensors developed by standard membrane transducers (SMT) which were developed by GA cross-linking of GOx without using zeolite. SMTs were developed as described in Chapter 3.2. 2.4.

#### 4.3.2.2 Sensitivity

The sensitivity of the biosensors developed by drop-coating method showed improved sensitivity but a slow response with respect to PEI method For example, obtaining a response to 1mM glucose took about 40 min as presented in Figure 4.23, which is a very long period for a typical biosensor analysis. This result can

be attributed to the significantly thicker layer of silicalite formed by drop-coating compared to PEI-coating as presented in Figure 4.24. The thickness of drop-coated silicalite on amperometric electrode was 15±0.1µm whereas the thickness was 1.65±0.3 µm in PEI-coated electrodes which correspond to 2-3 layers of silicalite. However, the response of DZMT based on GOx was three times more than of the biosensors based on SMT. Thus, to get a quick response by zeolite modified transducer, PEI modification was carried out using silicalite and nano BEA by reducing the thickness of the zeolite layer.

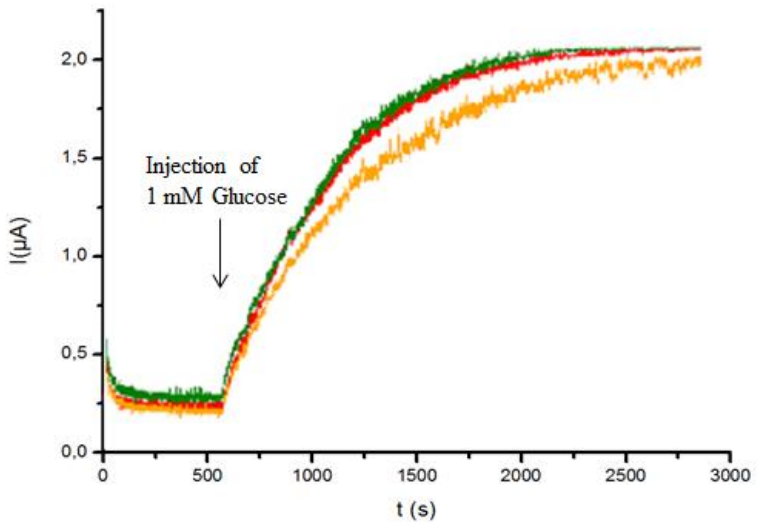


Figure 4.23 Response curve of amperometric biosensor developed by drop coating of silicalite

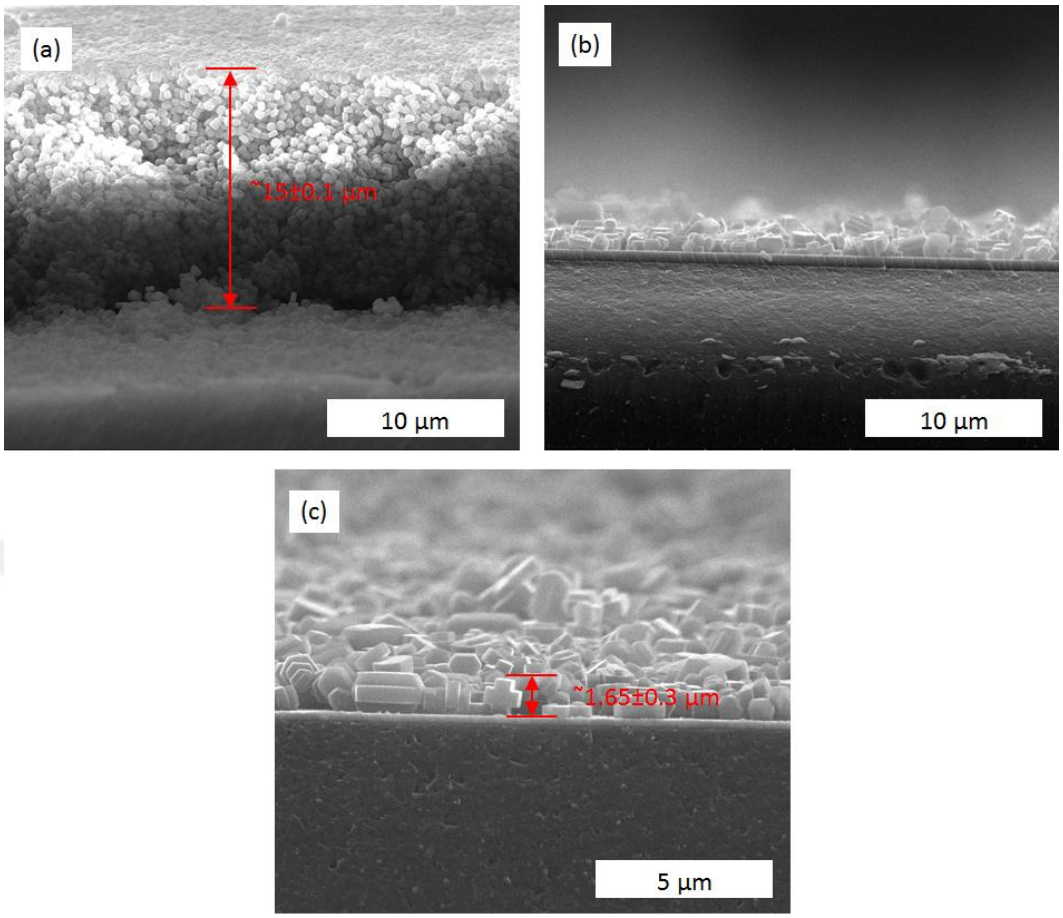


Figure 4.24 Cross sectional SEM images of amperometric electrodes with (a) drop-coated silicalite, (b) PEI-coated silicalite, (c) PEI-coated silicalite with a higher magnification

The characteristics of these PZMT based biosensors were compared with those of the biosensors based on the traditional immobilization in GA vapor (SMT). Since the sensitivity and linear range of measurement are the most important working characteristics of any biosensor, the influence of different types of immobilization on these parameters was investigated. The calibration curves presented in Figure 4.25 were obtained for each biosensor.

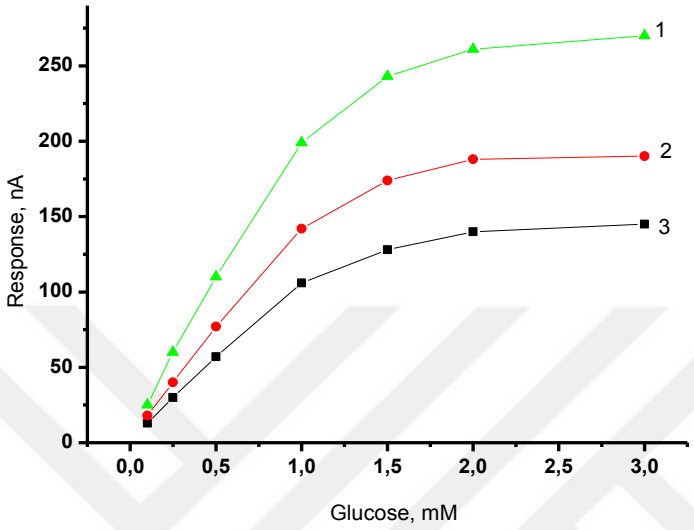


Figure 4.25 Calibration curves for glucose detection by biosensors based on GOx adsorbed on (1) nano BEA and (2) silicalite, and GOx immobilized in (3) GA vapor. Measurements were carried out in 5 mM HEPES buffer, pH 7.2

As shown in Figure 4.25, the linear ranges of measurement for all biosensors were identical, whereas the sensitivities were different. The biosensors based on using both zeolites were characterized by a higher sensitivity than the biosensors based on the GOx immobilized in GA vapor. Additionally, nano BEA zeolite based biosensors had higher sensitivity than silicalite based biosensors.

#### 4.3.2.3 Signal Reproducibility and Inter-Reproducibility

At the next stage, the reproducibility of responses of all three biosensors during several hours of continuous operation were investigated. One measurement of glucose took 3–5 min. The interval between measurements was about 20 min,

during which the biosensors were washed from substrates using working buffer solution. No considerable decrease in responses of all three sensors after 10 subsequent measurements was observed. As seen in Figure 4.26, all biosensors demonstrated high signal reproducibility. The relative standard deviation of responses to glucose belonging to nano BEA, silicalite coated and SMT were 2.5%, 3.2%, 5.6%, respectively.

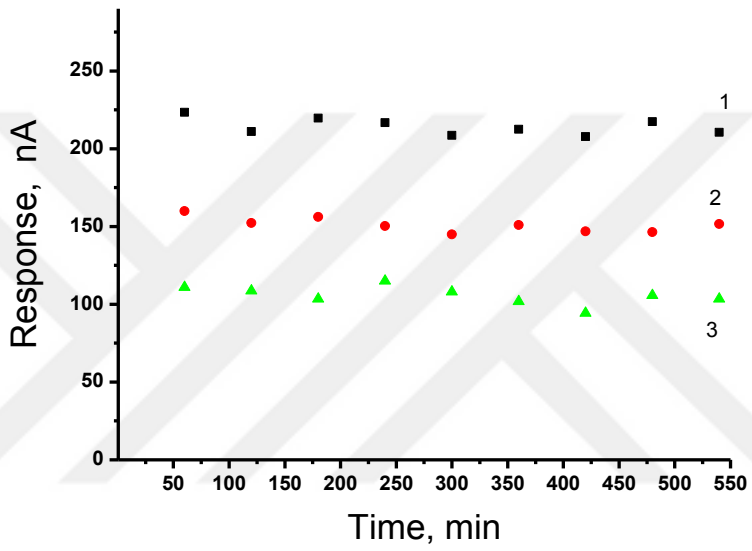


Figure 4.26 Reproducibility of responses of biosensors based on GOx adsorbed on nano BEA (1) and silicalite (2), and GOx immobilized in GA vapor (3).Glucose concentration – 1 mM. Measurements were carried out in 20 mM HEPES buffer, pH 7.2

As another important parameter for biosensors, reproducibility of biosensor preparation- inter-reproducibility was investigated and the results are shown in Figure 4.27. The new method of enzyme immobilization by PEI coating should have a better inter-reproducibility than SMT. As it was expected, the biosensors

based on the GOx adsorption on nano BEA and silicalite had better reproducibility as compared to the biosensors with enzyme immobilization in GA vapor.

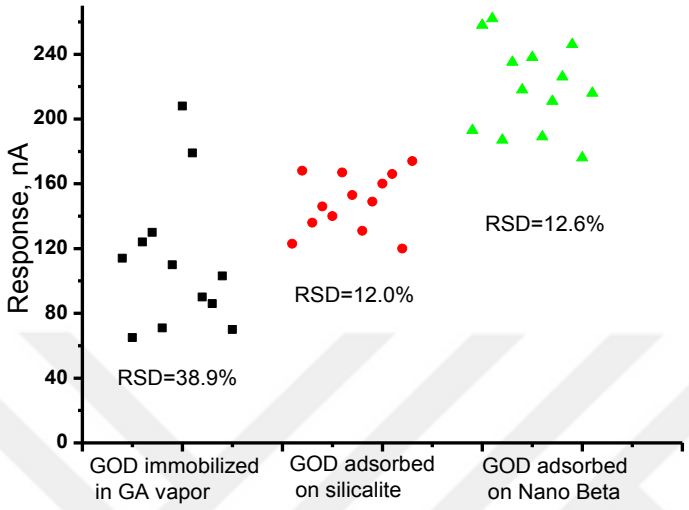


Figure 4.27 Inter-reproducibility of biosensors based on GOD adsorbed on nano BEA (1) and Silicalite (2), and GOx immobilized in GA vapor (3).Glucose concentration – 1 mM. Measurements were carried out in 20 mM HEPES buffer, pH 7.2

Eventually, the biosensors based on the GOx adsorbed on nano BEA zeolite were with higher sensitivity and inter-reproducibility. This type of immobilization was the most stable and reproducible method for amperometric biosensor production for GOx, and the biosensors were characterized with the highest and fastest responses [95].

### 4.3.3 ISFET Based Biosensors

#### 4.3.3.1 ISFET Based Biosensors for Urea

In this study, PEI coating method was applied to ISFET based biosensors using different types of zeolites: silicalite, nano BEA and Cal-Nano BEA to achieve urea detection. Obtained results were compared with the results of biosensors based on urease immobilization in GA vapor (SMT).

##### 4.3.3.1.1 Preparation of Zeolite Modified Transducers

The synthesis of silicalite, Nano-BEA and Cal-Nano BEA were described and characterized in Chapter 3.1.

PZMTs were prepared according to the method described in Chapter 3.1.2.2 using different zeolites. The obtained transducers were presented in Figure 4.28. (a-c) the bare transducer, the obtained PZMTs with (d-f) silicalite and (g-i) Nano-BEA , respectively at different magnifications.

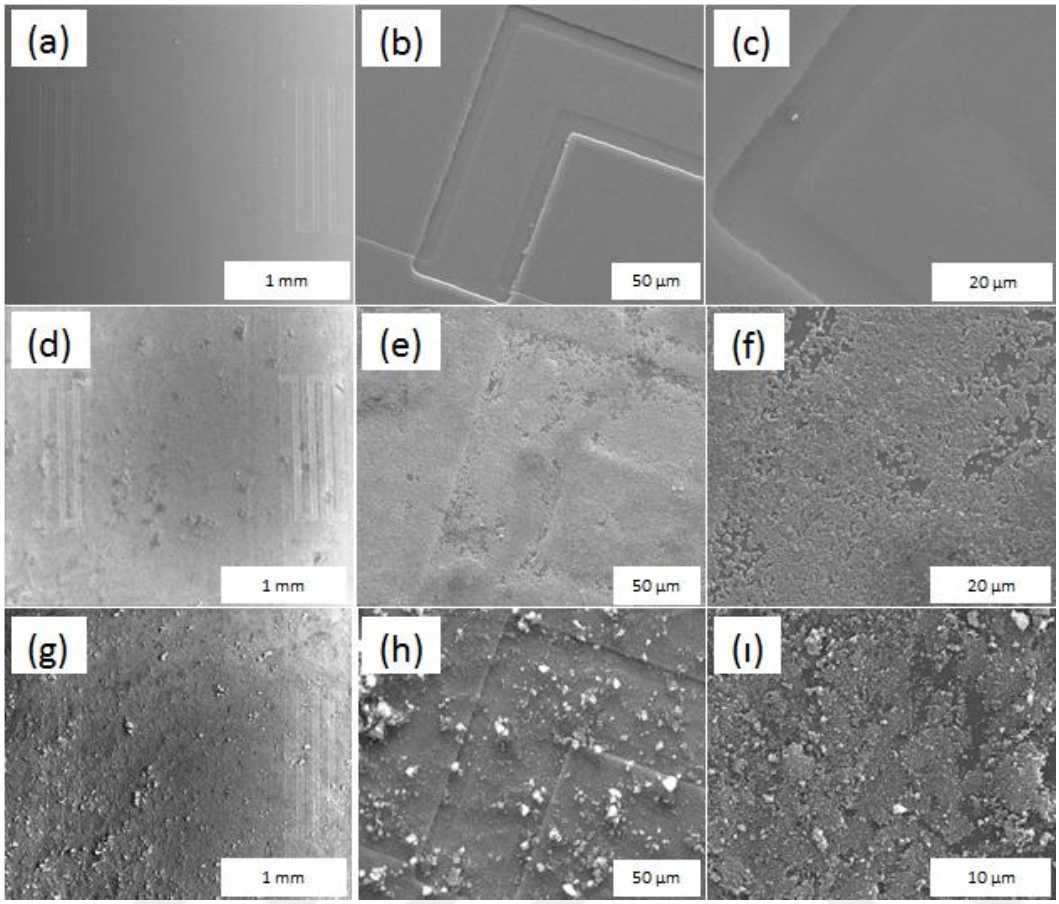


Figure 4.28 SEM images of the PZMTs developed by using zeolites at different magnifications: (a,-c) without zeolite, (d-f) Silicalite, (g-i) Nano BEA

As observed in Figure 4.28, all of the zeolites were coated onto the surfaces successfully. Almost a perfect monolayer of silicalite coating was obtained on the active zone of the transducer shown in Figure 4.29-f whereas as a thicker layer approximately 2-3 layers of zeolite was seen with nano BEA in Figure 4.29-i.

The enzyme immobilization onto these obtained transducers was done as it was explained in Chapter 3.1.2.3. For control, GA cross-linking was used (Chapter 3.2.1.4) as a traditional method for enzyme immobilization for comparison purposes.

#### 4.3.3.1.2 Sensitivity

For developing the bioselective membrane, urease was immobilized on PZMTs as described in Chapter 3.1.2.3. The efficiency of the proposed method of enzyme immobilization using PEI coating was tested firstly by comparing the typical responses of the biosensors obtained by PZMTs with traditional method in GA vapor i.e.; standard membrane transducers (SMT, Chapter 3.2.1.4). The biosensor responses to injection of 0.5 mM of urea for all developed biosensor are given in Figure 4.29.

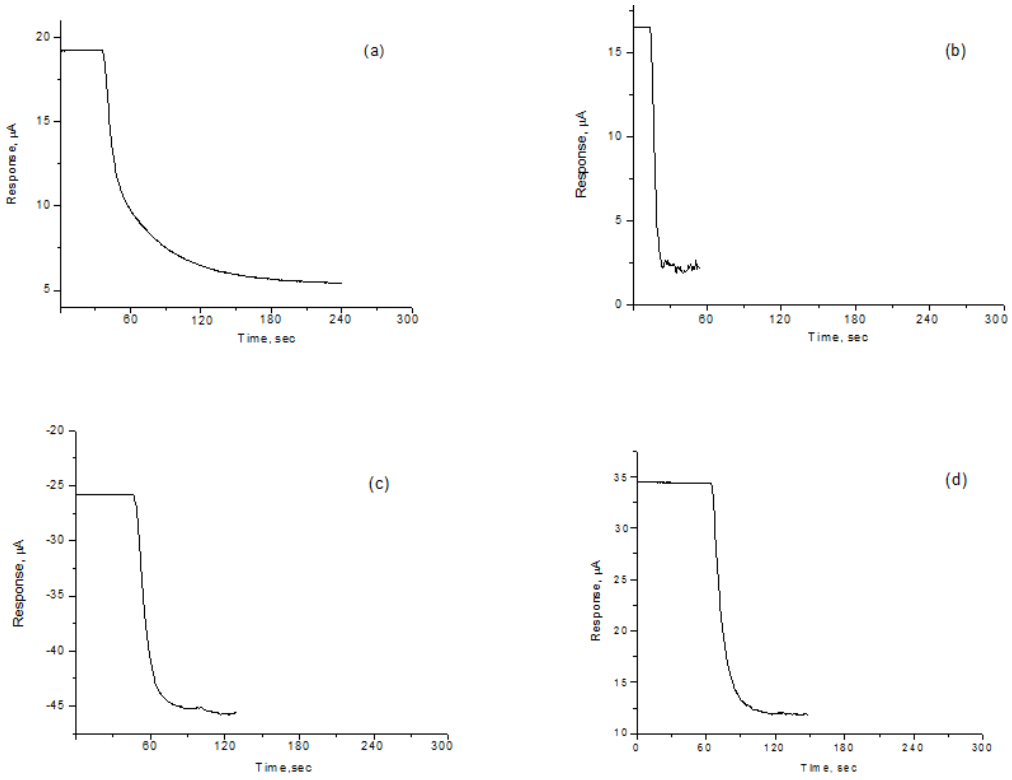


Figure 4.29 The responses to 0.5 mM of urea obtained with biosensors created by urease immobilization in (a) GA vapor, adsorption on (b) Silicalite, (c) Nano BEA, (d) Cal-Nano BEA. The measurements were carried out in 5mM phosphate buffer solution (pH 7.4)

As seen in Figure 4.29-b, the biosensor with urease adsorbed on silicalite demonstrated the response time to urea in about 1 min, which is three times less compared with that for the biosensor based on urease immobilized in GA vapor (Figure 4.29-a). Also, the other zeolites gave quicker responses than SMTs. This is an expected result since the GA layer was considered as a diffusion barrier. Thus, the proposed method of urease adsorption on zeolites using PEI-coating method can significantly reduce the time of biosensor analysis as also observed for previous amperometric biosensor studies reported in Chapter 4.3.2. Another important working characteristics of the biosensors for analysis of substances in real samples are their sensitivity and linear range of determination. Therefore, the calibration curves of the biosensors based on different types of immobilization were compared. For this reason, urea of various concentrations ranging from 0.1 mM up to saturation concentration was added to the measuring cell. The obtained calibration curves are given in Figure 4.30.

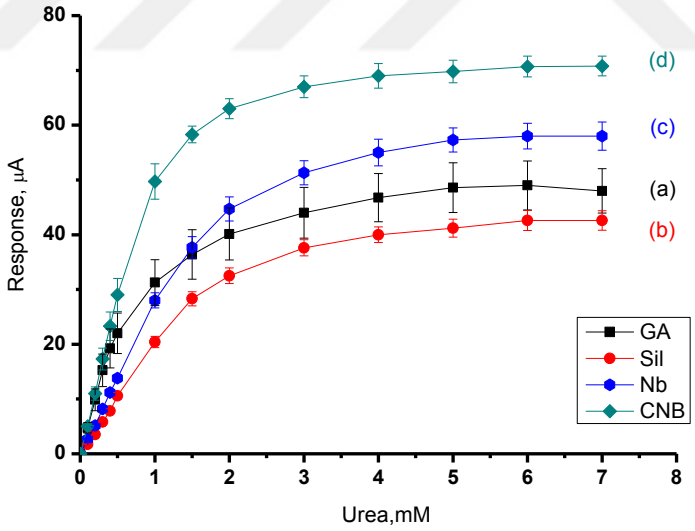


Figure 4.30 Calibration curves for urea determination obtained with biosensors created by urease immobilization in (a) GA vapor, adsorption on (b) Silicalite, (c) Nano BEA, (d) Cal-Nano BEA. The measurements were carried out in 5mM phosphate buffer solution (pH 7.4)

According to Figure 4.30-d, the highest sensitivity belongs to the biosensors based on urease adsorbed on Cal-Nano BEA. Biosensors with urease adsorbed on silicalite had the largest linear range while the smallest was revealed for the biosensor with urease immobilized in GA vapor. Cal-Nano BEA had higher sensitivity compared to nano BEA, which can be explained by the increased surface area (from 472 $m^2/g$ to 696 $m^2/g$ as shown in Table 4.1) due to the removal of template leading to a possible increase in the amount of immobilized enzyme. Additionally, all BEA-type framework based biosensors had higher sensitivities than MFI type framework based ones (silicalite).

#### 4.3.3.1.3 Signal Reproducibility and Inter-Reproducibility

At the next stage, the reproducibility and inter-reproducibility of the created biosensors were investigated, which are important for the biosensor stability. For this study, 0.5 mM of urea was added to the cell and after obtaining the response, sensors were cleaned away from reaction products in working buffer. This procedure was repeated for 10 times. The mean value calculated for all the responses was taken as 100% for certain type of immobilization. For each type of immobilization, the experiment was repeated for at least three times. As seen from Figure 4.31, the highest signal reproducibility belonged to the biosensor obtained by immobilization on nano BEA; the lowest was obtained for immobilization in GA vapor. The reproducibility data reported for the biosensors immobilized by adsorption on the surface of silicalite and Cal-Nano BEA were the same.

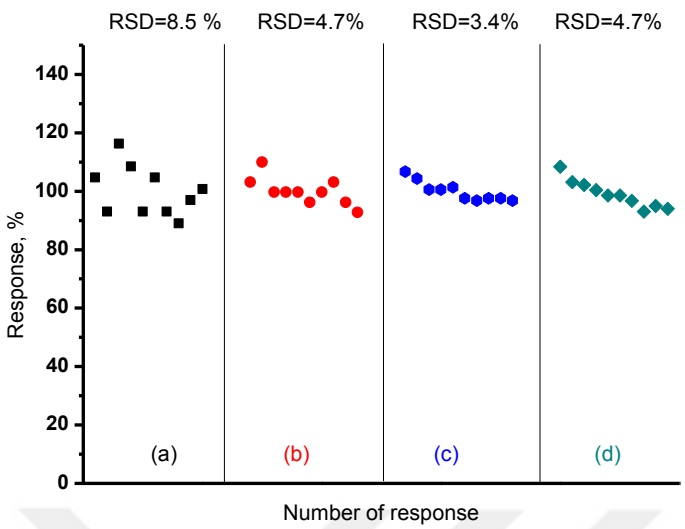


Figure 4.31 Reproducibility of the responses to the 0.5mM urea obtained with biosensors created by urease immobilization in (a) GA vapor, adsorption on (b) Silicalite, (c) Nano BEA, (d) Cal-Nano BEA. The measurements were carried out in 5mM phosphate buffer solution (pH 7.4)

Inter-reproducibility is known to be the reproducibility data obtained from the responses of a number of biosensors to the same substrate concentration on different transducers. For this purpose, ten different ISFETs with similar working characteristics were selected. 0.5 mM of urea was used for the substrate concentration which corresponds to the linear working range of the biosensors. After receiving the responses, the sensor was completely washed away from the enzyme and reference membranes, as well as from the zeolite attached onto the surface. Next, new immobilization procedure was carried out and responses to the same substrate concentrations were measured. The described procedure was repeated for ten times. For each sensor, the responses to certain concentration were obtained in three repetitions, and the average value was calculated as shown in Figure 4.32. A mean value calculated for all the responses was taken as 100% for

the corresponding type of immobilization. The slightest data dispersion was revealed for the biosensor obtained by urease immobilization on silicalite. whereas the highest data dispersion was observed for biosensors based on urease immobilized in GA vapor.

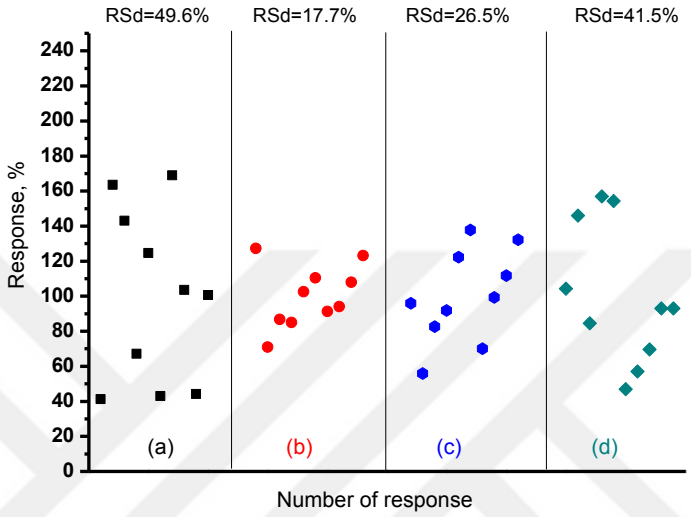


Figure 4.32 Inter-reproducibility of signals to urea concentration of 0.5mM obtained with biosensors created by urease immobilization in (a) GA vapor, adsorption on (b) Silicalite, (c) Nano BEA, (d) Cal-Nano BEA. The measurements were carried out in 5mM phosphate buffer solution (pH 7.4)

The comparative data (noise, baseline drift, minimum detection limit, linear range, error of signal reproducibility) for the biosensors based on different types of immobilization are summarized in Table 4.6.

Table 4.6 Comparison of operational characteristics of biosensors created using all types of urease immobilization

| Material | Response to 3 mM urea(μA) | Resp. Time(s) | Linear range, mM | Det. Limit, mM | RSD of Reprod. (%) | RSD of Inter-reprod., (%) | Noise, μA | Drift of base line, μA/min |
|---|---|---|---|---|---|---|---|---|
| GA vapor | 44 | 240 | 0-0.5 | 0.0015 | 8.5 | 49.6 | 0.02 | 0.010 |
| Silicalite | 38 | 60 | 0-1.5 | 0.0015 | 4.7 | 17.7 | 0.03 | 0.028 |
| Nano BEA | 51 | 120 | 0-1.0 | 0.0015 | 3.4 | 26.5 | 0.03 | 0.001 |
| Cal-Nano BEA | 67 | 120 | 0-1.0 | 0.0055 | 4.7 | 41.5 | 0.09 | 0.013 |

The obtained data in Table 4.6 show that in general adsorption on zeolites can promote sensitivity, linear range, a decrease in the error of response reproducibility, a decrease in response time and baseline drift. Nevertheless, the biosensors obtained by traditional immobilization in GA vapor can be characterized by lower baseline noise. Thus, the technique of PEI –coated zeolites for enzyme adsorption results not only to avoid the use of toxic substances (glutaraldehyde, etc.), but also to obtain potentiometric biosensors with improved analytical characteristics for the first time [96].

#### 4.3.3.2 ISFET Based Biosensor Applications for Creatinine

Creatinine is a marker of kidney glomerular filtration rate [97, 98] and considered as a general diagnostic indicator of kidney function. Its concentration in kidney should be determined, for muscular dysfunction and should be monitored for patients receiving hemodialysis. Therefore, firstly, silicalite coating with drop-coating method was applied and optimized for immobilization of creatinine deiminase onto ISFET surfaces for creatinine determination. Afterwards, this method was compared with PEI coating method for zeolite attachment and then the effect of zeolite morphology, particle size, gold nanoparticles were investigated.

#### 4.3.3.2.1 Preparation of Drop-coated Silicalite Modified Transducers

The synthesis of silicalite (Cal-Sil) was completed as it was described in Chapter 3.1.1.

Drop-coated zeolite modified transducers (DZMT) with silicalite (Cal-Sil; Chapter 3.1.1) was achieved as described in Chapter 3.1.2.1. The formed silicalite layer by drop-coating method was presented in Figure 4.33. Then, the creatinine deiminase (CD) immobilization onto these surfaces was carried out according to Chapter 3.1.2.3. For control, the traditional method for enzyme immobilization; GA cross-linking was used as known to be the traditional method for enzyme immobilization (SMT, Chapter 3.2.3.2.4).

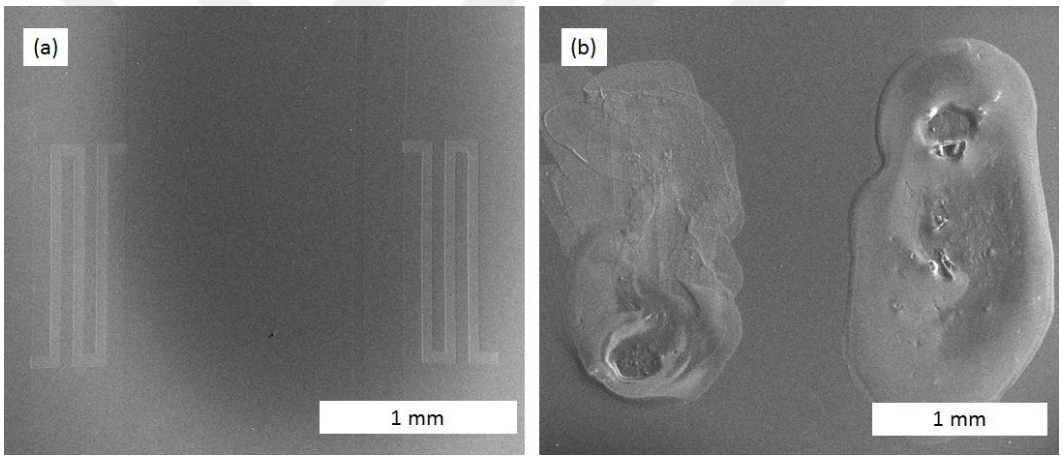


Figure 4.33 SEM images of potentiometric transducers (sensitive parts): (a) bare surfaces and (b) surface covered with silicalite

#### 4.3.3.2.2 Sensitivity

The enzymatic response of biosensors developed by adsorption on drop-coated silicalite was compared with GA cross-linked enzyme. Their calibration curves based on adsorption and cross-linking up to 10 mM creatinine concentration are presented in Figure 4.34-a and b, respectively.

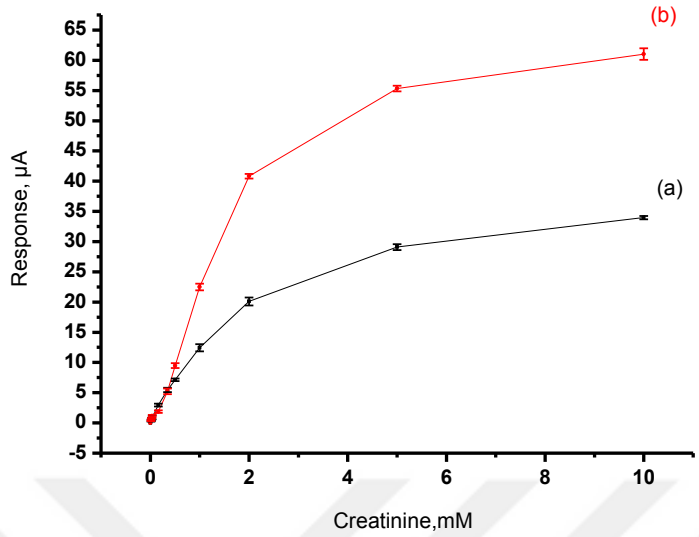


Figure 4.34 Calibration curves of creatinine biosensors: (a) covalent cross-linking in GA vapor and (b) adsorption on drop-coated silicalite. Measurements were carried out in 5 mM phosphate buffer solution, pH 7.4, at room temperature

The characteristics of biosensors such as: detection limit, response time, regeneration time and sensitivity are presented in Table 4.7. Application of adsorption on drop-coated silicalite resulted in an increase in the sensitivity to creatinine by almost three times, a decrease in response and regeneration time by nearly two-thirds, and a decrease by a half in detection limit when compared with covalent cross-linking in GA vapor as seen in Table 4.7. Additionally, the linear dynamic range remained the same for both methods of immobilization and ranged from 0 to 2 mM. Therefore, only drop-coated silicalite-modified biosensors were used for reproducibility and storage stability studies.

Table 4.7 Characteristics of creatinine biosensor based on different types of enzyme immobilization

| Key parameters | Covalent CD cross-linking in GA vapor | CD adsorption on drop-coated silicalite |
|---|---|---|
| Detection limit, μM | 10 | 5 |
| Response time, s | 240 | 90 |
| Regeneration time, s | 300 | 80 |
| Sensitivity, μA/mM | 7 | 18 |

#### 4.3.3.2.3 Signal Reproducibility and Operational Stability

To determine the signal reproducibility, the biosensor responses to 1 mM creatinine were measured through one working day. Biosensors were kept in continuously stirred buffer solution at room temperature during all the time intervals in between measurements. As seen from Figure 4.35, the responses of drop-coated silicalite-modified biosensors were highly reproducible. The relative standard deviation (RSD) for creatinine determination was 2.6 %.

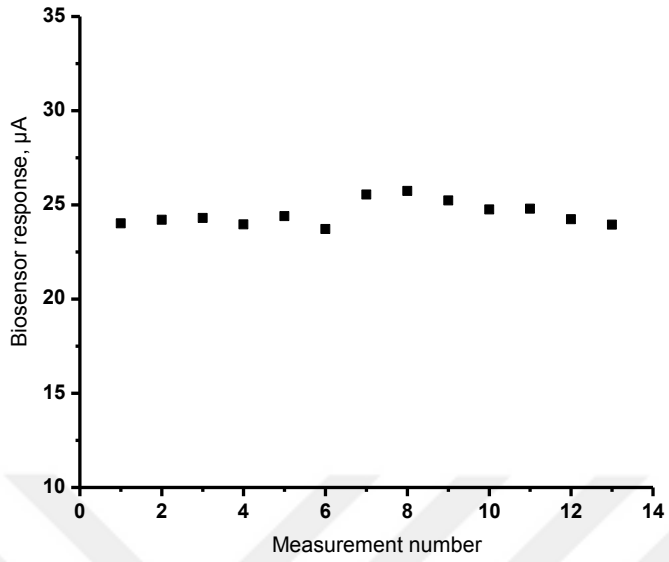


Figure 4.35 The reproducibility of the drop-coated silicalite modified biosensor. Measurements were carried out in the 5 mM phosphate buffer at a pH of 7.4 at room temperature. Concentration of creatinine was 1 mM

To investigate the storage stability, a special buffer with the addition of stabilizers and preservatives (10 mM phosphate buffer, pH 7.4 + 1 mM EDTA + 1 mM dithiothreitol + 0.1% $NaN_3$) was used. The biosensors were stored in this buffer at 4ºC. On the first day after adsorption of the enzyme on the drop-coated silicalite modified transducers, the biosensor responses to 1 mM of creatinine were measured in 5 mM phosphate buffer at a pH of 7.4. The responses of biosensors with initial activity were taken as 100%. Subsequent measurements were carried out after certain time intervals. It was shown that after more than one-year long storage, the activity of CD adsorbed on drop-coated silicalite based biosensor decreased to 43.3% (Figure 4.36). This is a very high stability, since CD is known as an unstable enzyme. This result can be attributed to the presence of silicalite as an enzyme

carrier at the immobilization providing increased surface area and microenvironment for the enzymes.

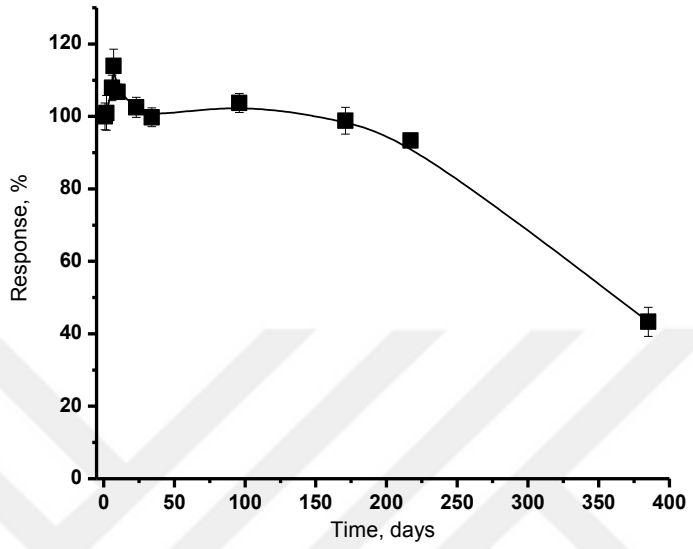


Figure 4.36 Storage stability of drop-coated silicalite modified biosensor, Measurements were carried out in 5 mM phosphate buffer, pH 7.4 at room temperature. Concentration of creatinine was 1 mM

#### 4.3.3.2.4 Effect of Solution Properties

The ultimate aim of these studies was to be able to use the created biosensors in real biological samples such as blood serum of patients with renal failure having the creatinine concentration is about 1000 μM. In fact, the blood serum is a complex medium containing several buffer systems, amino acids, electrolytes, carbohydrates, enzymes, lipoproteins, proteins, etc. The highest concentration belongs to sodium chloride (137-144 mM) and protein (7.5% on average).

For this reason, the biosensor responses to 1 mM creatinine were measured at the sodium chloride concentrations ranging from 0 to 200 mM. It was shown that the

value of responses affected by 2 to 7%. Since the 1:20 blood serum dilution and differential mode of measurements were planned to be used, an influence of NaCl could be neglected (Figure 4.37).

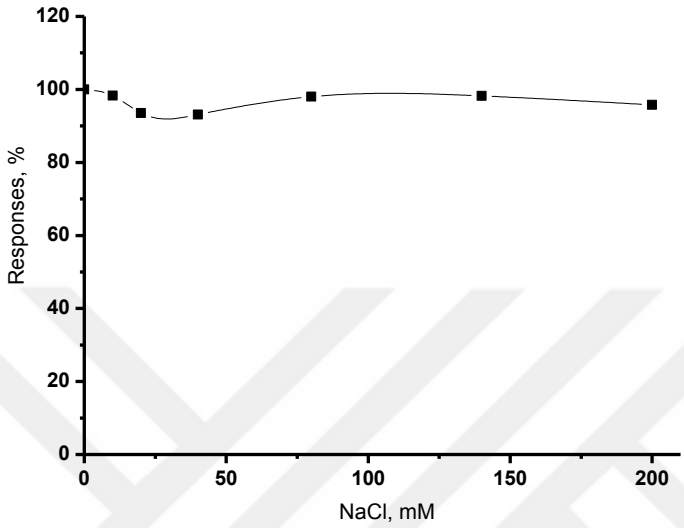


Figure 4.37 Dependence of response of drop-coated silicalite modified biosensor on NaCl concentration. Measurements were carried out in 5 mM phosphate buffer, pH 7.4, at different concentrations of NaCl and room temperature. Concentration of creatinine was 1 mM

Considering possible variants of blood serum dilution from 1:10 to 1:20, BSA was also added to the working cell in concentrations up to 1%, no signal to BSA was observed, and no significant influence of BSA on calibration curves of the biosensor was found as demonstrated in Figure 4.38.

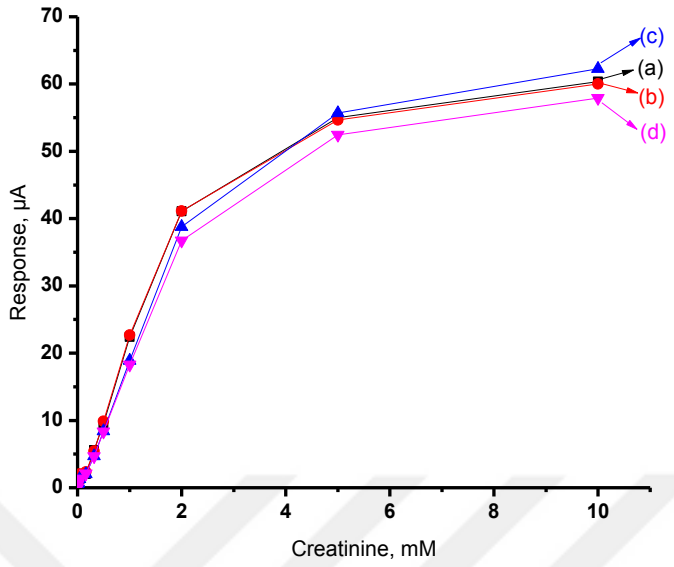


Figure 4.38 Calibration curves for creatinine detection in presence of protein at various concentrations: (a) 0 %, (b) 0.1 %, (c) 0.5 % and (d) 1%. Measurements were carried out in 5 mM phosphate buffer, pH 7.4 and room temperature

Thus, the presence of pre-diluted macromolecular BSA fraction in the buffer does not lead to a significant non-specific response and faintly affects its value.

In conclusion, the developed drop-coated silicalite modified biosensor has improved analytical characteristics; high storage stability, and selectivity towards interferences. Therefore, in the future it can be successfully used in the analysis of blood serum of patients with kidney disease [99].

#### 4.3.3.2.5 Comparison of Creatinine Adsorption on Silicalite Developed by DZMT and PZMT

PEI coating method (PZMT) was compared with drop-coating method (DZMT) for silicalite-modified creatinine biosensor based on ISFET.

#### 4.3.3.2.5.1 Sensitivity

Creatinine sensitive ISFET biosensors developed by PEI coating method as described in Chapter 3.1.2.2 and 3.1.2.3 was compared with only PEI including just enzyme, to be sure about the response is not due to PEI. These responses were compared with biosensor responses developed by drop-coated silicalite modified biosensor developed as described in Chapter 3.1.2.1 and 3.1.2.3. The responses of zeolite-based biosensor's analytical characteristics were compared with the GA vapor method (SMT) as described in Chapter 3.2.3.2.4.

The biosensor responses up to 10 mM of creatinine for the following types of immobilization: in GA vapor (SMT), in drop-coating method and PEI-coating method of silicalite are presented in Figure 4.39. Additionally, for comparison the biosensor response developed by only PEI with enzyme is presented.

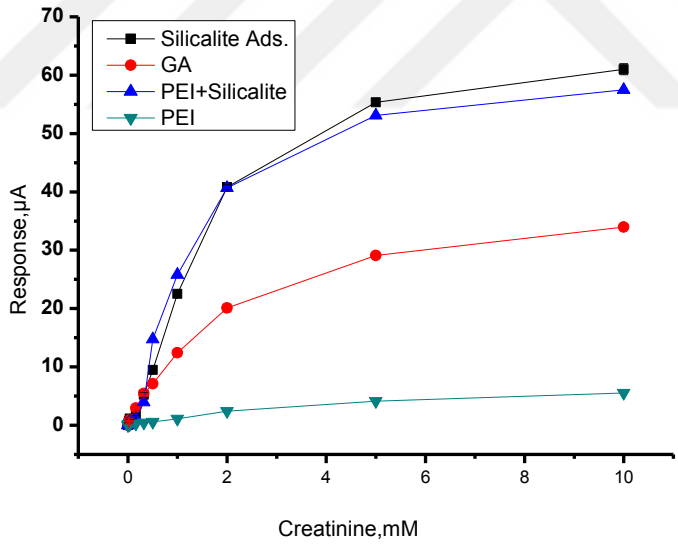


Figure 4.39 The calibration curves for determination of the creatinine in 5 mM phosphate buffer solution, pH 7.4.

As seen in Figure 4.39, the response of biosensor with only PEI and enzyme is the smallest and usage of combination of PEI and silicalite gave a higher response. Both drop-coating and PEI coating methods gave higher responses than SMT.

Additionally, characteristics of biosensors such as; sensitivity, linear range of detection, response time, regeneration time and detection limit are presented in Table 4.8.

Table 4.8 Comparison of characteristics of creatinine based biosensors

| Material | Sensitivity, μA/mM | Linear range, mM | Response time, s | Regeneration time, s | Detection limit, μM |
|---|---|---|---|---|---|
| SMT | 14 | 0-2 | 240 | 300 | 10 |
| DZMT | 20 | 0-2 | 90 | 60-120 | 5 |
| PZMT | 30 | 0-2 | 30 | 60 | 2 |

According to Table 4.8, the sensitivity of GA vapor (SMT) was 14 μA/mM, whereas zeolite including DZMT and PZMT had higher sensitivities as 20 and 30 μA/mM, respectively. All obtained biosensors resulted in the same linear range which was seen to be in the range of 0-2 mM of creatinine , but the response time were different, for SMT; 4 min, DZMT; 1.5 min whereas for PZMT response time was 30 seconds. Additionally when the regeneration time was determined; for SMT; 5 min, DZMT; 1-2 min, and for PZMT; 1 min. These results were similar with the studies conducted using urease where SMT had response time of 4 min and PZMT had response time of 60 seconds in Chapter 4.3.3.1.2. Additionally, detection limit for SMT was 10μM, for DZMT; 5μM whereas for PZMT; detection limit was 2μM. Consequently, the usage of zeolite resulted in two-fold increase in sensitivity, and quicker responses than SMT. This result was explained by more controllable thickness of zeolites for enzyme adsorption compared to SMT. Additionally, PZMT responses were quicker since PEI coating resulted in more thinner layers of zeolites, almost a degree of monolayer.

#### 4.3.3.2.5.2 Signal Reproducibility and Inter-Reproducibility

The calculated RSD values of signal reproducibility for both silicalite based biosensors are presented in Figure 4.40. The zeolite-based biosensors gave same reproducibility (3%) and they were higher than the SMT (12%).

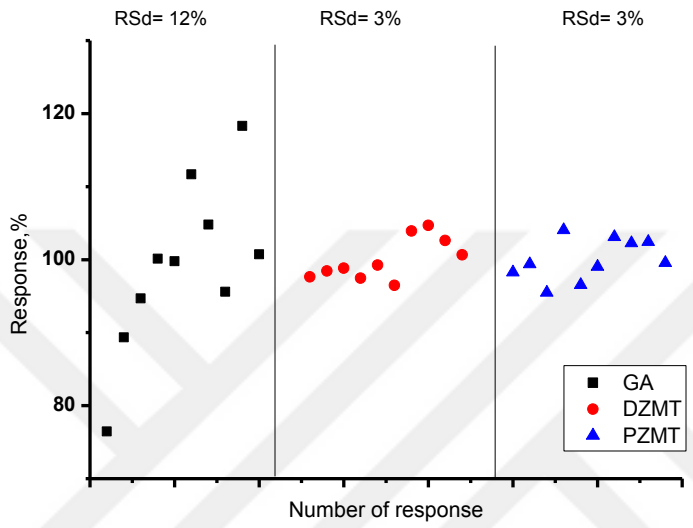


Figure 4.40 Results of the biosensor signal reproducibility for determination of creatinine content in 5 mM phosphate buffer, pH 7.4 at room temperature

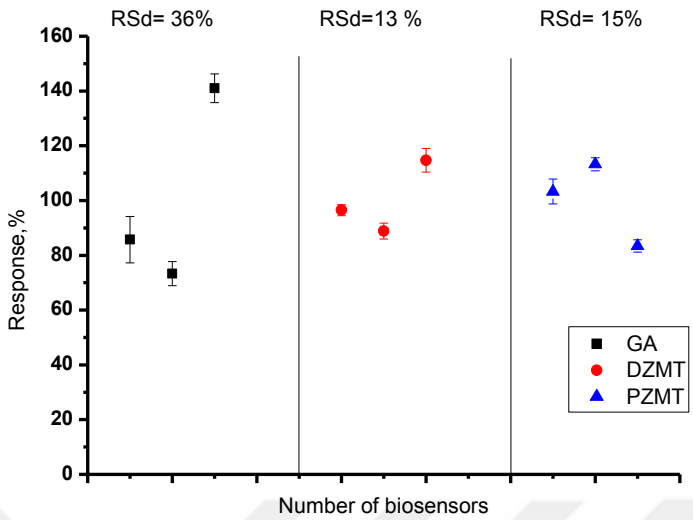


Figure 4.41 Results of the biosensor signal inter-reproducibility for determination of creatinine content in 5 mM phosphate buffer, pH 7.4 at room temperature

In Figure 4.41, inter-reproducibility values for all immobilization methods were presented. In this figure, it can be seen that both zeolite based enzyme adsorption methods having RSD of 13% for DZMT and 15 % for PZMT have lower dispersion of responses than the responses of biosensors based on cross-linking with GA vapor method having RSD of 36 %.

#### 4.3.3.2.6 Effect of Zeolite Morphology, Particle Size and Gold Nanoparticle on Drop-Coated Zeolite Modified ISFET Based Biosensors

The effects of different types of zeolite frameworks, particle size variation and the presence of gold on zeolites were investigated to improve the analytical characteristics of drop-coated zeolite modified ISFET based biosensors. Silicalite (Cal-Sil) and BEA zeolites were synthesized to be able investigate the effect of zeolite morphology. Gold nanoparticles were formed on BEA zeolites in order to

investigate the effect of gold nanoparticles in ISFET performance. Additionally, for particle size effect, nano BEA zeolites were synthesized.

The basic characteristics of all types of zeolites prepared for this particular study are summarized in Table 4.9.

Table 4.9 Summary of physicochemical characteristics of used zeolites

| Sample Name | Structure | Si/Al [a] | Particle Size[b] (nm) | $S_{BET}$ [c] ($m^2/g$) | $S_{EXT}$[d] ($m^2/g$) | Zeta Potential [e] (mV) |
|---|---|---|---|---|---|---|
| Cal-Sil | MFI | ∞ | ~470nm | 447 | 96 | -62.6 |
| Cal-BEA | BEA | 21.5±0.7 | ~1.2µm | 743 | 128 | -47.9 |
| BEA-Gold | BEA | 21.0±0.9 | ~1.2µm | 776 | 160 | -47.2 |
| Cal-Nano BEA | BEA | 20.8±0.8 | ~100nm | 696 | 183 | -36.6 |

a Measured by EDX
b Measured by SEM and Master sizer
c Measured by Multipoint BET
d Measured by t-plot Method
f Measured by Zeta potential at pH 7

According to Table 4.9, Cal-Sil which belongs to MFI-type framework has the lowest surface area (447 $m^2/g$) with the lowest zeta potential (-62.6 mV) and it has no aluminium inside whereas BEA-type of zeolites have similar Si/Al ratios with different particle sizes such as 1.2µm for Cal-BEA and 100 nm for Cal-Nano BEA. Gold nanoparticle formation on BEA resulted in a 20% increase in the external surface area which was thought to be important in enzyme immobilization.

#### 4.3.3.2.6.1 Preparation of Drop-coated Zeolite Modified Electrode

Drop-coated zeolite modified transducers (DZMT) with zeolites; Cal-Sil, Cal-BEA, BEA-Gold and Cal-Nano BEA were produced as described in Chapter 3.1.2.1.

In order to attain an idea about the zeolite thickness on the transducers, the exact developed methodology for drop-coating was applied an silicon wafers. In this

way, cross sectional views were obtained and the images collected for all zeolite modified surfaces are shown in Table 4.10 with corresponding AFM images and surface roughness values. As seen from the cross sectional SEM images, the thickness of the coated zeolite layer was in the range of 10-20µm. According to the obtained AFM images, electrode surfaces modified with nano BEA has the smoothest surface with a surface roughness value of 0.08±0.01 nm. On the other hand, BEA-Gold, Cal-BEA, and silicalite have similar surface roughness values of 48.85±8.3, 42.00±4.9, 44.45±4.03 nm, respectively.

Table 4.10 Cross sectional SEM and AFM images of silicalite, Cal-BEA, BEA-Gold and Cal-Nano BEA on silicon wafer with their representative surface roughness values (Ra)

| Zeolite Type (Particle size) | Cross sectional SEM image of zeolite coated on silicon wafer | 2-D Image | Roughness, Ra (nm) |
|---|---|---|---|
| Silicalite (450nm) | 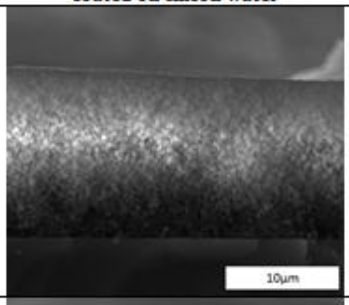  | 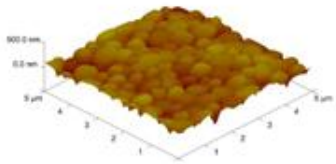 | Ra=44.45±4.03 |
| BEA (1.2μm) | 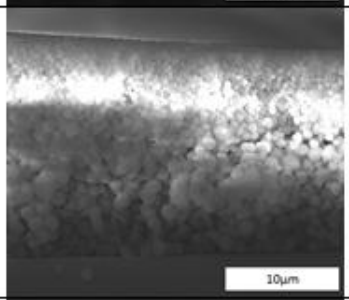  | 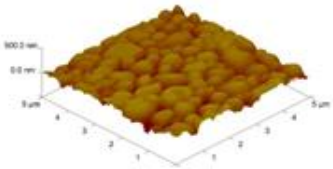 | Ra=42.00± 4.9 |
| Bea-Gold (1.2μm) | 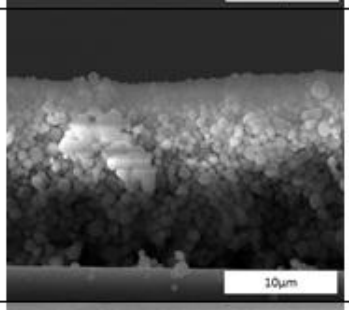  | 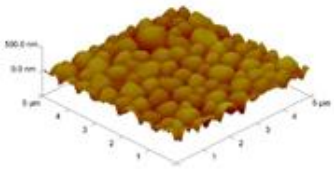 | Ra=48.85±8.3 |
| Nano bea (100nm) | 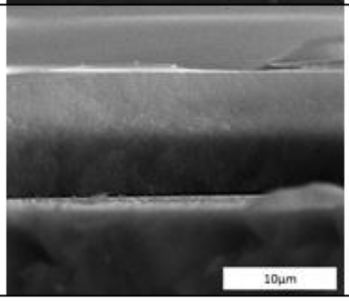  | 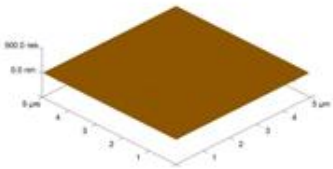 | Ra=0.08±0.01 |

Additionally, contact angle measurements were carried out on surfaces of drop-coated zeolite modified ISFET surfaces. According to the contact angle measurements presented in Table 4.11, zeolite coated surfaces were becoming more hydrophilic when compared to GA cross-linked surfaces. The contact angles were in the following order: BEA=BEA-Gold<nano BEA<silicalite<GA. This is an expected result, since it was known that a decrease in $Al^{3+}$ content, which is related to ion-exchange capacity of a zeolite, produces more hydrophobic nature [100].

Table 4.11 Contact angles of biosensor surfaces

| Sample Name | Contact Angle, Θ (°) |
|---|---|
| Plain Surface | 56 |
| GA | 66 |
| Silicalite | 29 |
| Cal-BEA | 6 |
| BEA-Gold | 5 |
| Cal-Nano BEA | 15 |

Then, the CD immobilization onto these surfaces was performed according to Chapter 3.1.2.3. The traditional method for enzyme immobilization; GA cross-linking was used as described in Chapter 3.2.3.2.4 for control.

#### 4.3.3.2.6.2 Sensitivity

GA cross-linking was used as a control group to compare the effect of zeolites on characteristics of zeolite modified potentiometric biosensors such as sensitivity, linear range, response time, detection limit and regeneration time. Therefore, firstly, the calibration curves for all biosensors up to 10 mM of creatinine concentration were obtained and the results are presented in Figure 4.42.

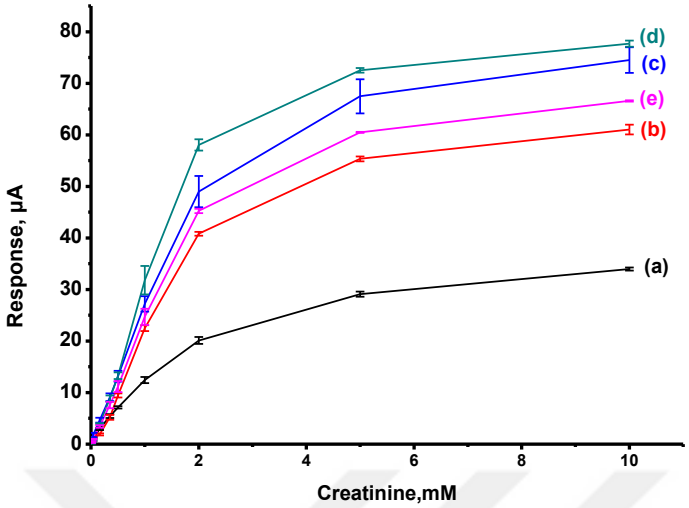


Figure 4.42 The calibration curves for determination of creatinine obtained with biosensors created by CD immobilization; (a) in GA vapor, adsorption on: (b) silicalite, (c) BEA, (d) BEA-Gold and (e) Nano BEA. The measurements were carried out in 5 mM phosphate buffer solution (pH 7.4)

As seen in Figure 4.42, all zeolite based biosensors had higher sensitivities than GA-based biosensors. The sensitivities of the biosensors decreased in the order of: BEA-Gold>BEA>nano BEA>silicalite>GA. BEA zeolites, having aluminium inside, regardless of its particle size, gave higher response than silicalite which has no aluminium in its structure. This result is consistent with our previous results showing that the sensitivity of urease biosensor based on ISFET developed by nano BEA coating is higher compared to silicalite coated one [96] and the same trend was observed for amperometric glucose biosensor [95]. This result can be attributed to the presence of aluminium in zeolite BEA and nano BEA, providing both hydrophilicity and Brønsted acid sites (Si-OH-Al) which are strongly effective in protein adsorption [26, 54]. Additionally, Tavolaro et al. studied the effect of different acidity owing to zeolite framework on protein immobilization and

concluded that the protein immobilization is proportional to effective acidity (AE) which is defined as:

$AE=m\ \alpha_0$

where m=Al/Al+Si and $\alpha_0$ is the efficiency coefficient [54]. In their study, they found the immobilization trend as FAU>BEA>MFI, which is similar with what was observed in the current study (BEA>MFI).

Biosensor responses were compared for BEA and nano-BEA samples to investigate the effect of particle size, since both zeolites had similar Si/Al ratios and identical zeolite framework (BEA). It was observed that BEA based one having higher surface area (743$m^2$/g) with larger particle size (~1.2μm) showed higher response. This result can also be related with its surface roughness since enzymes prefer rough surfaces rather than smooth surfaces [101-103].

In the current study, more hydrophilic surfaces gave higher sensitivities as consistent with the findings of Peng et al. They demonstrated that higher concentration of enzyme adsorption can be achieved on hydrophobic surfaces, whereas hydrophilic surfaces can be enzymatically more active [104].

Linear dependence between response current and creatinine concentration, the sensitivities of the obtained biosensors with the other characteristics such as detection limit (at an S/N of 3), response time and regeneration time for cross-linked and zeolite coated biosensors were presented in Table 4.12. As it can be seen, all zeolite based biosensors; silicalite, Cal-BEA, BEA-Gold and Cal-Nano-BEA showed good linear dependence with correlation coefficients of 0.9934, 0.9976, 0.9967, 0.9980, respectively. The highest sensitivity belongs to BEA-Gold, having threefold increase compared to GA. This can be attributed to more favorable microenvironment for CD created by the presence of gold that avoids denaturation as well as increased surface area for interaction upon modification by gold nanoparticles. Furthermore, when comparing BEA and BEA-Gold based

biosensors, it was observed that an increase in external surface area of about 20 % resulted in approximately similar increase in the sensitivity.

The linear dynamic range of 2 mM was the same for all biosensors, however, there was a significant improvement in the response time of about 60 % decrease in silicalite based biosensors and a minimal 40 % decrease in regeneration time of all BEA-type of zeolite based biosensors compared to respective values of GA based biosensors. Additionally, the detection limit was decreased by half for all types of zeolite based biosensors compared to GA based biosensors.

Table 4.12 Characteristics of creatinine based biosensors with different types of enzyme immobilization

| Material | Linear equation between response (y) and creatinine concentration(x) | Sensitivity, µA/mM | Det. limit, µM | Response time,s | Reg. time,s |
|---|---|---|---|---|---|
| GA | y=10.131x+0.9594, $R^2$=0.9807 | 10 | 10 | 240 | 300 |
| Silicalite | y=20.79x-0.3002, $R^2$=0.9934 | 21 | 5 | 90 | 80 |
| BEA | y=24.663x+0.6437, $R^2$=0.9976 | 25 | 5 | 150 | 180 |
| BEA-Gold | y=29.591x-0.3703, $R^2$=0.9967 | 30 | 5 | 150 | 120 |
| Nano-BEA | y=22.942x+0.0394, $R^2$=0.9980 | 23 | 5 | 120 | 120 |

#### 4.3.3.2.6.3 Signal Reproducibility and Inter-Reproducibility

The stability of the created biosensors was investigated through reproducibility and inter-reproducibility studies. In reproducibility studies, the responses of the biosensors to 1 mM concentration of creatinine were measured over one working day with 30-35 min time intervals and continuous stirring at room temperature to determine signal repeatability. During this study, after obtaining the response, the working cell was rinsed with buffer three times to discard the products of enzymatic reaction on the biosensor surface. This measurement was repeated for six times for every type of immobilization. Finally, the relative standard deviations (RSD) for determining creatinine were presented in Figure 4.43. As seen, the tested biosensors had rather good reproducibility as a sign of stable operation. The RSD

values for all biosensors were in the range of 1-5 % with BEA having the highest RSD value of 4.67 %, while the lowest RSD value belongs to the silicalite based biosensors (1.04%).

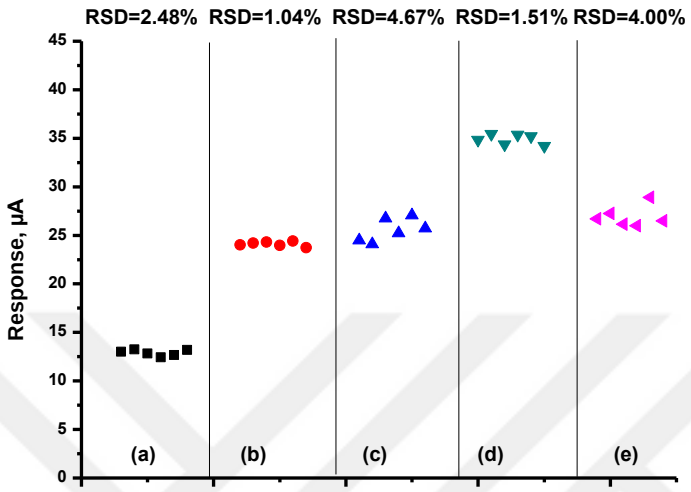


Figure 4.43 Reproducibility of signals obtained with biosensors created by CD immobilization; (a) in GA vapor, adsorption on: (b) Silicalite, (c) BEA, (d) BEA-Gold and (e) Nano BEA. The measurements were carried out in 5 mM phosphate buffer solution (pH 7.4)

For inter-reproducibility studies, several clean electrodes were drop-coated with zeolites and then CD was adsorbed onto these transducers as described in Chapter 3.3.1.2. After obtaining the response to 1 mM of creatinine in three repetitions, enzyme and zeolite particles were removed from the transducer surfaces with ethanol-wetted cotton. Thereafter the whole procedure was repeated three times and RSD values of biosensors were calculated. According to the results, the highest RSD (36.03 %) belonged to the traditional method prepared with GA and the least RSD belonged to BEA-Gold (3.19 %), while the intermediate values belonged to silicalite (13.27%), BEA (10.7%), and nano BEA (18.5 %). The lowest RSD for

zeolite based biosensors compared to GA based biosensors can be due to the better controlled procedure of adsorption. Additionally, low RSD of BEA-Gold can be due to the presence of gold nanoparticles, which will bind covalently the amine groups of the enzyme and actively stabilize the enzyme. This result is consistent with the study of Gole et al., where pepsin-gold colloid conjugates were prepared by just mixing under protein friendly conditions and then demonstrated that pepsin showed significant catalytic activity. They explained the binding mechanism of the enzyme to the gold nanoparticle by covalent interactions between thiol groups in cysteine residues as well as amine groups in lysine residues of pepsin with the surface of gold. This interaction resulted in a more stabilized enzyme with its activity [64,105].

# CHAPTER 5

## SUMMARY, CONCLUSION AND FURTHER SUGGESTIONS

In this study, the goal was improving and optimizing the zeolite usage in immobilization of bioselective membrane to obtain improved analytical characteristics of conductometric, amperometric and potentiometric (ISFET based) biosensors. Doing so, it was aimed to find an alternative for the mostly used toxic GA cross-linking agent for enzyme immobilization. For this reason, two different methodologies of zeolite coating were developed for enzyme immobilization; drop coating and PEI coating.

Firstly, conductometric transducers were optimized for urea detection by modifying the electrode surfaces using drop-coated silicalite. This procedure provided to discard usage of GA as the cross-linker for enzyme immobilization. Usage of zeolites enabled to produce a biosensor with enhanced sensitivity, reproducibility, inter-reproducibility and operational stability. The fabricated zeolite modified biosensors were tested in real blood serum successfully for the first time.

Then, drop coating method was applied to amperometric biosensor for glucose determination. However, it was observed that drop-coating method resulted in biosensors with a very long response time so PEI coating method was developed for the deposition of thinner zeolite layers. By this way, a new method of enzyme adsorption on zeolites was verified for development of amperometric biosensors with improved analytical characteristics.

The developed PEI method of zeolite attachment was adapted to ISFET based potentiometric urea biosensors. The fabricated biosensors using zeolite showed

shorter response time with higher reproducibility, linear range and high storage stability (nearly 1 year) compared to GA cross-linked enzyme based biosensors.

The characteristics of both drop coating and PEI coating for detection of creatinine were compared with standard membrane transducers using ISFET type biosensors. It was realized that PEI coating was producing quicker responses due to the controlled thickness of zeolites with almost a degree of monolayer. Additionally, there was a decrease in detection limit compared to drop-coated zeolite modified transducers. However, the reproducibility and inter-reproducibility of biosensors were the same for zeolite-based biosensors. Both of these methods were producing biosensors with low detection limit, quick response, higher reproducibility and inter-reproducibility compared to the conventional method of enzyme immobilization using GA cross-linker. Accordingly, developed two methods of enzyme immobilization using zeolites can be alternatives to GA cross-linking for production of bioselective membrane on biosensors.

Finally, the effect of different types of zeolite frameworks, particle size variation, and the presence of gold on zeolites were investigated to improve the analytical characteristics of drop-coated zeolite modified ISFET based biosensors. The incorporation of zeolite and gold nanoparticles for adsorption of creatinine deiminase on ISFET based biosensor was studied for the first time. The sensitivities of the obtained biosensors were decreasing in the following order: BEA- Gold > BEA > nano BEA > silicalite > GA. The BEA-Gold based biosensor resulted in increased sensitivity compared to GA based biosensor, which could be attributed to favorable microenvironment for CD to avoid denaturation as well as increased surface area produced by gold nanoparticles with good stability. This result showed that gold nanoparticles can be used with zeolites to improve the characteristics of ISFET based biosensors.

Consequently, it has been shown that the proposed methods of the enzyme immobilization by adsorption on zeolites are quite promising for further application in the development of biosensors.

## REFERENCES


[1] International Union of Pure and Applied Chemistry, Compendium of Chemical Terminology, Gold Book, Version 2.3.3, 2014-02-24, “https://goldbook.iupac.org/pdf/goldbook.pdf”, retrieved on 11.11.2017

[2] J. Yoon, “Introduction to Biosensors From Electric Circuits to Immunosensors”, Springer, New York, p. 5, 2013.

[3] D. O'Hare, “Biosensors and Sensor Systems”, In: Body Sensor Networks G.-Z. Yang (ed.), Springer-Verlag, London, p.58, 2014.

[5] O. Fesenko and L. Yatsenko (ed.), “Nanophysics, Nanomaterials, Interface Studies, and Applications: Selected Proceedings of the 4th International Conference Nanotechnology and Nanomaterials (NANO2016), August 24-27, 2016”, Lviv, Ukraine, 581

[5] D. Thévenot, K. Toth, R. Durst, G. Wilson, “Electrochemical Biosensors: Recommended Definitions And Classification”, Pure Appl. Chem. 71, pp. 2333-2348, 1999.

[6] J. Li and N. Wu, “Biosensors Based on Nanomaterials and Nanodevices”, Taylor & Francis Group, Boca Raton, FL, 2014

[7] N. Bhalla, P. Jolly, N. Formisano, and P. Estrela, “Introduction to biosensors”, Essays Biochem., no. June, pp. 1–8, 2016.

[8] N. Jaffrezic-Renault and S. V. Dzyadevych, “Conductometric microbiosensors for environmental monitoring”, Sensors, vol. 8, no. 4, pp. 2569–2588, 2008.

[9] S. Öztürk, “Immobilization Of Zeolite Crystals On Solid Substrates For Biosensor Aplications”, M. Sc. Thesis, METU, 2010.

[10] O. O. Soldatkin, V. M. Peshkova, S. V. Dzyadevych, A. P. Soldatkin, N. Jaffrezic-Renault, and A. V. El’skaya, “Novel sucrose three-enzyme conductometric biosensor”, Mater. Sci. Eng. C, vol. 28, no. 5–6, pp. 959–964, 2008.

[11] S. V. Dzyadevych, V. N. Arkhypova, A. P. Soldatkin, A. V. El’skaya, C. Martelet, and N. Jaffrezic-Renault, “Amperometric enzyme biosensors: Past, present and future”, Itbm-Rbm, vol. 29, no. 2–3, pp. 171–180, 2008.

[12] J. Wang, “Amperometric biosensors for clinical and therapeutic drug monitoring: A review”, J. Pharm. Biomed. Anal., vol. 19, no. 1–2, pp. 47–

53, 1999.

[13] I. Willner and E. Katz, “Bioelectronics: From Theory to Applications”, WILEY-VCH Verlag GmbH & Co. KGaA, Weinheim, Germany, 2005.

[14] I. Willner, E. Katz, “Integration of Layered Redox Proteins and Conductive Supports for bioelectronics applications ”, Angew. Chem. Int. Ed. Engl., vol. 39, pp. 1180–1218, 2000.

[15] S. V. Dzyadevych, A. P. Soldatkin, A. V. El’skaya, C. Martelet, and N. Jaffrezic-Renault, “Enzyme biosensors based on ion-selective field-effect transistors”, Anal. Chim. Acta, vol. 568, no. 1–2, pp. 248–258, 2006.

[16] M. Yuqing, G. Jianguo, and C. Jianrong, “Ion sensitive field effect transducer-based biosensors”, Biotechnol. Adv., vol. 21, no. 6, pp. 527–534, 2003.

[17] A. D. Pozzo, L. Vanini, M. Fagnoni, M. Guerrini, A. De Benedittis, and R. A. A. Muzzarelli, “Preparation and characterization of poly ( ethylene glycol ) -crosslinked reacetylated chitosans,” Carbohydr. Polym., vol. 42, pp. 201–206, 2000.

[18] X. Luo, J. Xu, Q. Zhang, G. Yang, and H. Chen, “Electrochemically deposited chitosan hydrogel for horseradish peroxidase immobilization through gold nanoparticles self-assembly,” Biosens. Bioelectron., vol. 21, pp. 190–196, 2005.

[19] Y. Yang, H. Yang, M. Yang, G. Shen, and R. Yu, “Amperometric glucose biosensor based on a surface treated nanoporous $ZrO_2$ / Chitosan composite film as immobilization matrix,” Anal. Chim. Acta, vol. 525, pp. 213–220, 2004.

[20] A. Sassolas, L. J. Blum, B. D. Leca-Bouvier, “Immobilization strategies to develop enzymatic biosensors”, Biotechnology Advances, vol. 30, no. 3, pp. 489, 2012.

[21] G. Evtugyn, “Biosensors: Essentials”, Lecture Notes in Chemistry 84, Springer-Verlag Berlin Heidelberg, 2014.

[22] I. Migneault, D. Dartiguenave, M. J. Bertrand, K. C. Waldron, “Glutaraldehyde: behavior in aqueous solution, reaction with proteins, and application to enzyme crosslinking”, Biotechniques, vol. 37, pp.790–802, 2004.

[23] A. Dwevedi, “Enzyme Immobilization”, Springer International Publishing Switzerland, 25, 2016.

[24] “http://www.iza-structure.org/DatabaseHistory.htm.”, retrieved on

10.11.2017

[25] “http://europe.iza-structure.org/IZA-SC/ftc_table.php.”, retrieved on 11.11.2017

[26] K. Sakaguchi, M. Matsui, and F. Mizukami, “Applications of zeolite inorganic composites in biotechnology: Current state and perspectives,” Appl. Microbiol. Biotechnol., vol. 67, no. 3, pp. 306–311, 2005.

[27] K. Sahner, G. Hagen, D. Schönauer, S. Reiss, and R. Moos, “Zeolites - Versatile materials for gas sensors,” Solid State Ionics, vol. 179, no. 40, pp. 2416–2423, 2008.

[28] E. P. Ng and S. Mintova, “Nanoporous materials with enhanced hydrophilicity and high water sorption capacity,” Microporous Mesoporous Mater., vol. 114, no. 1–3, pp. 1–26, 2008.

[29] P. Mehrotra, “Biosensors and their applications – A review”, J. Oral Biol. Craniofac Res., vol. 6, no. 2, pp. 153–159, 2016.

[30] E. B. Bahadır, M. K. Sezgintürk, “Applications of commercial biosensors in clinical, food, environmental, and biothreat/biowarfare analyses”, Analytical Biochemistry, vol. 478, pp. 107-120, 2015.

[31] R. Săndulescu, M. Tertiş, C. Cristea and E. Bodoki, “New Materials for the Construction of Electrochemical Biosensors”, In: Toonika Rinken ed. Biosensors- Micro and Nanoscale Applications, InTech, 2015

[32] C. Mousty, “Sensors and biosensors based on clay-modified electrodes-new trends”, Appl Clay Sci vol. 27, pp. 159–177, 2004.

[33] C. Mousty, “Biosensing applications of clay-modified electrodes: a review”, Anal Bioanal Chem, vol. 396, pp. 315–325, 2010.

[34] J. Wang and T. Martinez, “Trace Analysis at Clay-Modified Carbon Paste Electrodes”, Electroanalysis, vol. 1, pp. 167-172, 1989.

[35] A. Walcarius, M. Etienne, G. Herzog, V. Urbanova,and N. Vila`, “Electrode Materials (Bulk Materials and Modification)”, In: Environmental Analysis by Electrochemical Sensors and Biosensors ed. L. M. Moretto, K. Kalcher, Springer, New York, NY, 2014.

[36] D. Shan, C. Mousty, S. Cosnier, S. A. Mu, “New Polyphenol Oxidase Biosensor Mediated by Azure B in Laponite Clay Matrix”, Electroanalysis vol. 15, pp. 1506–1512, 2003.

[37] Z. Dai, G. Shao, J. Hong, J. Bao, and J. Shen, “Immobilization and direct electrochemistry of glucose oxidase on a tetragonal pyramid-shaped porous

ZnO nanostructure for a glucose biosensor", Biosens. Bioelectr., vol. 24, pp. 1286-1291, 2009.

[38] P. M. Ajayan, "Carbon nanotube from carbon", Chem. Rev., vol. 99 no. 7, pp. 1787-1799, 1999.

[39] W. Putzbach and N. J. Ronkainen, "Immobilization Techniques in the Fabrication of Nanomaterial-Based Electrochemical Biosensors: A Review", Sensors, vol.13, pp. 4811-4840, 2013.

[40] P. J. Britto, K. S. V Sunthanam, P. M. Ayajan, "Carbon nanotube electrode for oxidation of dopamine", Bioelectrochem. Bioenerg, vol. 41, pp.121–125, 1996.

[41] J. Wang, M. Musameh, Y. Lin, "Solubilization of carbon nanotubes by nafion toward the preparation of amperometric biosensors", J. Am. Chem. Soc., 125, pp. 2408-2409, 2003.

[42] C. Shan, H. Yang, J. Song, D. Han, A. Ivaska, L. Niu, "Direct electrochemistry of glucose oxidase and biosensing for glucose based on graphene", Anal. Chem., vol. 81, pp. 2378–2382, 2009.

[43] A. Walcarius, "Zeolite-modified electrodes in electroanalytical chemistry", vol. 384, pp. 1-16, 1999.

[44] S. Mintova, V. Valtchev, V. Engstro, B. J. Schoeman, and J. Sterte, "Growth of Silicalite-1 films on gold substrates", Microporous Mater., vol. 11, pp. 149–160, 1997.

[45] J. Sterte, S. Mintova, G. Zhang, and B. J. Schoeman, "Thin molecular sieve films metal substrates on noble", Zeolites, vol. 18, 5-6, pp. 387-390, 1997.

[46] Y. Zhang, F. Chen, W. Shan, J. Zhuang, and A. Dong, "Fabrication of ultrathin nanozeolite film modified electrodes and their electrochemical behavior", Microporous Mesoporous Mater. 65, vol. 65, pp. 277–285, 2003.

[47] J. S. Lee, J. H. Kim, Y. J. Lee, N. C. Jeong, and K. B. Yoon, "Manual assembly of microcrystal monolayers on substrates", Angew. Chemie - Int. Ed., vol. 46, no. 17, pp. 3087–3090, 2007.

[48] Pham T. C. T., Kim H. S. Yoon K. B., "Growth of Uniformly Oriented Silica MFI and BEA zeolite films on substrates", Science, vol. 334, no. December, pp. 1533–1539, 2011.

[49] S. Öztürk and B. Akata, "Oriented assembly and nanofabrication of zeolite A monolayers", Microporous Mesoporous Mater., vol. 126, no. 3, pp. 228–233, 2009.

[50] R. H. Carvalho, F. Lemos, J. M. S. Cabral, and F. Ramˆ, “Influence of the presence of NaY zeolite on the activity of horseradish peroxidase in the oxidation of phenol”, J. Molecular Catalysis B: Enzymatic, vol. 44, pp. 39–47, 2007.

[51] R. Wijntje, H. Bosch, A. B. De Haan, and P. J. T. Bussmann, “Influencing the selectivity of zeolite Y for triglycine adsorption”, J. Chromatogr., vol. 1142, pp. 39–47, 2007.

[52] J. E. Krohn and M. Tsapatsis, “Amino Acid Adsorption on Zeolite β”, Langmuir, vol. 21, no. 19, pp. 8743–8750, 2005.

[53] P. Vidinha, V. Augusto, J. Nunes, J. C. Lima, J. M. Cabral, and S. Barreiros, “Probing the microenvironment of sol – gel entrapped cutinase : The role of added zeolite NaY,” J. Biotechnol, vol. 135, pp. 181–189, 2008.

[54] P. Tavolaro, A. Tavolaro, and G. Martino, “Influence of zeolite PZC and pH on the immobilization of cytochrome c: A preliminary study regarding the preparation of new biomaterials”, Colloids Surfaces B Biointerfaces, vol. 70, no. 1, pp. 98–107, 2009.

[55] P. Tavolaro, S. Catalano, G. Martino, and A. Tavolaro, “Applied Surface Science Zeolite inorganic scaffolds for novel biomedical application : Effect of physicochemical characteristic of zeolite membranes on cell adhesion and viability”, Appl. Surf. Sci., vol. 380, pp. 135–140, 2016.

[56] H. Kotte, B. Gründig, K.D. Vorlop, D. Strehlitz, U. Stottmeister, “Methylphenazonium-modified enzyme sensor based on polymer thick films for subnanomolar detection of phenols”, Anal. Chem., vol. 67, pp. 65-70, 1995,

[57] J. Wang and A. Walcarius, “Zeolite containing oxidase-based carbon paste biosensors”, J. Electroanal. Chem., vol. 404, pp. 237–242, 1996.

[58] J. Q. Liu, B. H.; Hu, R. Q.; Deng, “Characterization of immobilization of an enzyme in a modified Y zeolite matrix and its application to an amperometric glucose biosensor”, Anal Chem., vol. 69, no. 13, pp. 2343–8, 1997.

[59] X. Zhou, T. Yu, Y. Zhang, J. Kong, Y. Tang, J. L. Marty, and B. Liu, “Nanozeolite-assembled interface towards sensitive biosensing”, Electrochem. commun., vol. 9, no. 7, pp. 1525–1529, 2007.

[60] O. Y. Saiapina, V. M. Pyeshkova, O. O. Soldatkin, V. G. Melnik, B. A. Kurç, A. Walcarius, S. V. Dzyadevych, and N. Jaffrezic-Renault, “Conductometric enzyme biosensors based on natural zeolite clinoptilolite for urea determination”, Mater. Sci. Eng. C, vol. 31, no. 7, pp. 1490–1497, 2011.

[61] E. Soy, V. Pyeshkova, V. Arkhypova, and F. V. Cedex, “Potentialities of zeolites for immobilization of enzymes in conductometric biosensors”, Sens. Electron. Microsyst. Technol., vol. 1, pp. 28-35, 2010.

[62] E. Soy, V. Arkhypova, O. Soldatkin, M. Shelyakina, S. Dzyadevych, J. Warzywoda, A. Sacco, and B. Akata, “Investigation of characteristics of urea and butyrylcholine chloride biosensors based on ion-selective field-effect transistors modified by the incorporation of heat-treated zeolite Beta crystals”, Mater. Sci. Eng. C, vol. 32, no. 7, pp. 1835–1842, 2012.

[63] S. K. Kirdeciler, E. Soy, S. Öztürk, I. Kucherenko, O. Soldatkin, S. Dzyadevych, and B. Akata, “A novel urea conductometric biosensor based on zeolite immobilized urease”, Talanta, vol. 85, no. 3, pp. 1435–1441, 2011.

[64] A. Gole, C. Dash, V. Ramakrishnan, S. R. Sainkar, A. B. Mandale, M. Rao, and M. Sastry, “Pepsin - Gold Colloid Conjugates : Preparation , Characterization , and Enzymatic Activity”, Langmuir, vol. 17, pp. 1674–1679, 2001.

[65] S. A. Ansari and Q. Husain, “Potential applications of enzymes immobilized on/in nano materials: A review”, Biotechnol. Adv., vol. 30, no. 3, pp. 512–523, 2012.

[66] A. L. Crumbliss, S. C. Perine, J. Stonehuerner, K. R. Tubergen, J. Zhao, and R. W. Henkens, “Colloidal gold as a biocompatible immobilization matrix suitable for the fabrication of enzyme electrodes by electrodeposition”, Biotechnol. Bioeng., vol. 40, no. 4, pp. 483–490, 1992.

[67] J. Crumbliss, A. L., Henkens , R. W., Perine, S. C., Tubergen, K. R., Kitchell, B. S., Stonehuerner, “Biosensor Technology: Fundamentals and applications”, New York: Marcel Dekker, 1990.

[68] J. Feng, G. Zhao, J. Xu, and H. Chen, “Direct electrochemistry and electrocatalysis of heme proteins immobilized on gold nanoparticles stabilized by chitosan”, Anal. Biochem., vol. 342, pp. 280–286, 2005.

[69] N. German and A. Ramanaviciene, “Glucose biosensor based on graphite electrodes modified with glucose oxidase and colloidal gold nanoparticles”, Microchim Acta, vol. 168, no. 3-4, pp. 221–229, 2010.

[70] S. Zhang, N. Wang, H. Yu, Y. Niu, and C. S. T, “Covalent attachment of glucose oxidase to an Au electrode modified with gold nanoparticles for use as glucose biosensor”, Bioelectrochemistry, vol. 67, pp. 15–22, 2005.

[71] A. B. Kharitonov, A. N. Shipway, and I. Willner, “An Au Nanoparticle / Bisbipyridinium Field-Effect Transistor for the Sensing of Adrenaline”, Anal. Chem., vol. 71, no. 23, pp. 5441–5443, 1999.

[72] J. Gun, D. Rizkov, O. Lev, M. H. Abouzar, A. Poghossian, and M. J. Schöning, “Oxygen plasma-treated gold nanoparticle-based field-effect devices as transducer structures for bio-chemical sensing”, Microchim. Acta, vol. 164, no. 3–4, pp. 395–404, 2009.

[73] J. Gun, M. J. Schöning, M. H. Abouzar, A. Poghossian, and E. Katzd, “Field-effect nanoparticle-based glucose sensor on a chip: Amplification effect of coimmobilized redox species”, Electroanalysis, vol. 20, no. 16, pp. 1748–1753, 2008.

[74] A. Poghossian, M. H. Weil, M. Bäcker, D. Mayer, and M. J. Schöning, “Field-effect devices functionalised with goldnanoparticle/ macromolecule hybrids: New opportunities for a label-free biosensing”, Procedia Eng., vol. 47, pp. 273–276, 2012.

[75] A. Poghossian, M. Bäcker, D. Mayer, and M. J. Schöning, “Gating capacitive field-effect sensors by the charge of nanoparticle/molecule hybrids”, Nanoscale, vol. 7, no. 3, pp. 1023–1031, 2015.

[76] K. Mukhopadhyay, S. Phadtare, V. P. Vinod, A. Kumar, M. Rao, R. V. Chaudhari, and M. Sastry, “Gold nanoparticles assembled on amine-functionalized Na - Y zeolite: A biocompatible surface for enzyme immobilization”, Langmuir, vol. 19, no. 9, pp. 3858–3863, 2003.

[77] L. Ren, J. Dong, and X. Cheng, “Hydrogen peroxide biosensor based on direct electrochemistry of hemoglobin immobilized on gold nanoparticles in a hierarchically porous zeolite”, vol. 180, no. 13-14, Microchim Acta, pp. 1333–1340, 2013.

[78] N. Chauhan, U. Jain, R. Gandotra, and V. Hooda, “Electrochimica Acta Zeolites-AuNPs assembled interface towards amperometric biosensing of spermidine”, Electrochim. Acta, vol. 230, pp. 106–115, 2017.

[79] M. Zahmakiran and S. Özkar, “The preparation and characterization of gold(0) nanoclusters stabilized by zeolite framework: Highly active, selective and reusable catalyst in aerobic oxidation of benzyl alcohol”, Mater. Chem. Phys., vol. 121, no. 1–2, pp. 359–363, 2010.

[80] P. Prokešová, S. Mintova, J. Čejka, and T. Bein, “Preparation of nanosized micro/mesoporous composites”, Mater. Sci. Eng. C, vol. 23, no. 6–8, pp. 1001–1005, 2003.

[81] J. J. Virgen-Ortız, J. C. S. dos Santos, A. Berenguer-Murcia, O. Barbosa, R. C. Rodriguese and R. Fernandez-Lafuente, “Polyethylenimine: a very useful ionic polymer in the design of immobilized enzyme biocatalysts”, J. Mater. Chem. B, vol. 5, pp. 7461-7490, 2017.

[82] L. T. Yin, Y. T. Lin, Y. C. Leu, and C. Y. Hu, “Enzyme immobilization on

nitrocellulose film for pH-EGFET type biosensors", Sensors Actuators B: Chemical, vol. 148, no. 1, pp. 207–213, 2010.

[83] A. P. Soldatkin, J. Montoriol, W. Sant, C. Martelet, and N. Jaffrezic-Renault, "A novel urea sensitive biosensor with extended dynamic range based on recombinant urease and ISFETs", Biosens. Bioelectron., vol. 19, no. 2, pp. 131–135, 2003.

[84] A. P. Pavluchenko, A. S.; Kukla, A. L.; Goltvianskyi, Yu. V.; Soldatkin, O. O.; Arkhypova, V. M.; Dzyadevych, S. V.; Soldatkin, "Investigation of Stability of the pH-Sensitive Field-Effect Transistor Characteristics", Sens. Lett., vol. 9, no. 6, pp. 2392-2396, 2011.

[85] Y. F. Yeong, A. Z. Abdullah, A. L. Ahmad, S. Bhatia, "Synthesis, structure and acid characteristics of partially crystalline silicalite-1 based materials", Microporous and Mesoporous Materials, 123, pp.129–139, 2009.

[86] K. Narasimharao, M. Hartmann, H. H. Thiel, and S. Ernst, "Novel solid basic catalysts by nitridation of zeolite beta at low temperature", Microporous Mesoporous Mater., vol. 90, no. 1–3 SPEC. ISS., pp. 377–383, 2006.

[87] B. Louis, A. Vincente, C. Fernandez, and V. Valtchev, "Crystal Size – acid sites Relationship Study of Nano- and Micron-Sized Zeolite Crystals Crystal Size – Acid Sites Relationship Study of Nano- and Micron-Sized Zeolite Crystals", J. Phys. Chem C, 115, pp. 18603–18610, 2011.

[88] S. Zeng, S. Ding, S. Li, R. Wang, and Z. Zhang, "Controlled growth of gold nanoparticles in zeolite L via ion-exchange reactions and thermal reduction processes", Inorg. Chem. Commun., vol. 47, pp. 63–66, 2014.

[89] P. Jiang, S. Xie, J. Yao, S. Pang, and H. Gao, "The stability of self-organized 1-nonanethiol-capped gold nanoparticle monolayer", J. Phys. D. Appl. Phys., vol. 34, no. 15, pp. 2255–2259, 2001.

[90] L. Gorton (ed.), "Biosensors and modern biospecific analytical techniques", Elsevier, Lund, Sweden, 2005.

[91] W. Y. Lee, S. R. Kim, T. H. Kim, K. S. Lee, M. C. Shin, and J. K. Park, "Sol-gel-derived thick-film conductometric biosensor for urea determination in serum," Anal. Chim. Acta, vol. 404, no. 2, pp. 195–203, 2000.

[92] I. S. Kucherenko, O. O. Soldatkin, B. O. Kasap, S. Öztürk, B. Akata, A. P. Soldatkin, and S. V. Dzyadevych, "Elaboration of Urease Adsorption on Silicalite for Biosensor Creation," Electroanalysis, vol. 24, no. 6, pp. 1380–1385, 2012.

[93] W. R. Fearon, “The carbamido-diacetyl reaction: a test for citrulline,” Biochem J., vol. 33, no. 6, pp. 902-907, 1939.

[94] O. O. Soldatkin, I. S. Kucherenko, S. V. Marchenko, B. Ozansoy Kasap, B. Akata, A. P. Soldatkin, and S. V. Dzyadevych, “Application of enzyme/zeolite sensor for urea analysis in serum,” Mater. Sci. Eng. C, vol. 42, pp. 155-160, 2014.

[95] O. O. Soldatkin, B. Ozansoy Kasap, B. Akata Kurc, A. P. Soldatkin, S. V. Dzyadevych, and A. V. El’Skaya, “Elaboration of new method of enzyme adsorption on silicalite and nano beta zeolite for amperometric biosensor creation,” Biopolym. Cell, vol. 30, no. 4, pp. 291–298, 2014.

[96] M. K. Shelyakina, O. O. Soldatkin, V. M. Arkhypova, B. O. Kasap, B. Akata, and S. V Dzyadevych, “Study of zeolite influence on analytical characteristics of urea biosensor based on ion-selective field-effect transistors,” Nanoscale Res. Lett., vol. 9, no. 124, 2014.

[97] F. E. Jurkiewicz M, Alegret S, Almirall J, García M, “Development of a biparametric bioanalyser for creatinine and urea. Validation of the determination of biochemical parameters associated with hemodialysis” Analyst, vol. 123, pp. 1321–7, 1998.

[98] W. Sant, M. L. Pourciel-Gouzy, J. Launay, T. Do Conto, R. Colin, A. Martinez, and P. Temple-Boyer, “Development of a creatinine-sensitive sensor for medical analysis,” Sensors Actuators, B Chem., vol. 103, no. 1–2, pp. 260–264, 2004.

[99] S. V Marchenko, O. O. Soldatkin, B. O. Kasap, B. A. Kurc, A. P. Soldatkin, and S. V. Dzyadevych, “Creatinine Deiminase Adsorption onto Silicalite-Modified pH-FET for Creation of New Creatinine-Sensitive Biosensor,” Nanoscale Res. Lett., vol. 11, no. 173, 2016.

[100] M. Matsui, Y. Kiyozumi, T. Yamamoto, Y. Mizushina, F. Mizukami, and K. Sakaguchi, “Selective adsorption of biopolymers on zeolites,” Chem. - A Eur. J., vol. 7, no. 7, pp. 1555–1560, 2001.

[101] K. Rechendorff, M. B. Hovgaard, M. Foss, V. P. Zhdanov, and F. Besenbacher, “Enhancement of protein adsorption induced by surface roughness.,” Langmuir, vol. 22, no. 26, pp. 10885–10888, 2006.

[102] U. B. Jensen, E. E. Ferapontova, and D. S. Sutherland, “Quantifying protein adsorption and function at nanostructured materials: Enzymatic activity of glucose oxidase at GLAD structured electrodes,” Langmuir, vol. 28, no. 30, pp. 11106–11114, 2012.

[103] S. K. Kirdeciler, C. Ozen, and B. Akata, “Fabrication of nano- to micron-sized patterns using zeolites: Its application in BSA adsorption,”

Microporous Mesoporous Mater., vol. 191, pp. 59–66, 2014.

[104] Y. Peng, H. Zhu-Ping, X. Yong-Juan, H. Peng-Cheng, and T. Ji-Jun, “Effect of support surface chemistry on lipase adsorption and activity,” J. Mol. Catal. B Enzym., vol. 94, pp. 69–76, 2013.

[105] B. Ozansoy Kasap, S. V. Marchenko, O. O. Soldatkin, S. V. Dzyadevych, and B. Akata Kurc, “Biosensors Based on Nano-Gold/Zeolite-Modified Ion Selective Field-Effect Transistors for Creatinine Detection,” Nanoscale Res. Lett., vol. 12, no. 162, 2017.

# CURRICULUM VITAE

## PERSONAL INFORMATION

Surname, Name: OZANSOY KASAP, Berna

Nationality: Turkish

Date and Place of Birth: 1982, Ankara

Phone: +90 312 210 7417 Fax: +90 312 210 7433

e-mail: bernaozansoy@gmail.com

## EDUCATION

M.Sc. Hacettepe University,Chemical Engineering, 2007

B.Sc. Hacettepe University,Chemical Engineering, 2004

## WORK EXPERIENCE

2006-Present, General Directorate of Mineral Research and Exploration, Chemical Engineer

2004-2006, Hacettepe University, Chemical Engineering, Research Assistant

## PUBLICATIONS

### A. THESIS

[1] **B. Ozansoy**, Preparation and characterization of quartz crystal surfaces by plasma polymerisation technique for a biosensor, M. Sc. Thesis, Hacettepe University, 2007

### B. JOURNALS

[1] O.V. Soldatkina, O. O. Soldatkin, **B. Ozansoy Kasap**, D.Yu. Kucherenko, I. S. Kucherenko, B. Akata Kurc, S.V. Dzyadevych, "A Novel Amperometric Glutamate Biosensor Based on Glutamate Oxidase Adsorbed on Silicalite", Nanoscale Research Letters, vol. 12, 260, 2017.

[2] **B. Ozansoy Kasap**, S. V. Marchenko, O. O. Soldatkin, S. V. Dzyadevych, and B. Akata Kurc, "Biosensors Based on Nano-Gold/Zeolite-Modified Ion Selective Field-Effect Transistors for Creatinine Detection," Nanoscale Res. Lett., vol. 12, 162, 2017.

[3] S. V. Marchenko, O. O. Soldatkin, **B. O. Kasap**, B. A. Kurc, A. P. Soldatkin, and S. V. Dzyadevych, "Creatinine Deiminase Adsorption onto Silicalite-Modified pH-FET for Creation of New Creatinine-Sensitive Biosensor", Nanoscale Res. Lett., vol. 11, 173, 2016.

[4] V. M. Pyeshkova, O. Y. Dudchenko, O. O. Soldatkin, **B. Ozansoy Kasap**, F. Lagarde, B. Akata Kurç, S. V. Dzyadevych, "Application of silicalite-modified electrode for development of sucrose biosensor with improved characteristics", Nanoscale Research Letter, 10, 149, 2015.

[5] I. S. Kucherenko, O. O. Soldatkin, **B. Ozansoy Kasap**, S. K. Kirdeciler, B. Akata Kurç, N. Jaffrezic-Renault, A. P. Soldatkin, F. Lagarde, S. V. Dzyadevych, "Nanosized zeolites as a perspective material for conductometric biosensors creation", Nanoscale Research Letter, 10 , 209, 2015.

[6] O. O. Soldatkin, M. K. Shelyakina, V. N. Arkhypova, E. Soy, S. K. Kirdeciler, **B. Ozansoy Kasap**, F. Lagarde, N. Jaffrezic-Renault, B. Akata Kurç, A. P. Soldatkin ,S. V. Dzyadevych, "Nano- and microsized zeolites as a perspective material for potentiometric biosensors creation", Nanoscale Research Letters, 10, 59, 2015.

[7] V. M. Pyeshkova, O. Y. Dudchenko, O. O. Soldatkin, I. S. Kucherenko, **B. Ozansoy Kasap**, B. Akata Kurc, S. V. Dzyadevych, "Application of silicalite for improvement of enzyme adsorption on the stainless steel electrodes," Biopolym. Cell, vol. 30, no. 6, pp. 462-468, 2014.

[8] M. K. Shelyakina, O. O. Soldatkin, V. M. Arkhypova, **B. O. Kasap**, B. Akata, and S. V Dzyadevych, "Study of zeolite influence on analytical characteristics of urea biosensor based on ion-selective field-effect transistors," Nanoscale Res. Lett., vol. 9, 124, 2014.

[9] O. O. Soldatkin, **B. Ozansoy Kasap**, B. Akata Kurc, A. P. Soldatkin, S. V. Dzyadevych, and A. V. El'Skaya, "Elaboration of new method of enzyme adsorption on silicalite and nano beta zeolite for amperometric biosensor creation," Biopolym. Cell, vol. 30, no. 4, pp. 291-298, 2014.

[10] O. O. Soldatkin, I. S. Kucherenko, S. V. Marchenko, **B. Ozansoy Kasap**, B. Akata, A. P. Soldatkin, and S. V. Dzyadevych, "Application of enzyme/zeolite sensor for urea analysis in serum," Mater. Sci. Eng. C, vol. 42, pp. 155-160, 2014.

[11] I. S. Kucherenko, O. O. Soldatkin, **B. O. Kasap**, S. Öztürk, B. Akata, A. P. Soldatkin, and S. V. Dzyadevych, "Elaboration of Urease Adsorption on Silicalite for Biosensor Creation," Electroanalysis, vol. 24, no. 6, pp. 1380–1385, 2012.

[12] S. Mutlu, D. Çökeliler, A. Shard, H. Göktaş, **B.Ozansoy**, M. Mutlu, "Preparation and characterization of ethylenediamine and cysteamine plasma polymerized films on piezoelectric quartz crystal surfaces for a biosensor", Thin Solid Films, vol. 516, 6, pp.1249-1255, 2008.

## C. CONFERENCE AND MEETING PRESENTATIONS

[1] **B. Ozansoy**, S. Dzyadevych, B. Akata Kurc, "Biosensors Based on Nano-Gold/Zeolite – Modified Ion Selective Field Effect Transistors for Creatinine Detection", Materials Research Society (MRS) Fall Meeting, Boston, USA, November 26-December 1, 2017.

[2] **B. Ozansoy**, S. Dzyadevych, B. Akata Kurc, "A Novel Amperometric Glutamate Biosensor Based On Glutamate Oxidase Adsorbed On Silicalite", Materials Research Society (MRS) Fall Meeting, Boston, USA, November 26-December 1, 2017.

[3] **B. Ozansoy Kasap**, Burcu Akata Kurç, "Zeolite Modified Electrodes and Their Influence on Biosensor Performance", Materials Research Society (MRS) Fall Meeting, Boston, USA, November 27-December 2, 2016.

[4] S. V. Marchenko, O. O. Soldatkin, I. S. Kucherenko, S. V. Dzyadevych, A.P. Soldatkin, I. I. Piliponskiy, O. O. Mamchur, **B. O. Kasap**, B. A. Kurç, "Development of a new biosensor by adsorption of creatinine deiminase on monolayers of micro- and nanoscale zeolites", 4th International Conference Nanotechnology and Nanomaterials (NANO2016), Lviv, Ukraine, August 24-27, 2016.

[5] **B. Ozansoy Kasap**, S. V. Marchenko, O. O. Soldatkin, S. V. Dzyadevych, B. A. Kurç, "Improvement of the analytical characteristics of creatinine biosensor based on ISFET using micro and nanosized zeolites", 4th International Conference Nanotechnology and Nanomaterials (NANO2016), Lviv, Ukraine, August 24-27, 2016.

[6] **B. Ozansoy**, K. S. Kirdeciler, B. Akata, "Production of Zeolite Including Microfluidic Channels for Advanced Biosensor Applications" The 6th Nanoscience and Nanotechnology Conference (NanoTR6), Çeşme, Turkey, 15-18 June, 2010.

**D. BOOKS**

[1] I. S. Kucherenko, O. O. Soldatkin, **B. Ozansoy Kasap**, B. Akata Kurç, V. G. Melnyk, L. M. Semenycheva, S. V. Dzyadevych, A. P. Soldatkin, "Biosensors based on urease, adsorbed on nickel, platinum, and gold conductometric transducers modified with silicalite and nanozeolites". In: O. Fesenko, L.Yatsenko (eds.), Nanocomposites, Nanophotonics, Nanobiotechnology, and Applications, Springer Proceedings in Physics 156, Springer International Publishing Switzerland, p. 271, 2015

**E. PATENTS**

[1] O. O. Soldatkin, I. S Kucherenko, D. Y. Kucherenko, S. V. Dzyadevych, A. P. Soldatkin, T. O. Borisova, A. A. Borisov, N. V. Krysanova, **B. Ozansoy Kasap**, S. Kaan Kirdeciler, B. Akata Kurç, "Amperometric biosensor for glutamate determination", Patent of Ukraine No 101165, 2015, deposited 26.03.2015, published 25.08.2015, V. 16.

[2] S. V. Marchenko, O. O. Soldatkin, S. V. Dzyadevych, A. P. Soldatkin, **B. Ozansoy Kasap**, S. Kaan Kirdeciler, B. Akata Kurç, "Potentiometric biosensor

based on recombinant urease for determination of urea in water solution", Patent of Ukraine No 101077, 2015, deposited 05.03.2015, published 25.08.2015, V. 16.

[3] O. O. Soldatkin, S. V. Marchenko, S. V. Dzyadevych, A. P. Soldatkin, **B. Ozansoy Kasap**, S. Kaan Kirdeciler, B. Akata Kurç, **"**Potentiometric biosensor based on creatinine deiminase for determination of creatinine in water solution", Patent of Ukraine No 101078, 2015, deposited 05.03.2015, published 25.08.2015, V. 16.

**AWARDS**

2009-2010 Academic Year METU Graduate Courses Performance Award